Department of Forest Products Technology

On the Refractive Index Contrast Modification in Paper and Printing Applications - Studies with Fillers and Coating Pigments

Kimmo Koivunen

Aalto University

DOCTORAL DISSERTATIONS

Aalto University publication series
DOCTORAL DISSERTATIONS 11/2011

On the Refractive Index Contrast Modification in Paper and Printing Applications - Studies with Fillers and Coating Pigments

Kimmo Koivunen

Doctoral dissertation for the degree of Doctor of Science in Technology to be presented with due permission of the School of Chemical Technology for public examination and debate in Auditorium (Forest Products Building 2) at the Aalto University School of Chemical Technology (Espoo, Finland) on the 11th of March, 2011, at 12 noon.

Aalto University
School of Chemical Technology
Department of Forest Products Technology

Supervisor
Professor Hannu Paulapuro

Instructor
Professor Patrick A. C. Gane

Preliminary examiners
Dr. John Husband
Professor Kaarlo Niskanen

Opponents
Dr. John Husband
Dr. Markku Leskelä

Aalto University publication series
DOCTORAL DISSERTATIONS 11/2011

ISBN 978-952-60-4034-9 (pdf)
ISBN 978-952-60-4033-2 (printed)
ISSN-L 1799-4934
ISSN 1799-4942 (pdf)
ISSN 1799-4934 (printed)

Aalto Print
Helsinki 2011

The dissertation can be read at http://lib.tkk.fi/Diss/

Publication orders (printed book):
julkaisut@aalto.fi

Author
Kimmo Koivunen

Name of the doctoral dissertation
On the Refractive Index Contrast Modification in Paper and Printing Applications - Studies with Fillers and Coating Pigments

Publisher School of Chemical Technology

Unit Department of Forest Products Technology

Series Aalto University publication series DOCTORAL DISSERTATIONS 11/2011

Field of research Paper and Printing Technology

Manuscript submitted 23.04.2010 **Manuscript revised** 12.11.2010

Date of the defence 11.03.2011 **Language** English

☐ **Monograph** ☒ **Article dissertation (summary + original articles)**

Abstract

In papermaking, fillers are traditionally added to the fibrous stock to extend expensive fibre, to improve the paper surface uniformity enabling beneficial liquid interactions during printing, and to improve the light scattering coefficient of paper. It is advantageous, therefore, to introduce as much filler as possible. However, fillers also have negative effects on paper properties, such as weakening the paper by preventing the formation of fibre-fibre bonds, which limit their use. Accordingly, fillers must be optimised to achieve the best functionality at controlled dose.

One objective of the work is to improve paper optical properties, which could later promote more efficient use of materials in papermaking. Light scattering potential of fillers can be controlled by changes in the particle size distribution (PSD), specific surface area (SSA), shape, surface chemistry and refractive index (RI). Refractive index has received the least attention of these approaches. Therefore, novel fillers displaying increased effective refractive indices were developed. The results suggest that the methods studied can improve the light scattering effects.

Since there are difficulties deconvoluting the boundary refractive index contrast from particle size in complex paper composites, which were highlighted in the first part, a second objective of the work was to study the complementary situation of reducing RI contrast by introducing liquid into a porous paper coating. The liquid distribution was then monitored by reflectance measurements. Knowledge of absorption behaviour of liquids into paper is essential for the print quality and controllability of printing processes. A relationship could be established, normalised for porosity, describing the reflectance change as a function of saturation level.

In conclusion, the local change of refractive index boundary in a porous medium can be monitored indirectly via light scattering, or vice versa modified to affect scattering, and the opportunities for enhancing the function of filler-containing porous media can be identified. The combination of the publications and complementary results bound together in this work suggest that the methods studied provide potentially important new means to utilise RI contrast modification in papermaking and printing applications.

Keywords Paper optical properties, light scattering coefficient, refractive index, coating-liquid interaction

ISBN (printed) 978-952-60-4033-2 **ISBN (pdf)** 978-952-60-4034-9

ISSN-L 1799-4934 **ISSN (printed)** 1799-4934 **ISSN (pdf)** 1799-4942

Pages 100 **Location of publisher** Espoo **Location of printing** Helsinki **Year** 2011

The dissertation can be read at http://lib.tkk.fi/Diss/

A! Aalto-yliopisto

Tiivistelmä

Aalto-yliopisto, PL 11000, 00076 Aalto www.aalto.fi

Tekijä(t)
Kimmo Koivunen

Väitöskirjan nimi
Taitekerroinerojen modifioinnista paperi- ja painatussovelluksissa – tutkimuksia täyteaineilla ja päällystyspigmenteillä

Julkaisija Kemian tekniikan korkeakoulu

Yksikkö Puunjalostustekniikan laitos

Sarja Aalto-yliopiston julkaisusarja VÄITÖSKIRJAT 11/2011

Tutkimusala Paperi- ja painatustekniikka

Käsikirjoituksen pvm 23.04.2010 **Korjatun käsikirjoituksen pvm** 12.11.2010

Väitöspäivä 11.03.2011 **Kieli** Englanti

☐ **Monografia** ☒ **Yhdistelmäväitöskirja (yhteenveto-osa + erillisartikkelit)**

Tiivistelmä

Paperissa käytettävien täyteaineiden tarkoituksena on parantaa paperin optisia ominaisuuksia ja painettavuutta, sekä alentaa materiaalikustannuksia. Näistä syistä on edullista lisätä paperiin mahdollisimman paljon täyteainetta. Täyteaineiden negatiiviset vaikutukset mm. paperin lujuuteen kuitenkin rajoittavat mahdollisuuksia nostaa paperin täyteainepitoisuutta. Täyteaineiden ominaisuudet on optimoitava, jotta rajoitetulla pitoisuudella voitaisiin saavuttaa mahdollisimman kilpailukykyiset ominaisuusyhdistelmät.

Työn ensimmäisenä tavoitteena oli parantaa paperin optisia ominaisuuksia uudenlaisia täyteaineita kehittämällä. Täyteaineiden valonsirontapotentiaalia voidaan parantaa niiden partikkelikokojakaumaa, ominaispinta-alaa, muotoa, pintakemiaa tai taitekerrointa modifioimalla. Näistä lähestymistavoista taitekertoimen modifiointia on tutkittu toistaiseksi vähiten. Työssä kehitettiin uusia, korotetun taitekertoimen omaavia täyteainetyyppejä. Tulosten mukaan niiden avulla voidaan parantaa paperin optisia ominaisuuksia.

Taitekertoimen noston vaikutus valonsirontaan on kuitenkin haasteellista erottaa muista tekijöistä kuten partikkelien rakenteen vaikutuksesta monimutkaisissa pohjapaperimatriiseissa. Tästä syystä työn toisessa osassa tarkasteltiin nesteen absorptiota ja jakautumista säännöllisemmän rakenteen omaavassa pigmenttipäällysteessä ja tästä aiheutuvan taitekerroinkontrastin muutoksen vaikutusta päällysteen pinnasta mitattuun reflektanssiin. Tieto nesteiden absorptiokäyttäytymisestä paperissa on oleellista painojäljen laadun ja painatuksen kontrolloitavuuden kannalta. Työssä kehitettiin päällysteen pinnasta mitatun reflektanssin ja absorboituneen nestemäärän välistä riippuvuutta kuvaava empiirinen kaava.

Paikallisen taitekerroinkontrastin muutosta voidaan siis karakterisoida epäsuorasti valonsirontaan perustuvalla mittauksella, tai kääntäen, valonsirontaan voidaan vaikuttaa modifioimalla taitekerroinkontrastia. Tämä havainnollistaa mahdollisuuksia parantaa täyteainepitoisen (kuitu)matriisin optisia ominaisuuksia. Työn erillisartikkeleissa julkaistut tulokset sekä yhteenvedon täydentävä tulosmateriaali tarjoavat uusia potentiaalisia keinoja hyödyntää optisia taitekerroineroja paperi- ja painatussovelluksissa.

Avainsanat Paperin optiset ominaisuudet, valonsirontakerroin, taitekerroin, päällyste-neste -vuorovaikutus

ISBN (painettu) 978-952-60-4033-2 **ISBN (pdf)** 978-952-60-4034-9

ISSN-L 1799-4934 **ISSN (painettu)** 1799-4934 **ISSN (pdf)** 1799-4942

Sivumäärä 100 **Julkaisupaikka** Espoo **Painopaikka** Helsinki **Vuosi** 2011

Luettavissa verkossa osoitteessa http://lib.tkk.fi/Diss/

"I say that the blueness we see in the atmosphere is not intrinsic colour, but is caused by warm vapour evaporated in minute and insensible atoms on which the solar rays fall, rendering them luminous against the infinite darkness of the fiery sphere which lies beyond and includes it…"

Leonardo da Vinci ca. 1500 AD

FOREWORD

In 2004, the supervisor of this thesis, Professor Hannu Paulapuro suggested that I seize the opportunity to improve light scattering performance of paper by considering the idea of modifying the refractive indices of materials used in papermaking. Finally, in 2006, after multistage preparations including some successes and failures, we launched a three-year project called "Improvement of Optical Properties of Paper by Increasing Refractive Indices of Materials", abbreviated "Nanopap", together with our financers and research partners. I want to warmly thank Professor Paulapuro for giving the input for this interesting and important topic, and for his encouragement and support at every turn during the long process required to complete this work.

I am grateful to Professor Patrick Gane, Head of Research and Development, Omya Development AG, Oftringen, Switzerland, for being the Instructor of this thesis, during the last years in particular, and for giving me the great opportunity to work with him and his professional team after 2008. I want to express my deep gratitude to him for his constant guidance and support during our cooperation, and for offering me an interesting research topic under his supervision in the field of printing technology that simultaneously complemented my thesis topic. I am most indebted to him for being always available to provide his excellent guidelines in any matters considering my thesis substance.

I want also to thank Dr. John Husband (Imerys Minerals Ltd., Cornwall, UK) and Professor Kaarlo Niskanen (Mid Sweden University, Sundsvall, Sweden) for reviewing the manuscript.

Funding from Tekes (The Finnish Funding Agency for Technology and Innovation), supporting companies, and other financers involved in Nanopap and THEOS (Thermal Effects and Online Sensing) projects, as well as financial support from PaPSaT (International Doctoral Programme in Pulp and Paper Science and Technology) are gratefully acknowledged.

I have been privileged to work with esteemed authorities on optical physics and light scattering. I want to express my sincere thanks especially to Professor Kai-Erik Peiponen (University of Eastern Finland, Department of Physics and Mathematics, Joensuu), and Professor Emeritus Kari Lumme (University of Helsinki, Department of Physics).

I want to thank warmly all co-authors involved in the publications of this thesis.

Thanks are also due to my workmates at the Department of Forest Products Technology. I wish to thank Dr. Philip Gerstner for pleasant cooperation,

M.Sc. Heli Järvelä, who completed her Master´s Thesis during the Nanopap project, and Minna Mäenpää for preparing most of the handsheets for my thesis.

Thanks are also due to Anne Forsström, Anne Jääskeläinen, and the rest of the great team of PPPS08.

I acknowledge Dr. Cathy Ridgway, Omya Development AG, Oftringen, Switzerland, for providing help in the model coating preparation, and for conducting the mercury porosimetry analyses.

My former research colleague at TKK, Dr. Kari Koskenhely (now with AFT), deserves thanks for many relaxing discussions, and for his valuable advice and motivation in the beginning of my doctoral studies.

I wish to express special thanks to Professor Emeritus Richard J. Kerekes, Department of Chemical and Biological Engineering, The University of British Columbia, Vancouver, Canada, for many inspiring discussions regarding the scientific approach.

My parents did not have the opportunity to become doctors, but, when I was a kid, they worked hard in the industry. They wanted to do their work perfectly, which was not always easy, so that I could have a better starting point for my life than they had had. I want to thank my mother and father heartily for their endless support and faith in me, especially during those years when I was a young student.

Last but certainly not least, I want to thank you, dear Johanna, for being such a wonderful wife for me and caring mother for our little princess Pinja Olivia, our sunshine.

Kimmo Koivunen

ABBREVIATIONS

BET	Brunauer, Emmet, Teller (method for SSA determination)
CMS	Carboxymethylated Starch
DDA	Discrete Dipole Approximation
EDS	Energy Dispersive X-ray Spectroscopy
GCC	Ground Calcium Carbonate
NIR	Near-Infra-Red
MBF	Moving Belt Former
MCC	Modified Calcium Carbonate
MFS	Multifunction Spectrometer
PCC	Precipitated Calcium Carbonate
PM	Paper Machine
PMMA	Polymethyl Methacrylate
PSD	Particle Size Distribution
RBA	Relative Bonded Area
RI	Refractive Index
RT	Radiative Transfer
SSA	Specific Surface Area
TGA	Thermogravimetric Analysis
WFU	Wood-free Uncoated
XRD	X-ray Diffraction

LIST OF PUBLICATIONS

I. Koivunen, K., Niskanen, I., Peiponen, K.-E., and Paulapuro, H. (2009): Novel nanostructured PCC fillers. J. Mater. Sci. 44(2): 477-482.

II. Koivunen, K., and Paulapuro, H. (2010): Papermaking potential of novel structured PCC fillers with enhanced refractive index. TAPPI J. 9(1): 4-12.

III. Juuti, M., Koivunen, K., Silvennoinen, M., Paulapuro, H., and Peiponen, K.-E. (2009): Light scattering study from nanoparticle-coated pigments of paper. Colloids Surf. A. 352: 94-98.

IV. Koivunen, K., Alatalo, H., Silenius, P., and Paulapuro, H. (2010): Starch granules spot-coated with aluminum silicate particles and their use as fillers for papermaking. J. Mater. Sci. 45(12): 3184-3189.

V. Kuutti, L., Putkisto, K., Hyvärinen, S., Peltonen, S., Koivunen, K., Paulapuro, H., Tupala, J., Leskelä, M., Virtanen, T., Maunu, S.-L. (2010): Starch-hybrid fillers for paper. Nord. Pulp Pap. Res. J. 25(1): 114-123.

VI. Gane, P.A.C., and Koivunen, K. (2010): Relating liquid location as a function of contact time within a porous coating structure to optical reflectance. Transp. Porous Med. 84(3): 587-603.

VII. Koivunen, K., and Gane, P. A. C. (2010): Optical reflectance as a function of liquid contact time and penetration depth distribution in coatings with mono and discretely bimodal pore size distributions. Proceedings of the TAPPI 11th Advanced Coating Fundamentals Symposium, Munich, Germany, Tappi Press, Atlanta, pp. 108-128.

AUTHOR´S CONTRIBUTION

I. First version of the manuscript excluding the description of the multifunction spectrometer. Development of spot-coated PCC, design of experiments, fabrication of the filler samples, handsheet preparation and analyses.

II. First version of the manuscript, design of experiments, fabrication of the filler samples, handsheet analyses.

III. Preparation of the pigment samples, parts of the manuscript.

IV. First version of the manuscript, design and analysis of handsheet experiments.

V. Design and analysis of handsheet experiments, calendering, parts of the manuscript.

VI. All experiments, parts of the manuscript.

VII. All experiments, first author of the manuscript.

TABLE OF CONTENT

- Part I – Refractive Index in Paper Applications -

1 INTRODUCTION

In papermaking, fillers are mixed with the fibrous stock in the approach flow of the PM wet end to improve paper optical properties and printability, and to reduce costs. The filler, in the presence of chemical additives, is further subjected to interaction with the fibres and fines through various deposition and flocculation mechanisms. During the removal of the large excess of water in the sequential unit operations a paper web is formed, then finished, and finally customised in various converting or printing processes, for specific end-uses.

Paper produced in such a process displays an extremely heterogeneous three-dimensional composite structure. First of all, the fibrous material itself, forming the skeleton of the composite, and, hence, affecting the resulting formation in a fundamental manner, may exhibit a wide range of particle sizes, morphologies, and chemistries, affected by the wood species, the pulping process, and consequent process stages, including bleaching, refining, and screening. It is well-known that fines formed in refining of mechanical and chemical pulp display distinctive chemistries and morphologies (Luukko 1999, Page 1989) and contribute to paper structure in different ways. In some grades also recycled fibres are included, which further increases the raw material diversity, including additional ash, and even non-paper components.

Secondly, mineral fillers available for paper applications also exhibit a multitude of different sizes, size distributions, shapes, chemistries, hardnesses, and solubilities. Filler can deposit on the fibre surfaces as individual particles, or become retained in the dewatering sheet via filler-filler flocculation, or together with fibre fines. Filler can also occur as rigid clusters, and can be introduced as a component of various filler blends. Retention by these mechanisms can, therefore, take place through adsorption or filtration. The latter typically emphasised in the case of larger particles. Removal of water can result in uneven filler distribution throughout the paper thickness, *z*-direction. Deposition of filler on fibres finally affects the paper strength development through preventing the formation of interfibre bonding as the fibres are pulled together by Campbell (capillary) forces at the final stages of web consolidation.

It is evident that the paper composite, formed by packing dissimilar particles together without specific control of individual particles, displays heterogeneous interparticle pore structure. Pores, empty spaces filled with air, typically occupy the majority, for instance 70 %, (Gill 1991) of the total volume of the paper skeleton, providing bulk, interfaces for interaction between light and the particles, and a connected medium for liquid transport. Pores occur in the complicated random network around fibres, fibre crossings, and fillers. Pore size and shape is greatly affected by the fibre properties, such as thickness and flexibility. When flexibility of fibres is increased, for instance, by refining, or when thin fibres are used, smaller pores are formed (Niskanen *et al.* 1998,

Retulainen *et al.* 1998). Filler size, size distribution, and shape, also affect the resulting interparticle pore structure in a fundamental manner.

Coatings, applied on the paper surface by various means, exhibit higher uniformity, usually lower porosity, and lower permeability, than the base paper. In coatings, pigments are introduced as dispersed particles in the presence of dispersion agents, instead of the floc-like configuration presented by base paper filler. Furthermore, in coatings the pigments are bound to each other and the base paper by dissolved polymeric or dispersed particulate binders. Coatings enhance the smoothness, gloss and printability, reducing the print through and enhancing print evenness, by promoting more controlled ink spreading and penetration through absorption mechanisms of capillarity and permeability, fixing the ink onto or in the surface structure of the coating in a controlled manner. Considering the instant when the liquid phase of the printing ink vehicle is contacted with the coating surface, i.e. at short timescales around nanoseconds, the liquid is wicked into the finest pores in an accelerating manner. These fine pores in initial contact are filled in practice before the retarding effect, caused by the viscous factors, becomes established, impacting in turn on observations at longer timescales. Inertial forces, as described in the models by Szekely *et al*. (1971) and Bosanquet (1923), simultaneously with the fine pore filling regime, retard the filling of the larger pores within short timescales, which are, hence, only filled at a distance behind the wetting front. With longer contact times, the filling of larger pores is completed, and the point of saturation gradually gains on the wetting front (Schoelkopf *et al.,* 2000a, b, 2003a, b, Gane *et al.* 2004).

Coatings also affect the electrical and thermal properties essential for toner transfer and fusing, in electrophotographic printing, respectively, and during ink drying in heatset web offset, as well as in converting processes, such as binding and gluing. An important function of coating is to further improve the paper optical properties, especially brightness and opacity. Coating pigments are typically finer than fillers and hence behave differently in terms of light interaction, creating many more light interacting pores within the coating structure. In coatings, some variation in the coating pore sizes is desired for printing, as liquid is most efficiently driven into coating structures displaying sufficient connectivity between fine capillaries and larger pores (Schoelkopf *et al.* 2000a, b, Gane *et al*. 2004, Ridgway *et. al.* 2006a). On the other hand, for optimising light scattering, the pore size regime needs to be more monodisperse. To maximise paper light scattering effects, therefore, much effort has to be focused on defining the particle size distribution, particle shape, and packing of pigments, and resulting interparticle pore structure.

Light propagation in paper follows that of a random medium, in which the interparticle distances vary. As light interacts with the heterogeneous network of base paper or coating, part of it is usually reflected as specular or mirror reflection, while the rest partially scatters diffusely from the surface, and partially propagates into the network in which additional diffuse light scattering effects take place, depending on the interparticle dimensions, distances, and

refractive index (RI) contrasts. These effects are of fundamental importance for the development of paper appearance, its brightness and opacity.

On the contrary to the random refractive index nature of paper and coating structure in respect to the arrangement of materials and their respective pores, the majority of the materials themselves, i.e. fibres, fines, fillers, coating pigments and binders, display similar optical refractive indices. This essentially limits the generation of light scattering at contact points between the materials, as light is exclusively scattered at interfaces with RI gradients. Thus, the limitation of scattering power from paper is given by the availability and arrangement of pores. The focus of the first part of this work has, therefore, been on increasing the refractive index contrasts to improve paper optical properties.

As predicted by current scattering theory, based on the considerations of the Mie scattering treatment (Mie 1908), valid for single spherical isotropic particles with no limitations in size, light scattering is most sensitive to changes in RI when the size of spherical particles is around half light wavelength. In this scale, light scattering effects, including reflection and refraction, are magnified by diffraction phenomena. With particles much smaller than the wavelength, the light scattering effects become significantly less intense, and the complexity of the Mie theory can be reduced to the more approximate treatment of Rayleigh scattering theory (Lord Rayleigh 1871). In the case of larger particles, such as fibres, light scattering is moderate, and dominated by refraction and reflection effects obeying laws of geometrical optics, such as described by Snell and Fresnel. RI contrasts, therefore, can be most efficiently increased by employing the light scattering potential of high refractive index fine particles. Therefore, it was considered beneficial to introduce fine, mono-sized high-RI particles into the paper structure. In coatings, the most convenient way to increase paper light scattering is to optimise coating structure (Gane 2001), where fine particles are beneficially dispersed and packed. In uncoated grades, however, such as woodfree uncoated (WFU), fillers play an exclusive role.

Low retention limits the use of fine, optically effective particles as fillers in the base paper. Fine fillers must be flocculated to larger structures to achieve sufficient retention. In homogeneous flocs of a single filler type, and consequently single RI, light scattering is, however, reduced (Pummer 1973, Alince & Lepoutre 1983, Alince 1986). Due to lack of interparticle RI differences in such flocs, limited contacts displaying interparticle distances around half the wavelength would be more beneficial. This has contributed to the emergence of various aggregated fillers, such as clustered PCC and calcined clay.

In view of the background discussed above, the thesis objectives can now be condensed as follows:

OBJECTIVE 1) is to improve the paper optical properties, especially diffuse reflectance through enhanced light scattering effects. The primary approach to achieve this is by incorporating RI contrast-enhancing agents into the base paper structure.

The first hypothesis is that filler(s) can be used as platforms for the RI contrast-enhancing agents in new ways in order to achieve the above-mentioned objective, i.e. increased light scattering by increasing refractive index gradient at the filler surface. The study is focused on finding new filler concept(s) rather than examining existing solutions. The approach a) includes:

a) Development of a new PCC filler displaying effective RI increased by incorporation of RI-enhancing additives or particles other than titanium dioxide (TiO_2)

   Background: simple blending of high-RI pigments in paper stock with regular filler is not considered an efficient solution with regard to light interaction. For instance, TiO_2, displaying exceptionally high refractive indices and light scattering potential, typically increases material costs and promotes wire abrasion. With high dosages, it tends to display reduction in the scattering efficiency through optical crowding. A lot of work has been, and continues to be, done with TiO_2, to improve optical properties of other materials, and to improve the optical efficiency of TiO_2 itself. However, an alternative approach is sought here by seeking to enhance the refractive index contrast boundary on the surface of typical low cost filler.

Organic fillers have advantages over traditional fillers, including low weight, low abrasivity, and combustability.

The second hypothesis is that organic filler particles can be utilised in novel ways with other materials to achieve Objective 1.

The third hypothesis is that Objective 1 can be achieved by modifying the refractive indices of organic bulk filler particles. The approach b), regarding the hypotheses II and III, includes:

b) Contribution to the development of new organic fillers with effective RI and light scattering properties.

   Background: Previous studies have covered utilisation of starch as a raw material for organic pigments.

Composite and aggregate filler structures are complex to define in terms of their convoluted properties of particulate size, internal void size and refractive index distribution. The importance of RI contrast, therefore, has further been

demonstrated in isolation in the second part, dealing with liquid absorption into a well-defined porous medium in the form of paper coating structures, representing the situation also during printing, detected with optical reflectance measurements.

OBJECTIVE 2) is to utilise RI contrast modification taking place at the pigment-pore and binder-pore interfaces within a paper coating due to liquid absorption, to establish the relationship between reflectance change and location of liquid absorbed into the porous structure. The information is considered to be useful in supporting current theoretical modelling of differential liquid distribution in porous networks, and for developing optical tools with the potential of providing real-time information about the dynamics of liquid absorption into porous paper coatings during printing.

The fourth hypothesis is that liquid distribution in the coating structure can be characterised by optical reflectance measurements. As air in the coating pores is replaced by a liquid displaying higher RI than air, RI gradient at the interface is reduced, i.e. the complementary case of enhanced scatter in Objective 1). This effect should be observable through reflectance measurements if at least part of the coating pore structure displays a size which is effective in terms of light interaction.

Previous studies (Schoelkopf *et al.,* 2000a, b, 2003a, b, Gane *et al.* 2004) have shown that with long timescales, after contacting the coating surface with the liquid phase of the printing ink vehicle, the point of saturation gradually gains on the initially rapidly propagating wetting front by filling the remaining air-filled pore structure. This increases the concentration gradient at the proximity of the furthermost point of the wetting front.

The fifth hypothesis is, therefore, that while filling of the finest pores with size around the Bosanquet inertially-defined optimum at short timescales (defined as < 100 nm by Schoelkopf *et al.* (2002) and Gane (2006)) results in zero to moderate effect in reflectance, more significant reduction can be observed with longer contact times due to filling of larger pores displaying size effective for light interaction. If observed, this phenomenon will be utilised to achieve Objective 2 and support the complementary first hypothesis.

> **Background:** Knowledge of *z*-directional liquid distribution plays a key role in print quality development, and control of printing processes.

2 INTERACTION BETWEEN LIGHT AND PAPER

2.1 General

Snell´s law (Equation 1), and the Fresnel equations (2) representing geometrical optics as applied to refraction and specular reflection, respectively, can be used as simple examples to illustrate the importance of RI contrast in cases where the particle dimensions exceed the wavelength of the illumination.

$$n_1 \sin\Theta_1 = n_2 \sin\Theta_2 \tag{1}$$

where n_1 and n_2 represent the refractive indices of the two media as presented in Fig. 1.

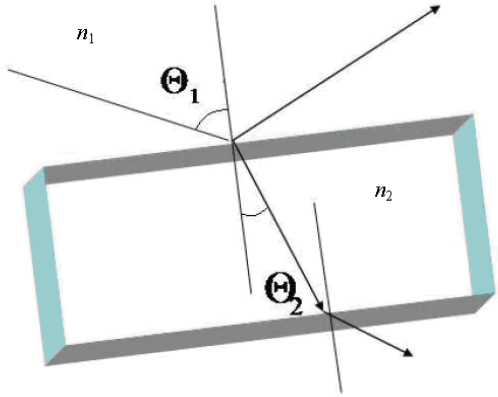

Fig. 1. Interaction between light and transparent material. A ray-optical illustration. Adapted from Publication II.

$$R_s = \left[\frac{n_1\cos(\Theta_1) - n_2\cos(\Theta_2)}{n_1\cos(\Theta_1) + n_2\cos(\Theta_2)}\right]^2$$

$$R_p = \left[\frac{n_1\cos(\Theta_2) - n_2\cos(\Theta_1)}{n_1\cos(\Theta_2) + n_2\cos(\Theta_1)}\right]^2 \tag{2}$$

where R_s and R_p are the reflection coefficients for light polarized in two planes, *s* perpendicular to the surface and *p* parallel to the surface plane. The Fresnel equations are valid for smooth surfaces. In practice, roughness reduces specular reflection and increases diffuse light scattering.

Scallan & Borch (1976) suggest that scattering from pulp fibres can be considered to be of the Fresnel type.

Paper optical properties are typically measured determining reflectance (Leskelä 1998, Pauler 1998). Reflectance from an illuminated object is, in practice, the ratio between reflected and incident light intensities. Brightness ($R457$) is diffuse reflectance measured from a stack of sheets with an effective wavelength of 457 nm. Opacity is a diffuse reflectance from a single sheet with black background divided by the intrinsic reflectance factor (Pauler 1998). Gloss is specular reflectance. Measurement details in each case depend on the standard used (Pauler 1998).

Diffuse reflectance can be utilised to calculate light scattering and absorption coefficients of paper, S and K, respectively, using a widely-used theory established by Kubelka and Munk in the 1930s (Kubelka & Munk, 1931). The theory is a simple approximation based on the radiative transfer (RT) approach, following the principles of geometrical optics, and is hence exact only in the case of systems displaying dimensions greater than the wavelength of light. In spite of this, it has been a popular means to describe light scattering properties of paper, as it has been considered to provide sufficient approximation in the practical papermaking environment. S and K are material related parameters describing the loss of intensity of a light stream travelling through paper per unit basis weight unit due to scattering and absorption, respectively. In the theory, paper is considered as a homogeneous material. Therefore, it cannot be used to predict the effects of or structural changes due to, for instance, filler particle size. It also fully ignores the interparticle discontinuity induced by air-filled pores.

Later, in the 1970s, Scallan and Borch presented a theory presenting paper as a stacked structure consisting of layers displaying specific transmittance and absorbance (Scallan & Borch 1972, Scallan & Borch 1974). In contrast to the K-M theory, the model includes the effect of sheet structure, as it presents paper as a stack of alternating (fibrous) layers of solid material and air. The number of layers is evaluated through specific surface area (SSA) measurements. However, the theory is based on the radiative approach as well, presenting the discrete form of the formulation, and must also be considered as an indicative method.

Both the Kubelka-Munk and Scallan-Borch approaches use Stokes' equations (Stokes 1860) to account for multilayer effects.

Leskelä (1997) has proposed an extension to the theory based on the Scallan and Borch approach, providing the link between particle properties and paper

optical properties using the void probability parameter. The model, for instance, enables the effect of particles with differing refractive indices to be examined.

All in all, light scattering effects are complex phenomena, and particularly so when considering how light interacts with porous material. In these three-dimensional networks, with their multitude of solid-air interfaces displaying refractive index differences, reflection, refraction and diffraction effects, the problem becomes virtually intractable if resolved into individual interactions. While reflection and refraction, following the laws of geometrical optics, are generally encountered in the case of individual macroscopic particles displaying a RI boundary gradient to the surrounding medium, diffraction as well as interference effects arising from interaction between closely located particles take place exclusively in small-scale structures exhibiting dimensions around the wavelength of light (Pauler 1998), such as in a base paper matrix or coating layer. Therefore, to be exact, a rigorous wave-optical approach, such as provided by Maxwell´s equations (Maxwell 1865) should be considered in paper applications instead of treatments based on geometrical optics.

A solution to Maxwell equations, covering scattering from single spherical isotropic particles, is provided by so called Mie theory (Mie 1908). However, due to the extremely complex interaction phenomena between closely located particles, it is hard to apply the exact multiple scattering approach in systems such as paper coating, although the computing power provided by modern supercomputers has brought this method partially within reach. As a shortcut, therefore, it has been usual to calculate the scattering from a single particle first according to the Mie treatment, and then expand the result to the multiple scattering environment through various radiative transfer (RT) approximations (Leskelä 1997).

One such example is the extended use of the Mie theory for coatings with low pigment concentration. The Mie theory can be strictly considered only if particles are located apart enough to scatter incident light only, and not multiply scattered light. In typical paper coatings, however, scattering from neighbouring particles due to high particle packing density regularly occurs, and one must account for these multiple scattering effects. Ross (1971) has found, that the scattering coefficient measured from coating displaying 8 % volume concentration is about two thirds of the scattering coefficient calculated by Equation (3)

$$S = 0.75(1-\cos\Theta)\cdot Q_{sca}\cdot(1.5/D)\cdot P \tag{3}$$

where

D	is the particle diameter
Q_{sca}	is the Mie scattering efficiency (depends on refractive index)
$(1-\cos\Theta)$	is asymmetry parameter of sphere (depends on refractive index)
P	is the pigment volume concentration

Also this equation is based on the RT approach (Borch & Lepoutre 1978), and so does not fully match with the measured values. As further suggested by Borch & Lepoutre (1978), in coatings displaying a volume concentration of 74 %, a more typical value in real paper coatings, the calculated values can be roughly ten times greater than the measured values. Importantly, both calculated and measured values suggest that maximum light scattering occurs when adopting particles displaying a size around half the wavelength of light. Furthermore, the effect of RI change on light scattering is the most significant with this particle size category (Borch & Lepoutre 1978). Hence, when considering the approach of increasing the light scattering effects in paper through RI modification, attention should be paid to fine fillers and pigments rather than fibres.

2.2 Contribution from fillers

Paper formed using beaten chemical pulp as the only raw material can have superior strength induced by the high degree of bonding, typically characterised by high relative bonded area (RBA), while its optical and printability properties are often not satisfactory for graphical applications. RBA controls the paper optical properties, and is hence traditionally determined with light scattering measurements (Ingmanson & Thode 1959). Fibre-fibre bonding in paper is closely related to the occurrence of solid-solid and solid-air interfaces, and, furthermore, to paper optical properties. According to Hemstock (1962), introduction of fillers affect light scattering through two mechanisms. Firstly, by increasing the specific surface area and, secondly, by preventing bonding between fibres. Both effects are related to the consequent emergence of RI gradients with regard to air.

Alince & Lepoutre (1985) have demonstrated the separation of SSA increase and debonding, and proposed that the role of fibre debonding in light scattering decreases as the refractive index of the filler increases.

As described by the current scattering theory based on the Mie solution, light scattering from pigment depends on the scattering cross-section, which is a function of pigment particle size in relation to the refractive index gradient at the particle interface. The RI gradient, in turn, depends on the intrinsic refractive index, or, in the case of birefringent materials, refractive indices of the pigment particle itself, and the medium surrounding the pigment. In paper applications, the relative distribution of other filler particles, fibres, fines, binders, moisture, and air-filled pores, define the RI of the surrounding medium.
With regard to maximum light scattering, this medium is beneficially air (RI 1.0), providing relatively high RI gradient at material boundaries.

The explanation of the RI of a material is described by Equation (4) (Feynman *et al.* 1964)

$$n = 1 + \frac{N{q_e}^2}{2\varepsilon_0 m\left({\omega_0}^2 - \omega^2\right)} \tag{4}$$

where

n is the refractive index
N is the number of charges per unit volume
q_e is the charge of an electron
ε_0 is the permittivity of vacuum
m is the mass of an electron
ω is the angular frequency of radiation
ω_0 is the resonant frequency of an electron

RI (n) decreases with increasing light wavelength (or decreasing frequency). This phenomenon, called optical dispersion, can be observed as rainbow colours developed in the passage of light through a prism. According to Equation (4), short wavelengths are refracted more than long wavelengths. Therefore, well-defined wavelengths are used when reporting RI values. Typically reported RIs correspond to the value corresponding to the spectral centre of yellow sodium emission, at the wavelength of 589.29 nm. More specific descriptions of the refractive index of a medium can be found in the literature (Feynman *et al.* 1964, Peiponen *et al.* 1999).

Due to the heterogeneous distribution and positioning of filler in paper, however, not all filler particles contribute to the scattering of light. In the fibrous matrix, filler can be located in interfibre pores, or on fibre surfaces between adjacent fibres displaying either closely sandwiched, inlaid position between fibres, or, more typically, expansive alignment resulting in interfibre disruption (Weigl *et al.* 1981). The fibres and filler particles typically display similar RI, and hence, do not provide significant RI gradients when contacted. RI for cellulose and lignin are 1.56 and 1.61, respectively (Scallan & Borch 1972, Giertz 1951). Of the various positions, therefore, the inlaid filler position is optically the least effective. To maximise interaction with light, filler should rather display limited contacting with regard to the adjacent particles, exhibiting sufficient air-filled interparticle spacing. In fact, light scattering of paper can be estimated considering the pores as light scattering bodies (Borch & Lepoutre 1978), rather than the matrix of solid material. Phenomenological understanding of the role of pores as light scattering bodies is especially important in the case of dense structures such as calendered papers or coatings (Bown 1997a). In base papers exhibiting open sheet structures, i.e. low density, such as uncalendered paper, light scattering is more dominantly controlled by the particles distributed within the structure (Bown 1997a).

Besides calendering, the pore structure is affected by other process parameters, such as wet-end chemistry, wet-pressing and drying, and further by material parameters including fibre properties (Niskanen *et al.* 1998, Retulainen *et al.*

1998), filler content, and filler properties, such as particle size distribution (PSD) and specific surface area (SSA). In addition, particle shape affects packing behaviour (Hagemeyer 1960). Considering particle packing with regard to the pore structure, as suggested by Bown (1997a, 1997b), the particle size should be considered together with size distribution, density, and aggregate properties. A broad particle size distribution results in closer packing, i.e. finer interparticle pores (Husband & Nutbeem 2001). Much work has been done to tailor the PSD of pigments. With spherical particles, size around half the wavelength of light, as discussed previously, and narrow size distribution, are beneficial (Borch & Lepoutre 1978). The optimum size, however, depends on the particle shape and RI - the higher the refractive index, the smaller is the optimum particle size (Penttilä & Lumme, 2004). Similarly, optimal pore size, for instance, in kaolin and calcium carbonate coatings, is around 0.15 μm – 0.30 μm (Climpson & Taylor 1976). Smaller pores (or particles) are not beneficial for light scattering (Rennel 1969, Alince 1986, Pauler 1998). Work done by Alince *et al.* (2002) suggests that when all pores display optimal size, and all particles have similar refractive indices, a linear dependence between light scattering and the internal surface provided by the pores can be found. Silenius (2002) demonstrates that filler-fibre composites can be utilised to boost the light scattering effect of filled sheets through even filler distribution resulting in advantageous pore structure.

Typical mineral fillers used in paper applications, display monotonous RI around 1.5-1.6. These include ground and precipitated calcium carbonate (GCC and PCC, respectively), kaolin clay, and talc, of which PCC is the most important, displaying 39 % share in 2004 (Laufmann 2006). The predominance of PCC as filler is based on the bulking properties it delivers to uncoated woodfree copy grades and the ability to produce on-site in cases where long haul land transport otherwise makes alternatives uneconomical. In addition speciality pigments displaying either light scattering voidage, such as calcined clay and structured PCC, or higher RI, such as titanium dioxide, synthetic silicas and silicates, and some organic pigments, displaying a greater particle number per unit weight addition, can be used. Today, however, only few speciality pigments display higher RI. Titanium dioxide (TiO_2) displays spherical shape and exceptionally high refractive index (RI 2.55-2.76 for anatase and rutile, respectively) (Laufmann 2006). Its particle size is typically close to the optimal. Its drawbacks are, however, high price and abrasivity, and its optical efficiency is dramatically reduced due to particle crowding.

As part of the light scattering arising from filler use is based on debonding (Hemstock 1962), one of the drawbacks of filler is decreased paper strength. Therefore, a common and useful way to obtain indication about papermaking potential of a specific filler is to plot the light scattering coefficient of the sheet as a function of strength (Alince 1989). Even, dispersed filler distribution usually contributes most to light scattering, and, hence, increases debonding. Low filler retention of dispersed fillers has negative impacts on the papermaking process, such as abrasion of wires and sizing agent consumption, as well as poor formation. Hence, to ensure sufficient development of

mechanical properties of paper, and runnability of the paper machine, as discussed for retention, fillers are typically introduced to paper as flocs.

Flocs can be formed between filler particles only (homoflocculation) (Holm & Manner 2001, Porubska *et al.* 2002) or together with fines (heteroflocculation) (Gavelin 1998). According to Holm & Manner, pre-flocculation leads to an improved strength at the expense of optical properties (2001). In addition, it is known that the scattering efficiency of filler decreases as the filler content in paper increases. This has often been explained by the crowding effect (Starr & Young, 1976, Alince & Lepoutre 1985, Howard 1983). Middleton *et al.* (1994) have suggested that this is because the filler particles are deposited randomly, a reference primarily to heteroflocculation.

Filler type and size affect the degree of strength reduction. Several studies (Bown 1997a, Adams 1993, Gill 1990, Papp 1989, Han & Seo, 1997, Fairchild 1992) indicate that small particles are more detrimental for paper strength. Coarse particles with narrow size distribution yield comparatively high strength. Filler selection is naturally case-dependent. If runnability and high filler content are preferred, coarse particles with narrow size distribution should be used, whereas fine pigments are more beneficial for optical properties (McLain & Wygant 2006).

We have seen from this summary of the interactive properties of fillers and fibres in the paper matrix and during the formation of paper itself, that most of the tools available for optimising light scattering are already regularly employed. The remaining variable arising out of the discussion is RI, provided it can be adjusted economically. Several studies regarding hollow pigments have been reported (for instance Enomae & Tsujino (2004), Walsh & Mann (1995), Hadiko *et al.* (2005), Bourlinos *et al.* (2001), Nelson (2007)). Hollow pigments display, in addition to the RI gradient with regard to the surrounding medium at the particle surface, an additional intraparticle RI gradient interface with regard to the medium filling the hollow space. Some studies have been conducted to increase RI of $CaCO_3$ by surface coating with another material (see for instance Lattaud *et al.* 2006). This limited work indicates that there are many practical obstacles to achieving a working system and product.

In contrast to many other materials, TiO_2 has been widely studied as an RI increasing additive, and applied to modify the optical properties of pigments such as silica (Hsu *et al.* 1993, Demirors *et al.* 2010) and other colloidal particles (Demirors *et al.* 2010). In the latter study, the process presented earlier by Eiden-Assmann *et al.* (2004) was further modified to introduce an amorphous TiO_2 layer with modifiable thickness on colloidal particles of silica, silver, gibbsite, and polystyrene, in a controlled manner. The advantage of coating materials with a TiO_2 shell is that cheaper material than TiO_2 can be used in the core, while the optical properties of the resulting composite are largely determined by the optically effective TiO_2 shell (Hsu *et al.* 1993). This is an especially important aspect in paper applications where attention must be paid to material costs. For the same reason, there is a need to develop further

the properties of TiO_2 itself, by providing new morphological features for anatase and rutile. Nelson (2007) has investigated modified TiO_2 grades designed to display improved interaction with light and fibrous components in paper applications. In this work by Nelson, polycrystalline TiO_2 nanoparticles showed advantages in optical properties over a commercial rutile based reference.

The results of the above-mentioned studies, included here as examples, show that TiO_2 based modification can be utilised to achieve structures with enhanced performance when contrasted with corresponding unmodified materials. Although from a reaction kinetics point of view it has been challenging to control the growth of TiO_2 coatings on core materials, additives have been found to be beneficial in controlling the reaction rate (Eiden-Assmann *et al.* 2004, Demirors *et al.* 2010).

All in all, while the prior art RI research has been much focused on TiO_2 modification, alternative materials, with for instance lower abrasivity, have been less examined. This is the challenge taken up here in moving on to investigate ways to achieve Objective 1.

3 DEVELOPING SPOT-COATED PCC WITH INCREASED EFFECTIVE REFRACTIVE INDEX

3.1 Background

Precipitated calcium carbonate, PCC, is a synthetic pigment, typically produced through carbonation by reacting calcium hydroxide, or slaked lime, with carbon dioxide gas. The crystal form as well as morphology of PCC can be tailored by controlling precipitation conditions. These can include supersaturation (see for instance Silenius 2002), or the use of crystal habit modifiers, such as certain sugars to promote growth of certain crystal facets whilst suppressing others (Agnihotri *et al.* 1999). Some examples on utilising additional ions or polymers to improve the functionality of PCC, including optical properties and acid resistance, for instance, have also been reported (Kim *et al.* 2005, Baumeister & Hofmann 1980, Suhara *et al.* 1983, Fujiwara *et al.* 1987, Yakushiji *et al.* 1993, Buijnsters *et al.* 2001, Jaakkola & Manner 2001, Hatakeyama *et al.* 2005). Xyla *et al.* (1991) have suggested that orthophosphates, oxalates, Cd^{2+}, and Zn^{2+} affect the crystal growth through adsorption on the crystal surfaces. However, information about the effects of such process additives on the RI development of the resulting PCC particles has been lacking.

Industrially produced crystal forms of PCC include calcite and aragonite. Calcite can be crystallised in rhombohedral, prismatic, colloidal, spherical, scalenohedral and clustered scalenohedral mophologies. Aragonite is needle-like, and can occur in both separate and clustered configurations (Gane 2001).

RIs for calcite and aragonite are 1.58 and 1.63, respectively (Lide 1990). The difference in RI is due to distinct atom coordination. In calcite, each calcium atom is coordinated by six oxygen atoms. In contrast, the aragonitic calcium displays more dense atomic packing, induced by coordination with nine oxygen atoms (Merrill & Bassett 1975). For calcium carbonates, the size of the cation has significant impact on the resulting crystal form. Preferred crystal form is moved from calcite to aragonite when cation size exceeds 1.1 Å (= 0.11 nm). The dimorphous nature of calcium carbonate is partly due to size of the calcium ion, which is around this value (Evans 1954), and partly due to the possible presence of hydrated water. The atomic configuration determines the space available for hydrated water in the crystal. Passe-Coutrin *et al.* (1995) have demonstrated the effect of water of hydration on aragonite-calcite phase transition in coral and mineral based aragonite samples.

3.2 Materials and Methods

To build versatile data based on both practical experimentation and modelling, the studies were conducted in three stages:

1) *Measurement of light scattering using particulate RI modifiers*. Tablets were compressed from blends of standard PCC and nano-sized particles of ZnS and Al-silicate, and light scattering was measured from the tablets using ellipsometry.
2) *Effect of soluble metal salts, acting as RI modifying agents*. Soluble metal salts were added in the conventional PCC fabrication process, and their effects on RI, structure, and papermaking potential of PCC were studied.
3) *Computer modelling*. Light scattering from selected PCC samples obtained in stage 2) was studied by computer modelling, applying the wave-optical Discrete Dipole Approximation (DDA) approach, namely the ADDA code (Draine & Flatau 1994, Yurkin *et al.* 2007), and the RT-based SCIAPOL code (Rozanov & Kokhanovsky 2006) for the single aggregates, and the model coating consisting of several aggregates, respectively.

In the first stage, the purpose was to examine the relevance of the approach of introducing particulate RI modifiers on the PCC surface. The potential of this approach was evaluated by examination of light scattering from tablets compressed from blends of standard PCC and various nanoparticles using ellipsometry. Dry standard PCC powder (S-PCC, described below) was mixed either with commercial ZnS[1] or Al-silicate[2] nano-sized particles, displaying average (primary) particle size around 80 nm and 30 nm, respectively, estimated from SEM micrographs such as presented in the Results section (Fig. 2). The mixing was done in 0.2 dm^3 deionised water by stirring vigorously with a Diaf mixer to obtain samples with 10 w-% and 18 w-% nanoparticle content. Mixing was continued for 15 minutes, during which the particles were self-assembled without being subject to additional chemicals. The resulting blend slurry was dried and pulverised in a mortar, pressed to tablets, and the light scattering from the tablet surfaces was analysed using an ellipsometer as described in Publication III.

In the second stage, PCC samples were fabricated in batches by carbonation using a cylindrical reactor (5.0 dm^3) supplied with thermo-element casings, centrifugal impeller mixer, a rotameter-controlled gas flow system for feeding CO_2 gas, and sensors for controlling pH and temperature.

Powder calcium hydroxide (50 g -100 g), from J. T. Baker, was mixed in deionised water (2.0 dm^3) together with the dissolved additive, and added into the reactor. Pro analysis grades of $ZnCl_2$, $SrCl_2$, $Sr(NO_3)_2$, $BaCl_2$, $MgCl_2$, KCl, KBr, and NaCl, were used as RI modifying additives. M/Ca mol ratios around 0.10 - 0.25 were used, where M stands for the additive cation.

A reference PCC, referred to as "S-PCC", with clustered calcitic scalenohedral (rosette-like) particle morphology, and several modified PCC samples ("Nano-

[1] Sachtolith L, a product name of Sachtleben Chemie GmbH.
[2] Hydrex P, a product name of J. M. Huber Corporation.

S-PCC") were then prepared. Formation of calcium carbonate in the carbonation stage takes place according to Equation (5):

$$Ca(OH)_2 + CO_2 \rightarrow CaCO_3 + H_2O \quad (5)$$

Initial pH of carbonation was around 12.5. Carbon dioxide gas was fed during mixing until pH dropped to 7. Mixing was continued for some time (e.g. 15 minutes) to stabilise pH to about 8.5. The resulting pigment was filtered with a glass filter (grade 4, used for fine precipitates), washed with deionised water, dried at 105 °C, and pulverised in a mortar.

The samples were characterised in detail. An Hitachi S-3400N VP-SEM (Variable Pressure SEM) was used to study the sample morphologies. Quantitative EDS (Energy Dispersive X-ray Spectroscopy) analysis was performed to determine the realised average additive content. This was done using the NSS202E-EDS system (Thermo Electron) with the SEM. Micromeritics FlowSorp II 2300 analyser was used for SSA. The SSA measurements were made in accordance with the BET (Brunauer-Emmet-Teller) theory (Brunauer *et. al.* 1938) covering adsorption of gas molecules on a surface. A Philips PW1710 diffractometer was used to analyse X-ray diffraction patterns (XRD), using CuKα radiation. A Netzsch STA 449C device, combined with a capillary to Netzsch QMS 403C mass spectrometer was used to conduct thermal gravimetric analyses (TGA).

Refractive indices were measured using a multi-function spectrometer MFS. In the method, pigment (about 0.50 g) is mixed with an immersion liquid (15 cm^3) with known refractive index, consequently illuminated with a xenon lamp, and the backscattering intensity is then recorded. The measurement wavelength and the temperature were 589.6 nm and 22 °C, respectively. As immersion liquids, mixtures of acetone-methylene iodide with a range of refractive indices from 1.54 to 1.73, displaying 0.01-0.05 intervals, were used. A graph was then plotted, presenting backscattering intensity as a function of immersion liquid RI. The best match between the RIs of the liquid and the sample is at the point of minimum backscattering intensity. A more detailed technical description of the MFS can be found in the literature (Niskanen *et al.* 2006).

Particle size distributions (PSD) of the fillers were determined with a Beckman Coulter LS 13 320 particle size analyser, the function of which is based on the current light scattering theory. The samples were dispersed by magnetic stirrer in 0.1 % sodium hexametaphosphate solution, which was further dosed into the water-filled liquid module of the analyser. Ultrasound treatment was applied in the water-filled module prior to the measurements, and the throughput was set to around 50 % of the maximum to avoid the formation of air bubbles. It is recognised that the Coulter method depends strongly on the scattering cross section of the material particulates. Since in this study the particulates are agglomerates, containing solid material and air, and furthermore have contrasting RI surfaces, the scattering cross section is too complex to define systematically. In this respect, an average parameter approach is adopted, which

reveals a relative particle size distribution without specific reference to the changes of RI contrast generated by the sample design. Whilst this is unsatisfactory as an absolute measure of the particle size, it can be correlated with scanning electron microscopy (SEM), and the correlation was found to be reasonable.

An indicative handsheet test series with the standard sheet mould was conducted using some of the novel fillers, as described in Publication I.

For more specific evaluation of the papermaking potential of the fillers, in particular the fillers displaying more moderate degree of modification, the papermaking process was simulated under laboratory conditions using a Moving Belt Former (MBF) sheet forming apparatus, described by Räisänen (1998), and subsequent calendering tests.

Birch and pine chemical pulp sheets from Finnish pulp mills were mixed to achieve 70/30 birch/pine fine paper, or Wood-Free-Uncoated, WFU, furnish. The furnish was beaten in a Valley Hollander to °SR 18 in accordance with the Standard SCAN-C 25:76 and further diluted to 3 gdm^{-3} consistency for handsheet preparation.

Dry-strength starch (Raisamyl 50021) was cooked in water at 95 °C for 25 minutes prior to handsheet preparation. Fennopol K 3400R was used as a retention agent. 80 gm^{-2} handsheets were prepared with the MBF. The fibrous stock was first added into the MBF container. Additives were then introduced as presented in Table I. The procedure was to mimic the wet end operations as might be found in practice in a typical paper machine environment. The stock in the container was continuously mixed.

Target filler contents of the handsheets were 15 w-%, 25 w-%, and 35 w-%, with ±1.5 w-% unit deviation, determined by the increase of the dry weight of the sheet due to the addition of filler. The sheets were wet-pressed and drum-dried, further stored in accordance with the Standard SCAN-P 2:75. Sheets were calendered through a single nip on an EP-210 laboratory calender using 70 kNm^{-1} line load, 70 °C hot roll surface temperature, and 35 $m.min^{-1}$ speed. The sheets were tested adopting Standard Methods. The sheets were also examined with EDS (NSS202E-EDS, Thermo Electron) to confirm that the additives had retained.

Specific pore volume and pore size distribution of selected handsheets (including both uncalendered and calendered sheets) were analysed by mercury porosimetry using an Autopore IV porosimeter (Micromeritics), and corrected with Pore-Comp[1] software to account for mercury and penetrometer effects, as well as sample skeleton compression applying the equation given by Gane *et al.* (1996).

[1] Pore-Comp is a program software name of the Porous Media Research Group at the University of Plymouth, U.K.

Table I. Introduction of additives in the MBF experiments. Adapted from Publication II.

Component	Point of addition, s *	Dosage, $mg \cdot g^{-1}$
Starch	11	5
Filler	30	Determined by target filler content
Retention aid	40	0.2

** the delay after the addition of the fibrous stock*

In the third stage, light scattering from the PCC aggregates, modified with $ZnCl_2$ in stage 2, was examined by computer modelling. In this part, the author´s role was to prepare the samples, and process the initial data needed, whereas University of Helsinki implemented the actual modelling (Penttilä & Lumme 2008). First, the standard PCC (S-PCC) aggregate structure, the number and relative arrangement of individual PCC particles in the aggregate, and the distribution of additive introduced in the form of solid ZnO spot structures, displaying size around 150 nm, on the PCC surface, was studied from the SEM images such as presented in Figs. 5-6. Then, model aggregates were created accordingly, using a specific algorithm, and further deposited in a model matrix containing several aggregates. However, examination in fibrous matrix was out of reach, as it would have required huge computing power. For simplification, aggregates were deposited in a model coating matrix environment instead, without binders.

Multiple scattering from single aggregates was examined using a rigorous wave-optical approach based on Discrete Dipole Approximation (DDA), or the ADDA code (Draine & Flatau 1994, Yurkin *et al.* 2007). However, as the ADDA approach is valid for single aggregates only, light scattering from the model piece of coating was done using the SCIAPOL code (Rozanov & Kokhanovsky 2006) based on the RT approach. The RT calculations provide brightness values corresponding to ISO brightness, while through the ADDA method the backward-scattered intensity from single aggregates can be obtained.

The modelling was done for two cases:
In case I, intrinsic RI of the standard PCC bulk particles was increased from 1.58 to 1.70 without including additional particles. Both random and rosette-like clusters were examined.
In the case II, effective RI of the PCC aggregates was increased through introducing spot-like fine particles with RI and average particle size around 2.0 and 150 nm, respectively, onto the PCC surface (corresponding the majority of the ZnO structures observed in Figs. 5-6). In this case, the ZnO content was used as variable. ZnO contents of 5 vol-% and 10 vol-%, corresponding to effective RIs around 1.60 and 1.62, respectively, were studied.

3.3 Results

In stage 1, the microscopic examination of the tablets compressed from the pigment mixtures suggested introduction of the nanoparticles on the PCC surfaces in a relatively dispersed manner, as illustrated in Fig. 3. However, some localised agglomeration of the nanoparticles was observed. Hence, the illustration in Fig. 3 is indicative. The particles introduced display local RI contrasts on the PCC surface, enhancing the interaction with light, further observed as increased light scattering. Fig. 4 illustrates the diffuse and specular reflection measured using the ellipsometer from tablets compressed from regular PCC (90 w-%) and nano-sized particles of Al-silicate (10 w-%) displaying size around 30 nm. The results suggest increased scattering due to the local index mismatches imparted by the nanoparticles, as they only had a minor effect on the particle size of the resulting composite pigment comprising the PCC host and the nano-sized particles, respectively.

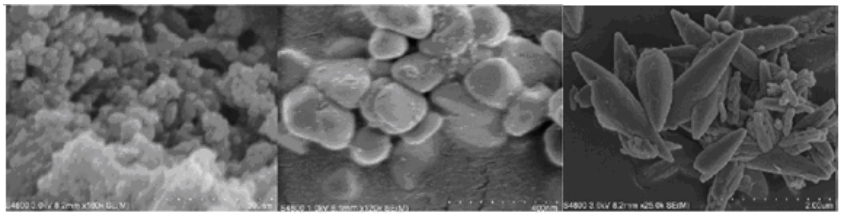

Fig. 2. Al-silicate (left) and ZnS particles (middle), used in mixtures with standard PCC (right) in the ellipsometric light scattering study using tablets compressed from the mixtures. Adapted from Publication III.

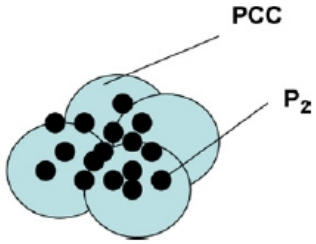

Fig. 3. Schematic illustration of the observed distribution of Al-silicate or ZnS based nanoparticles (P2) on the PCC surface in the compressed tablets. Adapted from Publication III.

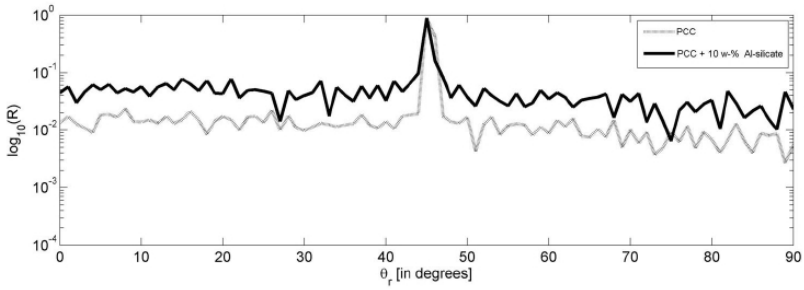

Fig. 4. Diffuse and specular reflection of reference PCC and PCC treated with 10 w-% Al-silicate particles as a function of detection angle. Adapted from Publication III.

These results were considered to provide a reasoned basis for the further experiments in stages 2 and 3.

In stage 2 (the effect of soluble RI modifiers), all additives were found to result in changes in PCC particle size and shape. Beneficial development of RI, and light scattering potential, were observed with Zn and Sr additives.

Achieving spot-coated structures through Zn modification

Figs. 5-6 show micrographs of the Zn modified PCC samples. Zn is seen to occur as solid particles, distributed in a discrete manner on the PCC surface. Through examination with EDS and XRD, the chemical composition of the particles was verified to be ZnO. The particles can be distinguished, especially in the backscattering images (Fig. 6), as bright spots. The reference PCC, typical scalenohedral rosette-like calcite, is shown in Fig. 8 (left).

ZnO provides various important functionalities in different industrial applications, including optical waveguides, UV-light emitters, phosphors (displaying phosphorescence), and transparent conductive materials. The optical properties of various ZnO nanostructures, as well as doped ZnO, have been discussed in the literature (see for instance Djurišic & Leung 2006). It displays relatively high RI, around 2.0 (Lide 1999), and has been considered an environmentally sound material (Djurišic & Leung 2006).

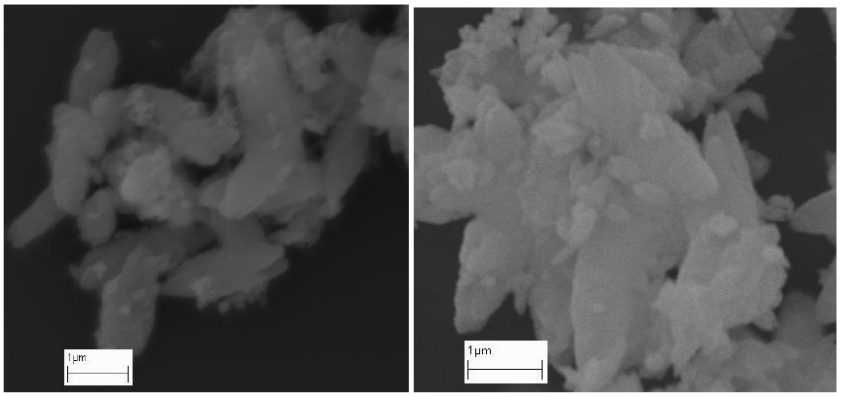

Fig. 5. PCC with 10 w-% (left) and 18 w-% (right) Zn content. Adapted from Publication II.

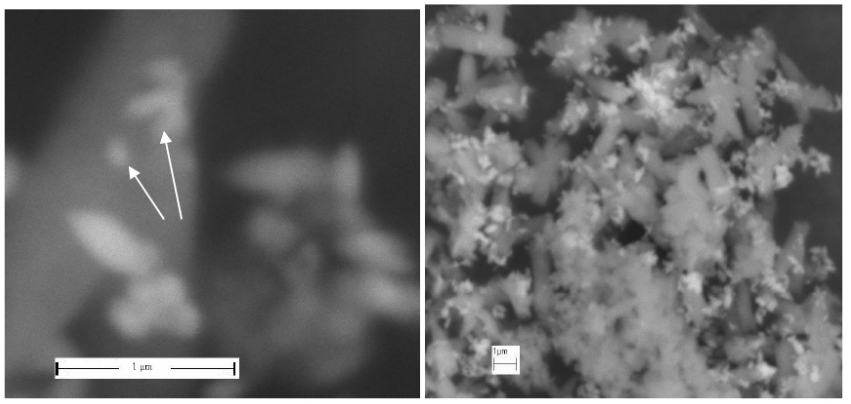

Fig. 6. ZnO particles on the PCC surface: backscattering images. Nano-sized structures (≤ 100 nm) are marked with arrows. Adapted from Publication II.

The samples presented in Fig. 5 displayed effective RIs of 1.63 (left) and 1.67 (right), measured with the MFS. Fig. 7 shows the backscattering intensity curves of the samples against RI of the immersion liquid.

With birefringent materials, such as calcium carbonate, back scattering intensity measured from suspension never achieves zero. For birefringence, also the minimum scattering intensity is further increased through RI contrast with regard to the ZnO particles introduced.

The formation mechanisms of the spots observed in Figs. 5-6 remains to be examined in further studies. However, the results of this study, based on repeated experiments, suggest beneficial precipitation of PCC in the presence of $ZnCl_2$ additive, yielding complete scalenohedral PCC particles coated with ZnO spots displaying at least partially desired size and inter-spot distance. This was

observed to take place with 60 °C starting temperature, 2.3 % $Ca(OH)_2$ concentration, and 1.0 dm^3min^{-1} CO_2 flow.

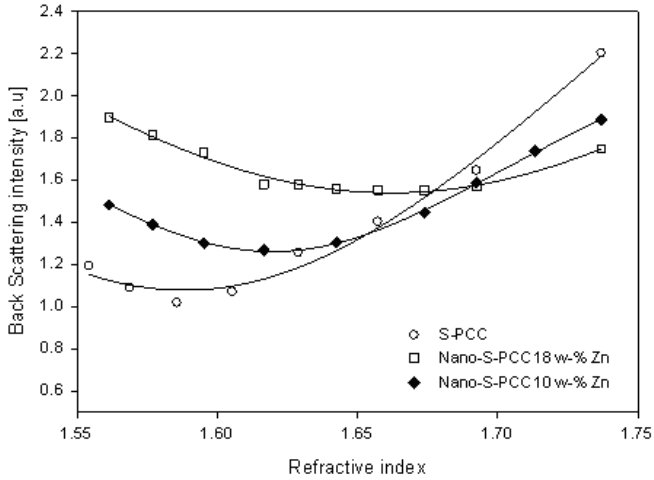

Fig. 7. Back scattering intensity measured from mixtures of PCC, and acetone – methylene iodide immersion liquid, as a function of the immersion liquid RI. Adapted from Publication I.

Morphological changes in the host particles – Sr modification

Effects of Sr can be observed as altered host particle morphologies Fig. 8 (image on the right). The host particles display needle-like structure, characteristic of aragonite carbonates. This might be an indication of Sr incorporation in the host particles through a substitution mechanism. Substitution of ions in a crystal may take place if the size of the substitute does not differ from the site provided by the original ions to be substituted by more than 15 % (Jaffe 1996). The size of Sr is close to that of calcium; hence such a mechanism could work. The XRD analysis verified the aragonitic crystallography. Relative amounts of calcite and aragonite in the sample were not examined.

It is well-known that additives incorporated in the crystal structure of calcium carbonate tend to change the particle morphology. In a previous study, the presence of Sr has been observed to contribute to aragonite formation, yielding more stable aragonite than calcium (Klein & Hurlbut 1999). Also the presence of magnesium and cobalt has been found to promote formation of aragonite (Kitano 1962, Braybrook *et al.* 2002).

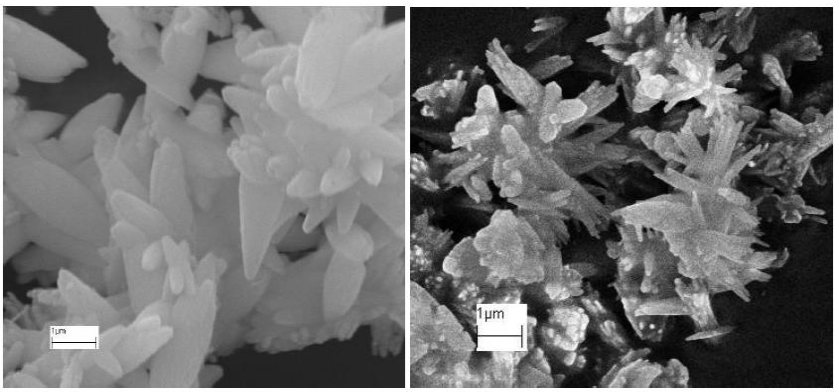

Fig. 8. Reference PCC (left) and PCC with 3.5 w-% $SrCO_3$ content (right). Adapted from Publication II.

Incorporation of ions into calcium carbonate crystals has been widely studied in the field of geochemistry. According to Nasrallah-Aboukais *et al*. (1996) ions can be incorporated into the crystal structure of calcium carbonate by substitution for calcium, interstitial substitution between lattice planes, substitution due to defects, and adsorption due to charges.

Alkali metals coprecipitate into calcite and aragonite via different mechanisms (Plummer & Busengerg 1982, White 1975, White 1977). According to White (1977), sodium and potassium coprecipitate into aragonite via substitution of calcium. In contrast, in calcite, sodium and potassium coprecipitate into interstitial positions (Ishikawa & Ichikuni 1984, Okumura & Kitano 1986). Coprecipitated amounts may also differ significantly. Coprecipitated amounts of alkali metals, especially sodium, are shown to be higher in aragonite (Okumura & Kitano 1986).

Papermaking potential of moderately modified samples

The preliminary handsheet tests made using the ZnO-modified fillers presented in Fig. 5, and the reference filler presented in Fig. 8 (left), suggested some improvement (5 % - 8 %) in the light scattering coefficient due to the ZnO-modified samples. The preliminary experiments are described in Publication I and will not be repeated here.

Papermaking potential was further examined in detail with the MBF apparatus using samples with moderate degree of Zn and Sr modification. Zn and Sr contents, as well as other sample data, are listed in Table II. Particle size distributions of the fillers are presented in Figs. 9-10.

The effective refractive index (n_{eff}) of a composite pigment consisting of a host particle (h) and a coating layer of particles (c) can be approximated from the

refractive indices (n) and the volume fractions (V) of the host and the particle layer, respectively, according to Equation (6)

$$n_{eff} = \frac{V_h n_h + V_c n_c}{V_h + V_c} \tag{6}$$

Accordingly, the effective RIs of the moderately modified samples were calculated, using the chemical content data obtained with TGA (presented in Table II), and additional density and RI data provided in the literature. The densities and refractive indices of ZnO are 5.606 gcm^{-3} and 2.0, respectively (Lide 1990). Corresponding values of $SrCO_3$ are 3.7 gcm^{-3} and 1.516 (Lide 1990). Density and refractive index of calcium carbonate (calcite) used in the calculation are around 2.71 gcm^{-3} and 1.58, respectively (Lide 1990).

Light scattering coefficient against filler content with different fillers is presented in Fig. 11. The differences in cluster sizes, particle shapes, and the resulting pore structures of the handsheets must be considered.

In the light of the current scattering theories discussed in the Introduction, and as discussed earlier briefly under Materials and Methods, it must be pointed out that the particle size data presented here are obtained using a light scattering technique that should be used predominantly for spherical isotropic pigments, well dispersed in the surrounding fluid. In the analysis of pigments displaying differing shape and optically active structure, such as presented in this study, the data should be critically inspected, and most predominantly evaluated together with supporting information from other sources such as sedimentation based particle size distribution measurements and/or micrographs. Therefore, the cluster sizes and size distributions presented in Table II and Figs. 9-10, respectively, are presented as indicative values only. Additional information about the size and shape characteristics of the pigments studied, and the sheet void structure, is provided by the SEM images, and the mercury porosimetry analyses, respectively.

The particle size data, shown in Figs. 9-10, display a primary peak centred around 5-10 µm, and a minor peak at or below 1 µm. Nano-S-PCC3 displays a single peak distribution with more evenly declining tail in the size range of the fine particles.

The clustered scalenohedral PCC samples of this study presumably contain intracluster void space, as could be observed from Figs. 5, 6, and 8. The intracluster void space arises from the limited packing of individual scalenohedral particles in rosette-like or more irregular configurations. As a matter of fact, the emergence of clustered PCC and other structured pigments such as calcined clay has been contributed by the fact that intraparticle air-filled pores displaying size corresponding to half the wavelength of visible light are beneficial for light scattering. The role of internal voids as light scattering bodies is emphasised in the case of such pigments. Bown (1997a) has suggested, that the characteristic size of a filler with internal pore volume

corresponds to that of the size of the pores. In the case of calcined clay with weight median particle size d_{50} and internal void size around 1.5 µm and 0.6 µm, respectively, the characteristic size is 0.7 µm (Bown 1997a). This is consistent with the current understanding according to which the role of pores as light scattering bodies is emphasised in compressed structures such as heavily calendered papers, as also discussed by Bown (1997a).

If the cluster is rigid enough to maintain its structure when dispersed in liquid, the air in the internal voids is replaced with the liquid. Due to the reduced RI contrast with regard to the inner pigment surface, the effect of the voids as light scattering bodies is reduced. However, even after filling with the liquid phase, significant RI contrast may still be present at the void-pigment interface. This can further affect the nature of backscattering, and increase the probability for misleading data in light scattering phenomena based particle size measurements valid for solid spherical particles. In this case, furthermore, the clusters are not uniform, but display local differences in density and refractive index. The internal pore volume and the heterogeneity of the particles significantly complicate the cluster size evaluation through the light scattering techniques. It is for these reasons that the second part of the thesis (from page 71), studying a well-defined porous medium filling with liquid, is undertaken to illustrate the RI-contrast effect using a complementary experimental design.

According to the light scattering based particle size data, which, as described above, should be critically inspected, Nano-S-PCC 3 displays smaller cluster size than Nano-S-PCC 1 (or Nano-S-PCC 2) but is close to that of the commercial reference PCC (S-PCC (Com). Evaluation of the micrographs supported this order of magnitude.

Nano-S-PCC 3 yields higher light scattering than any of the other fillers. At least part of the Nano-S-PCC 3 particles display aragonitic crystallography, and hence, RI around 1.63. Furthermore, the aragonitic shape of Nano-S-PCC 3 significantly differs from the shape of the other samples, and results in different packing and pore structure of the sheet. This effect will be discussed below. The influence of crowding can be envisioned in the case of Nano-S-PCC 3.

Table II. Characterisation of filler samples used in the MBF experiments. The cluster size denotes the volume-based size of filler clusters such as observed in Fig. 5. Adapted from Publication II.

Sample	Cluster size, µm		SSA, $m^2 \cdot g^{-1}$	ZnO, w-%	SrCO3, w-%	SrO, w-%	n_{eff}
	Mean	Median					
S-PCC	7.380	7.273	5.6	-	-	-	1.58
S-PCC (Com)	4.099	3.567	6.4	-	-	-	1.58
Nano-S-PCC 1	7.989	7.748	6.2	1	-	-	1.582
Nano-S-PCC 2	5.940	5.781	8	8	-	-	1.597
Nano-S-PCC 3	4.341	3.823	10.5	-	3.5	1	1.578 - 1.63*

** depends on the relative amount of aragonite in the sample (not examined)*

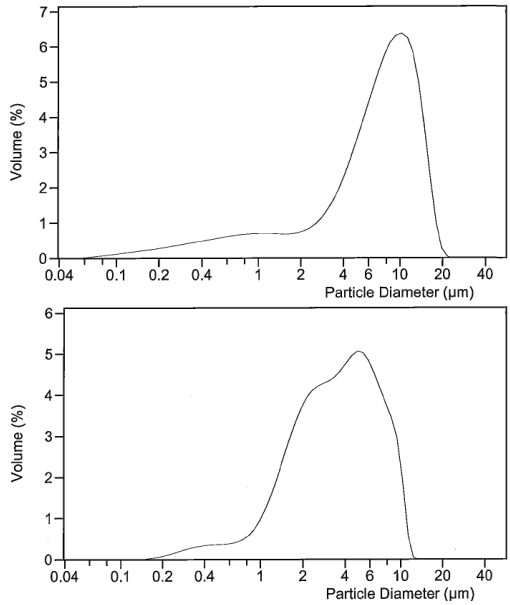

Fig. 9. Volume-based particle size distributions of S-PCC (top) and S-PCC (Com) (bottom).

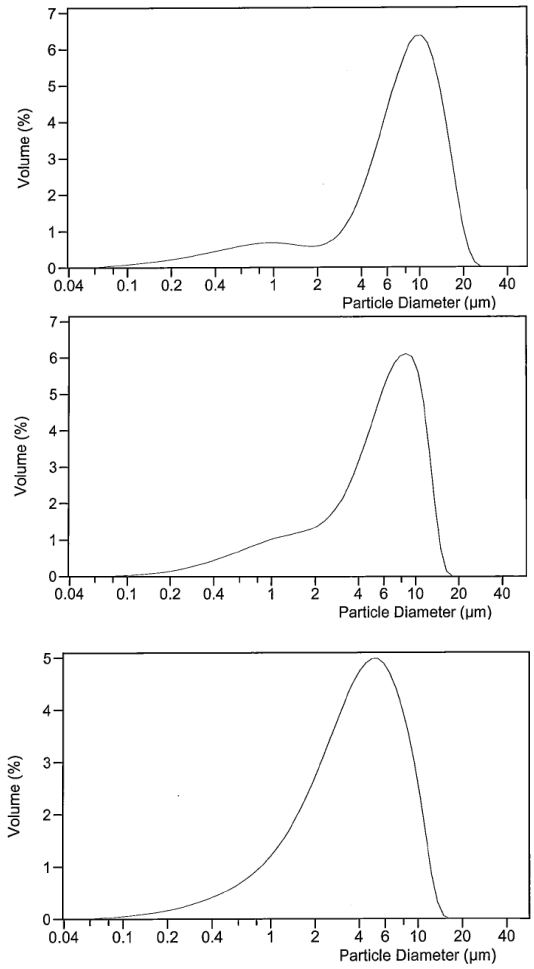

Fig. 10. Volume-based particle size distributions of Nano-S-PCC1 (top), Nano-S-PCC2 (middle), and Nano-S-PCC3 (bottom).

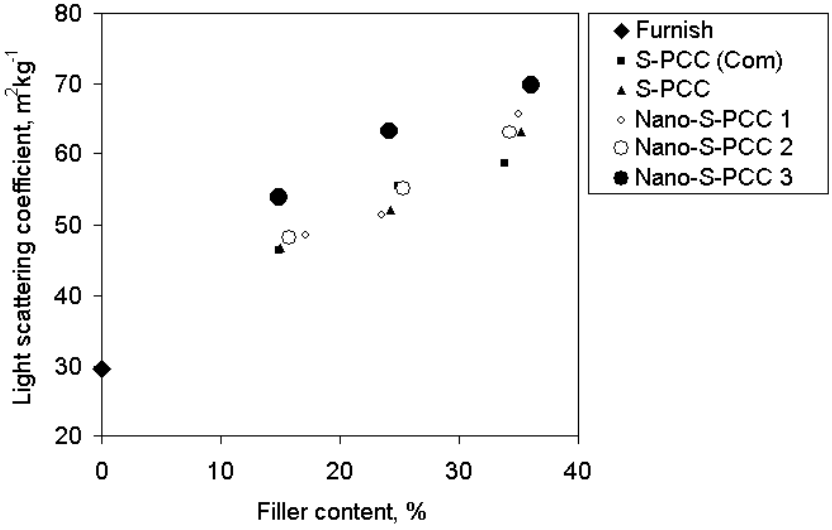

Fig. 11. The effect of filler type on light scattering coefficient. Adapted from Publication II.

Qualitative inspection of the Nano-S-PCC1 and Nano-S-PCC2 filled handsheets with EDS confirmed that ZnO had retained. No benefits in optical properties were observed in these cases. According to the ZnO content data presented in Table II, the ZnO contents are relatively low. Hence, only a limited number of ZnO particles displaying advantageous size and location with regard to the surrounding medium may be present. The observed zero to moderate effect of Nano-S-PCC1 and Nano-S-PCC2 on light scattering is also consistent with the Rayleigh scattering calculation discussed below (paragraph 3.4 Discussion).

It can be observed from Fig. 12 that the light scattering coefficient is increased in a predominantly straightforward manner with regard to the decreasing tensile index. The fillers, hence, do not provide synergistic benefit together with the fibres, but may display a more or less disruptive alignment between the adjacent fibres instead, such as suggested by Weigl *et al.* (1981). The resulting increase in the light scattering is, therefore, at least partly contributed by the debonding effect. However, the Nano-S-PCC 3 gives the highest light scattering coefficient at a fixed tensile index. This is an indication that the filler itself contributes to the light scattering, more so than in the case of the other fillers.

Particle size affects both optical and strength properties and can influence combinations of the two as well. As suggested by Bown (1997b), small particles sized approximately 2 µm can yield better combinations of these properties than large particles (6 µm). If we assume that the cluster size has a

similar effect in our case, this could explain results here, in addition to the effects discussed above.

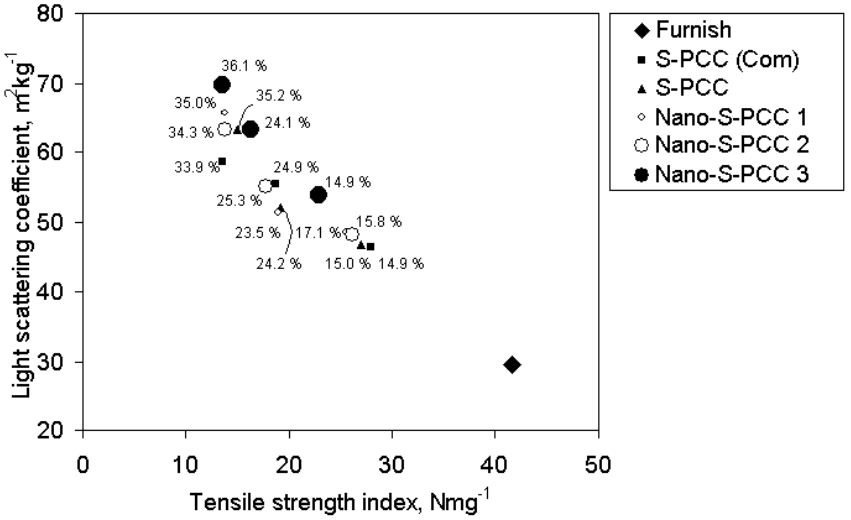

Fig. 12. Effect of filler type on the property combination of light scattering coefficient and tensile index. Adapted from Publication II.

Nano-S-PCC 3 yields the lowest bulk and air permeability (Figs. 13-14). This is consistent with the findings of, for instance, Breunig *et al.* (1990), according to which air permeability tends to decrease with higher SSA fillers. Lower SSA fillers Nano-S-PCC 1 and Nano-S-PCC 2 yield more open sheet structure. This is also in line with the assumed debonding effect.

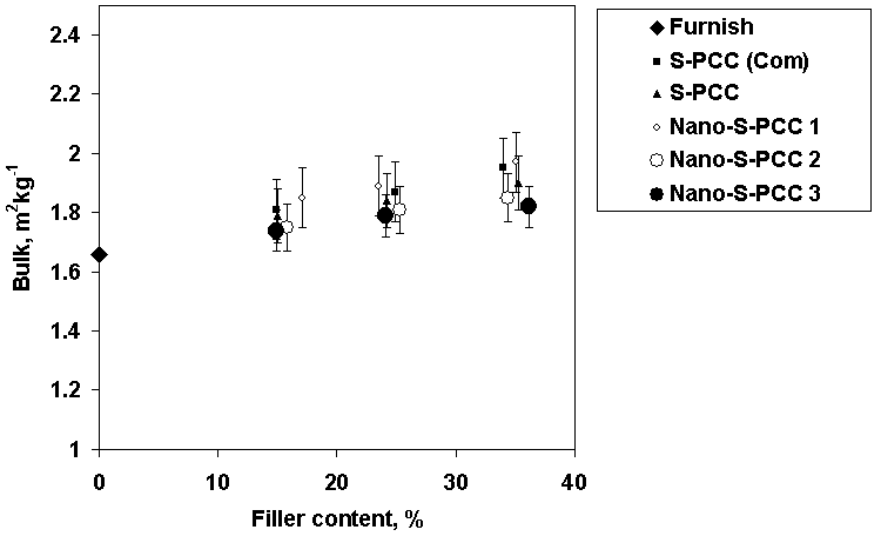

Fig. 13. Effect of filler type on bulk. Adapted from Publication II.

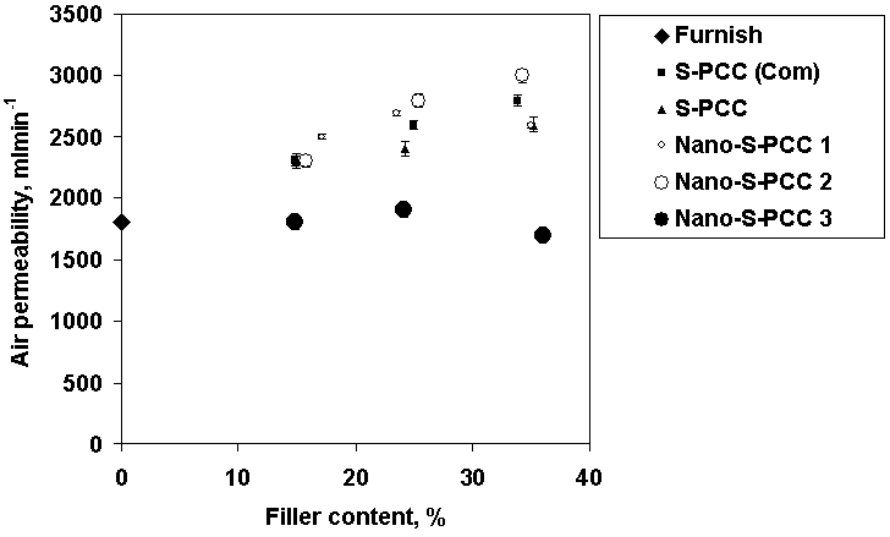

Fig. 14. Effect of filler type on air permeability. Adapted from Publication II.

The properties of calendered sheets are presented in Figs. 15-17. Calendering typically reduces pore volume and can therefore affect light scattering. After calendering, Nano-S-PCC 3 yields higher light scattering compared with the

other pigments. The advantage observed in the property combination of light scattering and strength properties in the case of uncalendered sheets has been reduced on calendering. Nano-S-PCC 3 yielded still the lowest air permeability.

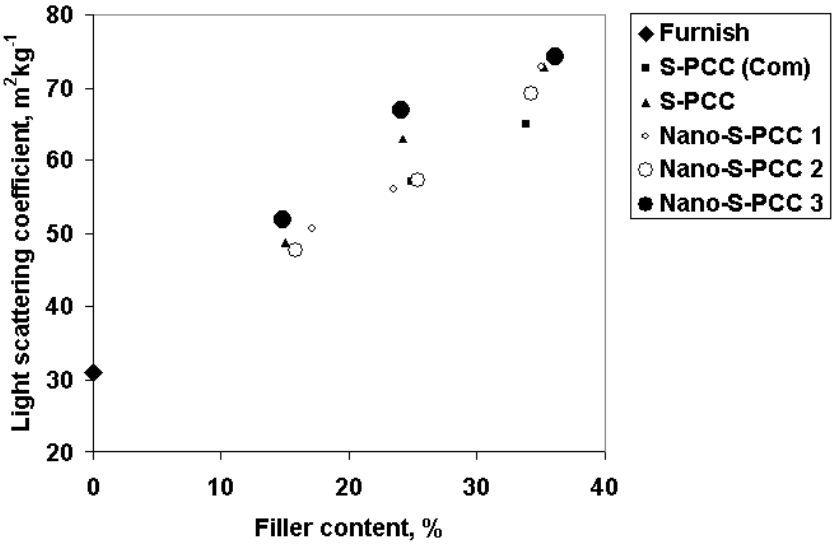

Fig. 15. The effect of filler type on light scattering coefficient. Calendered sheets. Adapted from Publication II.

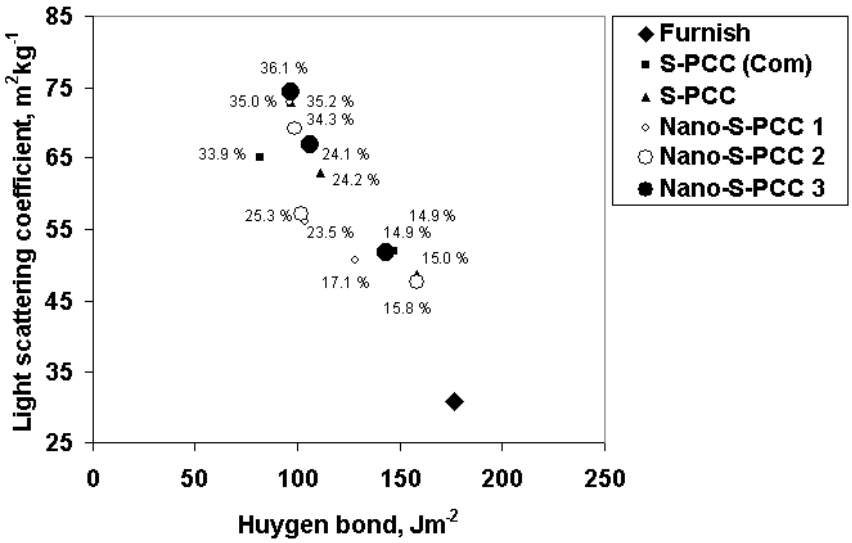

Fig. 16. The effect of filler type on the property combination of light scattering coefficient and Huygen bond. Calendered sheets. Adapted from Publication II.

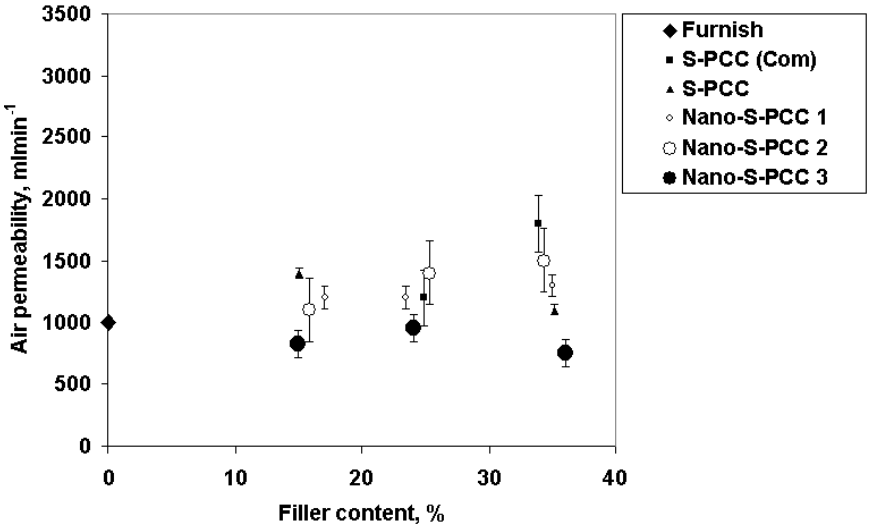

Fig. 17. The effect of filler type on air permeability. Calendered sheets. Adapted from Publication II.

Closer examination of the handsheet pore size distributions (shown in Figs. 18-19), based on the mercury porosimetry analyses, suggest beneficial effect of both Zn and Sr based structuring on the pore structures of the filled sheets in respect to potential light scattering.

Fig. 18 presents the cumulative pore size distributions of uncalendered and calendered sheets filled with S-PCC (Com), Nano-S-PCC 2, and Nano-S-PCC 3. According to a previous study (Ridgway & Gane 2003), irreproducible differences imparted by the occlusion effect due to the surface fibre irregularity are often encountered with pores with an equivalent Laplace diameter greater than 10 µm. The evaluation of the total volume would require supporting analyses through, for instance, oil absorption techniques (Ridgway & Gane 2003). The truncated curves, shown in Fig. 18 (below), provide information about the relative porosity with pores displaying equivalent Laplace diameter less than 10 µm.

The vertical lines in Fig. 19 illustrate the pore size range, which is the most effective for the interaction with light. The results suggest that, in the case of uncalendered sheets, S-PCC (Com) yields the lowest volume of optically effective pores, but displays the higher volume of bigger pores around the size of 1 µm. The big pores could contribute to the relatively high bulk and air permeability shown in Figs. 13-14. Slightly higher volume in the size range of optically effective pores is observed with Nano-S-PCC 2, indicating a beneficial spacing effect due to the ZnO structures, yielding more optimal interparticle distances. As suggested by Fig. 11, with 35 w-% filler content, Nano-S-PCC 2 yields a higher light scattering coefficient than S-PCC (Com). The possibly very fine ZnO particles, in spite of their high RI, do not have significant contribution to light scattering when contacted with micrometre-sized PCC particles, as will be illustrated by the Rayleigh calculation in paragraph 3.4. However, the RI contrast imparted by larger ZnO particles, with diameter around 300-500 nm, might be expected to play a more beneficial role. The effect of ZnO particles, displaying size of 350 nm, deposited on potassium silicate, has been discussed by Johnson *et al.* (2003).

Nano-S-PCC 3 yields the most beneficial structure displaying the highest volume of optically effective pores before calendering. This is consistent with the light scattering results presented in Figs. 11-12. All sheets filled with Nano-S-PCC 2 and Nano-S-PCC 3 display discrete bimodal pore size distributions with the primary peak around 1.0 µm (with Nano-S-PCC 3 yielding to some extent smaller average pore size), and a small secondary peak around 40 nm.

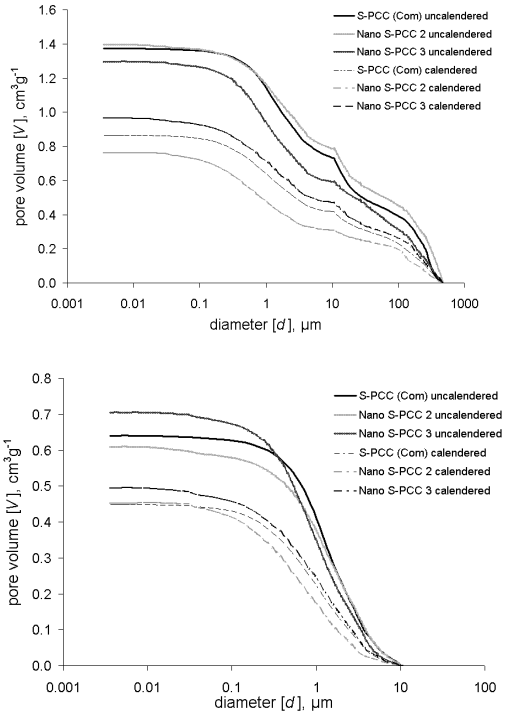

Fig. 18. Cumulative mercury intrusion pore size distribution data of selected handsheets. 35 w-% filler content. The irreproducible occlusion effects due to surface fibre irregularity (see Ridgway & Gane 2003) are eliminated in the lower figure, presenting the data truncated at 10 µm.

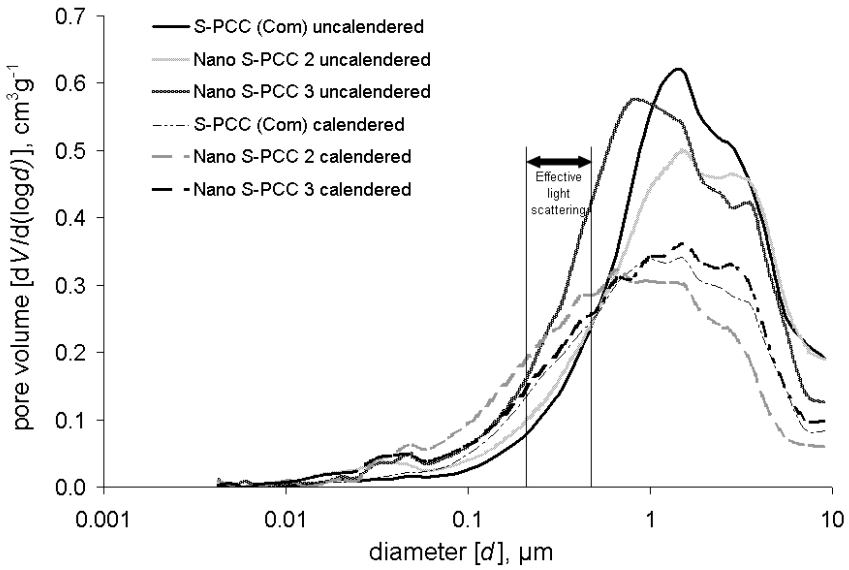

Fig. 19. Differential pore size distribution data of selected handsheets. 35 w-% filler content. The optically effective pore size interval is marked in the figure.

As Fig. 19 illustrates, calendering significantly decreased the volume of larger pores around 1 µm, whereas the effects on the pore volume in the case of optically effective pores depended on the filler type.

Calendering had a beneficial effect on volume of optically effective pores with Nano-S-PCC 2, whereas with Nano-S-PCC 3 the volume was reduced. In spite of this, Nano-S-PCC 3 yielded the highest light scattering coefficient, as was shown in Fig. 15, and suggests the effectiveness of including the higher RI material. This further indicates that the RI contrast introduced through the partially aragonitic particles is the more dominant factor rather than the resulting pore structure. However, this result applies to the examined filler content only. The situation could be different in ultra-highly filled papers displaying higher relative volume of optimal pores.

Considering Figures 12, 16, and 19 together, it is possible to observe a synergistic benefit with high filler content of Nano-S-PCC 2 in the calendered sheets. With conventional fillers, a more or less straightforward increase of light scattering coefficient is allied with a decrease of tensile index, as typically encountered when increasing filler loading. In contrast, with Nano-S-PCC 2 the change in filler content from around 25 w-% to 35 w-% in calendered sheets increases light scattering coefficient without adverse effects on bonding (Fig. 16), suggesting the positioning of the additional particles is in interfibre pores, rather than between the adjacent fibres. Extrapolation to filler contents beyond 35 w-% would further suggest an increasing advantage through this synergistic

effect. As can be observed from Figs. 15-16, the light scattering efficiency through the pore-optimised, compressed Nano-S-PCC 2 filled sheets is increased with high filler content, whereas an indication of the crowding effect, i.e. reduced light scattering efficiency, can be observed in the case of Nano-S-PCC 3 filled sheets. This suggests that with further increased filler contents Nano-S-PCC 2 could provide even more beneficial light scattering than Nano-S-PCC 3 through increased volume of optically effective pores.

Fig. 19 further shows that calendering significantly increased the volume of optically effective pores with Nano-S-PCC 2, and also with S-PCC (Com). Both fillers exhibit clustered scalenohedral morphology, whereas ZnO particles are present only on Nano-S-PCC 2. This suggests that besides imparting RI contrasts, the ZnO particles provide additional spacing, yielding advantageous pore structure, emphasised in compressed sheets.

Modelling study

The shape of the model particles, used to mimic the individual PCC particles observed in Figs. 5-6, was chosen to be prolate spheroidal (Penttilä & Lumme 2008). Spheres were used to represent the ZnO particles.

The ADDA approach (Draine and Flatau 1994, Yurkin *et al*. 2007) suggested 9 % increase in backscattering intensity from single aggregates in the reference case (case I), in which the bulk RI was increased from 1.58 to 1.70, without introduction of ZnO particles. In the model coating including several aggregates, 1 % - 4 % increase in brightness, based on the RT calculations, was observed.

The relative arrangement of the particles in the PCC aggregate didn't significantly affect the resulting light scattering, as both randomly clustered, and regular rosette-like aggregates (Fig. 20) were examined

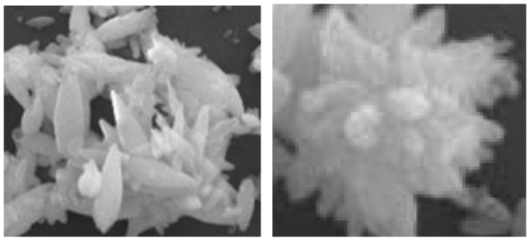

Fig. 20. Clusters of scalenohedral PCC displaying differing arrangement of individual particles. Random arrangement (left), and regular, rosette-type arrangement (right).

In contrast, 5 vol-% and 10 vol-% introduction of ZnO particles on PCC, corresponding to effective RIs around 1.60 and 1.62, respectively, resulted in

10 % - 20 % increase in backscattering from single aggregates, while brightness from the model coating increased 4 % - 7 %.

Due to the approximations used, the modelling results should be considered indicative.

ISO Brightness from handsheets displaying 20 % filler content was measured for comparison. Reference PCC, and PCC with 10 vol-% ZnO content (effective RI 1.62) were examined. Increment in ISO Brightness due to ZnO in this case was 2.1 %. The lower value compared to the modelling result was not surprising, as in coatings the particles are usually more beneficially located, displaying closer packing, and probably more beneficial pore size distribution than in fibrous matrices. The fibres themselves display relatively low brightness (around 84 % ISO, as measured from unfilled 60 gm^{-2} reference sheets). It is also noteworthy that in the modelling study the exact value of the imaginary part of the complex refractive indices, determining the absorption, were not known, while the approximation $0.00001 < n_i < 0.0001$, based on measured brightness values, was used.

3.4 Discussion

The results suggest that

- the Kubelka-Munk theory based *light scattering coefficient* measured from PCC-filled handsheets,
- and, as studied in the modelling section, *backscattering intensity* in addition to *RT based brightness*, calculated using model structures of single pigment clusters and model coatings consisting of several clusters in close proximity to each other, allowing multiple scattering from neighbouring particles, respectively,

can be increased by replacing standard clustered scalenohedral PCC filler with the newly developed ZnO spot-coated PCC filler pigment displaying enhanced effective refractive index.

The laboratory scale sample fabrication followed by simple sheet mould tests and more comprehensive MBF tests, complemented with the study of the calendering effects, suggest that

- scalenohedral PCC filler can be used as a platform in using fine spot-like particles as means to introduce RI contrasts in paper structure without significant adverse effects in sheet fabrication in the examined scale.

The EDS study confirmed that ZnO had retained in the handsheets. This is also suggested by the pore size distribution data indicating differing structures

between ZnO containing Nano-S-PCC 2 filled sheets and standard PCC filled sheets. This supports the first hypothesis of the thesis.

The effective refractive index of PCC was increased up to 1.67 as verified by the extended index matching method by the multi-function spectrometer MFS. That the method of refractive index matching gave successful extinction demonstrates that the particles act as an averaged refractive index medium and not as discrete optical elements. In this way, discrete introduction of fine particles with size close to the Mie-defined optimum onto the filler surface, and the consequent effect on the optical properties of the model coating, was contrasted by the effect of increasing the RI of PCC bulk particles without changes in the particle structure. The results indicate that, comparing the two approaches, introduction of fine particles on the PCC surface is more effective, yielding higher light scattering with a given effective refractive index. This is consistent with the considerations of the Mie treatment (1908). However, due to the observation that both effective RI and SSA of the resulting filler cluster were increased, the relative effects of these two factors were not quantitatively differentiated in this study. As it is a physical fact that increasing RI gradient on an optically active interface always increases the interaction with light, it is, however, justified to conclude that the fraction of ZnO particles displaying effective size for light interaction enhances light scattering at least partly through the RI mechanism.

More specifically, it is suggested that the ZnO particles, when introduced on PCC surface, influence light scattering through the following four ways.

First of all, the ZnO particles manifest local refractive index contrasts on the PCC surface. A significant fraction of the particles display size around 100 nm – 500 nm. Also nano-sized (≤ 100 nm) structures could be observed (Fig. 6). Tailoring the refractive index of various nanocomposites has gained attention in the field of optical physics (Zeng *et al.* 1988, Shalaev 2002, Aspnes 1982, Chylek & Videen 1998, Lakhtakia 2001, Scaffardi & Tocho 2006, Boyd & Sipe 1994).

When subjected to interaction with light, nano-sized particles display, generally, relatively moderate scattering effects, following the theory of Lord Rayleigh (1871). For instance, our perception of the sky as a blue medium is due to the scattering of the shortest visible wavelengths of light from the molecular scattering centres distributed in the atmosphere.

The Rayleigh criterion includes the size parameter α (Equation 7) for a particle in air

$$\alpha = \frac{2\pi a}{\lambda_0} \tag{7}$$

where

a is the radius of the spherical particle (effective scattering size)
λ_0 is the incident scattering wavelength component in air, i.e. the wavelength in the scattering medium, which in this case is air.

In the case where the scattering medium is not air, the incident wavelength is defined as

$$\lambda = \frac{\lambda_0}{m} \tag{8}$$

where

λ_0 is the incident wavelength value in air
m is the refractive index of the surrounding medium.

These relations show that the particle size, a, in relation to the wavelength effective within the refractive index contrast environment, created by the particle and its surrounding, plays a defining role, where, m, the complex refractive index of the scattering body is given by

$$m = n - ik \tag{9}$$

where

n is the real refractive index
k is the imaginary part of the refractive index

The Rayleigh criterion states that when $|m| \cdot \alpha << 1$, Rayleigh scattering may occur. For particles larger than this the scattering is defined by Mie theory.

The Rayleigh criterion can be applied under simple linear assumptions to obtain an indication of relative scattering power. In the case of a composite pigment comprising the host particle, acting as the surrounding material on one side of the additional scattering particle (attached onto the host), which in turn has its further contrast boundary to air or fibre on the other side. The additional particle will contribute to the light scattering more effectively than just by the Rayleigh scattering alone, if $|m| \cdot \alpha \approx 2\pi a_{max}/\lambda$, where a_{max} is the respective scattering size at maximum scatter for illuminating light of wavelength λ.

First, considering the case of a host PCC particle with an optimum scattering particle size, around a_{maxPCC} = 200 nm, its Rayleigh criterion, assuming the illuminated wavelength in air is 457 nm, is given by

$|m| \cdot \alpha$ = 1.0 x 2π x 200 nm / 457 nm = 2.75

Therefore, it is not, by definition, a Rayleigh scatterer. However, this optical value expresses the optimum for calcium carbonate, and can be considered an optimum for our system.

The additional very fine scattering particle, ZnO, displaying a radius of 50 nm surrounded by air, gives

$$|m| \cdot \alpha = 1.0 \text{ x } 2\pi \text{ x } 50 \text{ nm} / 457 \text{ nm} = 0.69$$

and is, therefore, an efficient Rayleigh scattering centre, which can lead to a background scattering effect, if present in sufficient number, just like the abovementioned blue sky effect. Analogous calculation would show that contact with a neighbouring fibre (on the opposite side of the ZnO particle) would result in moderate scattering.

Now, if we consider the ZnO particle neighbouring a medium of PCC, where PCC and ZnO display RI values of 1.58 and 2.0, respectively (Lide 1999), we obtain

$$|m| \cdot \alpha = 1.58 \text{ x } 2\pi \text{ x } 50 \text{ nm} / 457 \text{ nm} = 1.09$$

for light travelling toward the ZnO particle from the PCC, and right on the border of Rayleigh scattering, i.e. its scattering efficiency is reduced. However,

$$|m| \cdot \alpha = 2.00 \text{ x } 2\pi \text{ x } 200 \text{ nm} / 457 \text{ nm} = 5.50$$

for light travelling toward an optimally sized PCC (for scattering in air) through a medium of ZnO. This, too, is far from the optimum for particles larger than the Rayleigh criterion, i.e. 5.50 > 2.75 for PCC in air. These two latter cases are to be expected as the refractive index contrast is much less than for an air boundary.

If we form an average of these scattering centre calculations we obtain for the ZnO particle a value of $(0.69 + 1.09)/2 = 0.89$ for it surrounded on one side by air and on the other by PCC. Similarly, for the PCC surrounded to an approximation by air and ZnO we obtain $(2.75 + 5.50)/2 = 4.13$. If we have a 1:1 layer occurrence of the particle types then we could expect a linear approximated average of $(0.89 + 4.13)/2 = 2.51$, which is quite close to our defined optimum of 2.71 for the known optimally sized PCC.

Therefore, we can conclude that the addition of ZnO nanoparticles to the surface of an optimal PCC particle (defined as optimal in air) follows relatively closely the optimal scattering criterion of PCC alone. This means that the scattering from a filled paper, assuming no other interactions, is synergistically enhanced per unit composite filler volume, and hence weight, only if the addition of the ZnO nanoparticles provides changes in structural behaviour in respect to intra-cluster pore size, filler spacing or fibre matrix disruption.

The RI contrasts should be considered together with the resulting overall paper structure, and not alone. The Rayleigh approximation expression applied above ignores the effect of interparticle pore size distribution yielded by a high number of particles in the fibrous matrix. The ZnO particles not only modify the local RI contrasts, but also affect the interparticle pore size distribution of the paper structure. As discussed in paragraph 3.3, the ZnO particles have a beneficial effect on the pore structure, emphasised in highly-filled, calendered papers. Nonetheless, these calculations suggest that there is still much room for optimising the relative sizes of PCC and ZnO to give the maximum efficiency in terms of particle number, and weight, even given the crude approximations applied. When introducing a PCC with larger particle size, or placing the filler on/next to fibre, the PCC scattering effect is reduced. In contrast, larger ZnO particles could have a positive contribution, even when introduced on the larger PCC host particle (both also shown in Figs. 5-6). Nanoscale materials for light scattering are not always optimal.

Secondly, as already mentioned, the ZnO particles raise the SSA (see Table II), which might further lead to an increase in interparticle or inter-aggregate spacing as illustrated in Fig. 21. In optics, interparticle spacing, displaying no less than 200 nm interparticle distances, has the most significant contribution to light scattering.

The importance of spacing has been highlighted by some recent publications. Spacing of high-refractive-index pigments has been presented by Holm (2007). Spacing through fine particles in GCC coatings has been discussed by Gane (1998).

When packing density of fillers increases throughout paper, i.e. by calendering, or locally by filler particle flocculation (Holm & Manner 2001, Porubska *et al.* 2002), solid-air interfaces are replaced by solid-solid interfaces. This leads to reduction of light scattering. As presented by Gavelin (1998), fillers form flocs together with fines (heterogeneous flocculation as defined in the above paragraph 2.2). From the optics viewpoint, the effect is analogous, as fines and fillers display similar refractive indices. The light scattering effect reduces when interparticle distance goes below 200 nm. Flocculation is, however, inevitable if one is to achieve sufficient retention. Therefore, thirdly, it is beneficial that not all particles in a floc display similar indices.

The fourth mechanism suggested here is related to the distribution of the spot structures on host particles. In an ordinary blend consisting of filler particles and very fine additional particles, separation between two particle types may take place due to colloidal attraction within the fine particle fraction. Segregation of two filler types with differing morphologies has been explained earlier by Gane *et al.* (1999). When the particles are attached onto the host particles, the separation is prevented, and the number of solid-solid contacts displaying refractive index contrast is maximised.

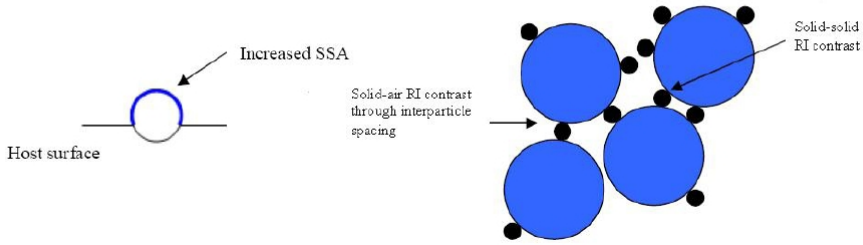

Fig. 21. Schematic figure illustrating the suggested mechanisms of light scattering generation through the novel filler. Left: increased SSA due to the fine particles. Right: spacing effect and RI contrasts occurring in a filler aggregate. Adapted from Publication II.

The effective refractive indices calculated according to Equation 6 are used as indicative values, basically giving information about the degree of RI modification with regard to the average refractive index of PCC (1.58). The deficiency in the concept of the effective refractive index is that it fails to distinguish between homogeneous fillers, exhibiting no birefringence at all, and composite structures exhibiting local RI contrasts, and consequently, increased birefringence. Furthermore, the effective refractive index concept does not provide information on how the applied way of modification in question will impact the resulting light scattering. Namely, two fillers with similar effective refractive indices may display distinctively different local RI distribution, and consequently, different effects on the light scattering. The nature of birefringence was earlier illustrated in Fig. 7. Furthermore, as suggested by the Rayleigh calculation, nano-sized particles with high RI do not significantly contribute to the light scattering. As was suggested in the modelling study, it is more beneficial to increase the effective RI of PCC by introducing RI contrasts on the PCC surface in the form of high-RI particles with size suitable for interaction with light, than by increasing the intrinsic RI of the PCC bulk particles themselves.

More detailed discussion on the various effective medium approximations can be found in the literature (Videen & Chylek 1998).

In summary, RI gradients in the paper structure can be increased through using ZnO spot coated PCC as a filler. Furthermore, light scattering of the resulting paper is increased through the incorporated RI gradients provided that the ZnO particles display size close to the Mie-defined optimum. Nano-sized particles (<

100 nm) are less effective. However, the overall response in light scattering depends on the resulting pore structure.

Sr based modification results mainly in conventional aragonitic crystals. In contrast to ZnO spot coated PCC, features supporting the first thesis hypothesis were not observed with this approach.

4 CONTRIBUTION TO THE DEVELOPMENT OF NOVEL STARCH BASED FILLERS

4.1 Approaches

Stock starch, after being gelatinised and solubilised through cooking in water, is typically added in the fibrous stock to provide paper dry-strength, reduced by the effects of fillers. To avoid operational problems at the PM, the dosage of stock starch is limited. Starch can also be applied onto the paper web surface at the size press.

Due to the use of inorganic fillers and coating pigments, huge amounts of inorganic material are separated from fibrous suspensions in deinking lines. Over half of the deinking sludge formed for instance in the flotation stage can be clay and calcium carbonate based material (Hanecker 1994). Deinking sludge is dewatered and used for landfill, used in industrial purposes, or combusted (Hamm 1998). The European Union has set goals for increased recovery of metal, glass, and paper. However, in incineration of paper based waste, significant formation of ash takes place. New solutions would be beneficial to avoid the ash generation, and further ease the use of paper based waste in energy production. Considering the non-toxic, inert landfill applicability that ash still provides, however, the production of the organic material for paper filling purposes must support sustainable development as well if they are to be considered viable. The land space, fertilisers etc. needed for large-scale cultivation of, for instance, starch, for industrial purposes, should be carefully re- evaluated on the basis of both economical and environmental effects.

Efforts have been made to develop organic pigments, such as plastic pigments, urea-formaldehyde pigments, and various modified starch based pigments (Krogerus 1998, Heiser & Shand 1973, Gruber *et al.* 1998, Varjos *et al.* 2004). Besides combustibility, organic fillers possess additional paper technical advantages such as light weight and low abrasivity.

To achieve semi-organic or organic filler pigment with enhanced RI or light scattering potential, three alternative approaches were studied:

1) spot coating of uncooked starch granules with inorganic material displaying high light scattering potential[1],
2) complexation between soluble starch and ions with high specific refractivity to obtain insoluble semi-organic hybrids[2],
3) incorporation of aromatic groups[1] in a starch based filler granule.

[1] Input by M-real Oyj, sample modification and analysis by LUT, paper technical testing by TKK
[2] Idea, sample modification, and analysis by VTT, paper technical testing by TKK

Hence, the first two approaches provide enhancement of starch filler optical performance through incorporation of inorganic material, giving semi-organic fillers, while the third approach provides 100 % organic pigment.

The approaches were studied in research cooperation as described in the footnote.

4.2 Materials and Methods

Spot coated starch granule fillers

Al-silicate was deposited in spots on uncooked starch granules (delivered by Raisio Group) reacting sodium silicate (Zeopol, Huber Engineered Materials) with aluminium sulphate, or alum (2331350, Kemira Oyj), in a 4.0 dm^3 reactor in the presence of the granules. Three different spot coated starch samples were fabricated.

First, a starting solution containing some alum and the granules was prepared. In the second stage, the sodium silicate, and additional alum were dosed in a controlled manner to form Al-silicate precipitates on the starch granules.

The variables were starch type (native vs. anionic) and the rate of reagent addition. The samples are described in Table III. The samples were designed to exhibit 80 w-% Al-silicate content.

Table III. The spot coating conditions of the starch granules. Adapted from Publication IV.

	Sample		
Initial solution	1	2	3
Alum, g	6.6	6.6	6.6
Starch, g	31.0	31.0	31.0
Starch type	Native	Anionic	Anionic
$Mg(OH)_2$, g	2.0	1.1	1.0
Water, g	1 000.0	1 000.0	1 000.0
***T*, °C**	40.0	40.0	40.0
Silicate deposition			
Silicate, g	414.0	414.0	414.0
Alum, g	67.5	67.4	67.4
Water, g	389.0	389.0	389.0
Duration, min	10.0	5.0	9.0

[1] Idea by the author, sample fabrication by VTT, paper technical testing by TKK

The size distributions and morphologies were studied with Coulter LS 130 and SEM, respectively.

Dried chemical pulp, consisting of 70 w-% birch and 30 w-% pine, was disintegrated and beaten according to the standard SCAN-C 25:76 until a 50 $Nm.g^{-1}$ tensile index without fillers was achieved. 60 gm^{-2} handsheets were prepared by applying the standard SCAN-C 26:76.

The filler contents were controlled by silicate content determined through ashing. Silicate content targets were 6 % and 14 %, relative to the weight of the base paper.

Laboratory handsheets are customarily dried at 23 ºC or 60 ºC. In this study, the wet-pressed handsheets were subjected to elevated temperature (90 ºC) for ten minutes in a fan drier specifically constructed for the experiment. This was done to correspond better with the drying conditions to be expected on a PM. The shape of starch particles may change in the presence of water due to dissolution of the polymer chains at the gelatinisation temperature (Ketola & Andersson 1998). Subsequently, the drying under standard conditions (23 ºC, 50 % RH) was completed. The sheets were analysed with Standard Methods.

A commercial silicate filler was used as a reference.

Complex starch hybrid fillers

The complexation idea as well as preparation and chemical characterisation of hybrid fillers were conducted solely by VTT, and are therefore not described as a part of this thesis summary. More details on this can be found in Publication V.

Papermaking potential of the hybrid fillers was investigated at TKK in laboratory handsheet experiments including calendering. The hybrid fillers examined were carboxymethylated starch complexed with barium chloride (CMS + $BaCl_2$), and CMS complexed with zirconyl nitrate hydrate (CMS + $ZrO(NO_3)_2.xH_2O$).

Handsheets were prepared with a Moving Belt Former (MBF) apparatus described by Räisänen (Räisänen 1998). Dried chemical pulp samples were mixed to obtain a blend furnish with birch and pine contents of 70 w-% and 30 w-%, respectively. The blend was beaten to reach Schopper Riegler value 18 and diluted to 3.0 gdm^{-3} fibre consistency.

Targeted basis weight of the sheets was 80 gm^{-2}. Target filler contents were 15 %, 25 %, and 35 % relative to the base paper weight.

Sheet preparation and calendering were done according to the methods described in the section covering spot-coated PCC.

Two commercial PCC grades (aragonitic and rhombohedral), and one GCC grade, were used as reference fillers. Particle size description of the reference fillers can be found in Table IV.

Table IV. Volume-based particle size data of the reference fillers (Beckman Coulter LS particle size analyser). Adapted from Publication V.

Sample ID	Description	Particle size, µm	
		Mean	Median
R-PCC	Rhombohedral precipitated calcium carbonate	3.353	1.873
A-PCC	Aragonitic precipitated calcium carbonate	3.498	3.092
GCC	Ground calcium carbonate	1.959	1.586

Aromatic starch based filler

Refractive indices of polymer materials can be approximated by using the Lorentz-Lorenz equation (Seferis 1999, Paquet *et al.* 2004)

$$R = \frac{n^2 - 1}{n^2 + 2}\frac{M}{\rho} \tag{10}$$

or the Gladstone-Dale equation

$$R = (n - 1)\frac{M}{\rho} \tag{11}$$

where

R is the molar refraction
n is the refractive index
M is the molecular weight
ρ is the density.

Molar refraction can be calculated by summing up all chemical group or bond refractivities constituting the molecule. For homopolymers, $R = DP*R_M$, where R_M
is the refractivity of its monomer unit, and DP the degree of polymerisation.

Aromatic groups display exceptionally high polarisability and refractivity compared with many other organic functional groups. Different chemical group or bond refractivities are listed in the literature (see for instance Krevelen 1976).

In the case of heterogeneous polymers, such as polymer blends, copolymers, or semicrystalline polymers with phase dimensions lower than the wavelength of light, Maxwell´s equations are applicable. RI, or its upper and lower boundaries, can be calculated using dielectric constants of constituent phases ($k = n^2$) (Seferis 1999, Partington 1960)

In organometallic chemistry, refractive index of metallocenes, a group of organometallic compounds, has been widely investigated (Paquet *et al.* 2004, Olshavsky and Allcock 1997). In this field, small scale tailoring through addition of functionalities with high molecular polarisability, incorporation of inorganic particles or high molar refraction elements have been utilised.

Heiser and Shand (1973) have covered using polymethyl methacrylate (PMMA) as a coating pigment. Examples of modification of PMMA for different applications can be found in the literature. Rasmussen (2001) has synthesised high refractive index polymers and copolymers to be used in eyeglasses by incorporating carbazole and other aromatic groups into methacrylates to get improved optical properties compared to PMMA.

Polyimide materials – which often contain aromatic groups in the molecules – can be tailored on the molecular level to achieve RIs up to 1.8 (Flaim *et al.* 2004).

Based, for instance, on the above findings reported in the literature, the author suggested utilising aromatic groups as a means to increase the RI and light scattering potential of a starch based pigment. The advantage of aromatic modification is that 100 % organic pigment can be obtained.

Therefore, novel aromatic starch benzoate pigments were synthesised at VTT as described in the Patent application by Mikkonen *et al*. (2008).

A commercial pearlescent pigment, and three calcium carbonate pigments (A, B, and C) displaying weight median particle size (d_{50}) around 5.6 µm, and 2-3 µm, respectively, were used as inorganic reference fillers. A starch acetate filler, synthesised earlier by VTT, was used as the organic reference filler.

Both of the organic fillers, i.e. starch acetate, and starch benzoate, displayed a porous structure made of particles with size below 1 µm.

RI of starch acetate has been reported earlier (Karvinen *et al.* 2007). RI of the starch benzoate filler was estimated through visual microscopic examination. First, a few drops of the immersion liquid (Cargille Laboratories, New Jersey, USA), displaying known refractive index in the range of 1.40 – 1.70, with intervals of 0.05, were applied on a filler sample. The immersed sample was then exposed to light from a quartz halogen lamp (Ernst Leitz Wetzlar GMBH, Germany), and further examined with an optical transmission microscope (Leitz Diaplan type 020-437.035). The procedure was repeated several times,

by subjecting the examined sample to contact with different immersion liquids, to find the best matching point between the refractive indices of the two, observed as disappearance of the filler sample. The RI evaluation was made by VTT.

Paper technical properties were examined at TKK with ordinary laboratory sheet moulding. Dried pulp (70 % birch, 30 % pine) was beaten to tensile strength index ~ 50 $Nm.g^{-1}$ and was used as furnish.

60 gm^{-2} handsheets were made in accordance with standard SCAN C 26:76. The handsheets were drum dried, air-conditioned, and analysed.

4.3. Results

Spot coated starch granule fillers

The PSD of the spot coated starch filler sample 2 (Table III) is presented in Fig. 22. The particle size gamut displays discrete bimodality in the particle size distribution, dominated by a large fraction of coarse starch granules (coated with fine Al-silicate particles as described below). The volume-defined median particle size, d_{50}, of this particle fraction is around 30 μm, an order of magnitude roughly ten times greater than the size exhibited by conventional fillers. In addition, a small fraction of fines material exhibiting a respective particle size around 300 nm can be observed. The fines fraction could indicate that not all Al-silicate particles are attached to the starch granules but are segregated instead. The reference filler has more typical particle size, the average value being around 5 μm, as estimated from the SEM images, such as presented in Fig. 24.

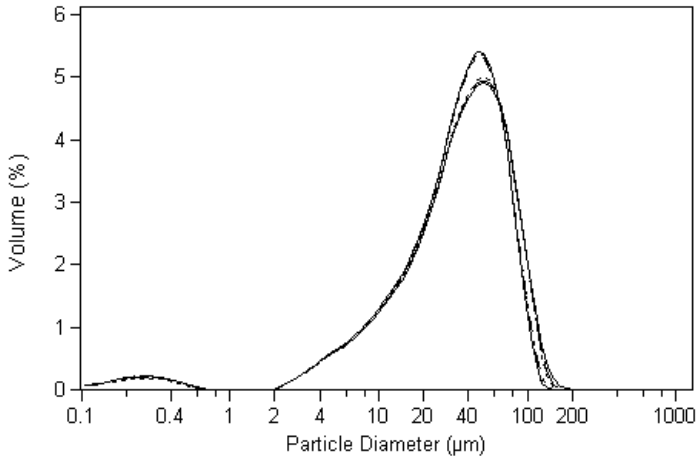

Fig. 22. Differential particle size distributions (the two curves represent replicated measurements) of a spot coated starch granule filler (sample 2). Adapted from Publication IV.

The surfaces of Al-silicate coated starch granules are presented in Fig. 23. The figures suggest an even introduction of fine Al-silicate particles on the coarse starch granules. The estimated size of the silicate particles varies in the range of 50 nm – 500 nm (as suggested also by Fig. 22, *viz.* the lower peak of the bimodal particle size distribution possibly presenting the unattached fine material fraction). This is around the optimum for effective interaction with light. Fig. 23 also suggests that the silicate particles have been usually deposited at an optimum spacing (≥ 200 nm) on the starch granules, displaying air-imparted RI contrasts between the particles, which is considered also beneficial for the light interaction.

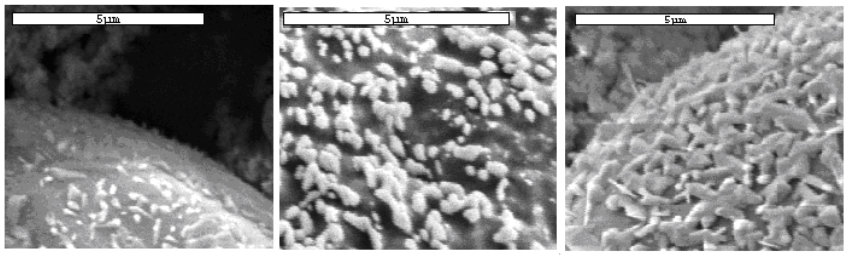

Fig. 23. Spot structures in samples 1 (left), 2 (middle), and 3. Adapted from Publication IV.

The reference Al-silicate filler is presented in Fig. 24. The filler consists of closely aggregated fine spherical aluminium silicate particles, building up

irregularly shaped highly porous larger pigment structures. The size of the fine particles is around 100-200 nm.

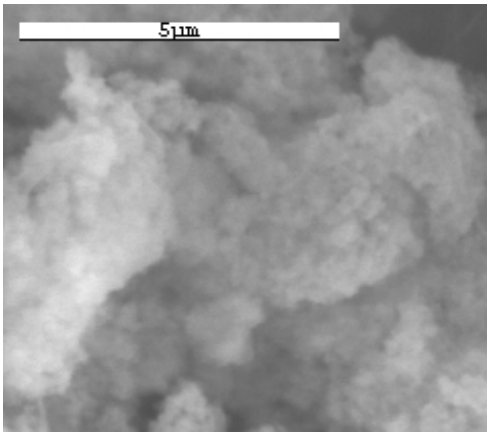

Fig. 24. Al-silicate based reference filler. Adapted from Publication IV.

In contrast to the starch filler samples 1-3, in the case of the reference the fine particles are arranged in a relatively densely packed configuration, displaying less spacing and probably more contact points to the surrounding particles. Due to the lack of refractive index (RI) contrast between the particles, light scattering is not as effectively generated in the absence of suitable interparticle spacing, i.e. effective surface porosity. In an optical sense, interparticle spacing displaying no less than 200 nm distance between the particles would be more beneficial.

The handsheet property combination of light scattering coefficient and Scott bond, provided by sample 2, is presented in Fig. 25. The results suggest significant benefits in the property combination when Al-silicate is introduced in paper on the starch particle surfaces instead of through the conventional free addition manner. This is suggested to be due to the synergy provided by the finely dispersed silicate and the coarse host starch granules. Being attached to the host particles, the silicate particles provide effective light scattering, but may not excessively disrupt the fibre network which would probably be the case if introduced in the conventional way. The restrained deterioration of strength is likely achieved due to coarse particle size provided by the starch host granules.

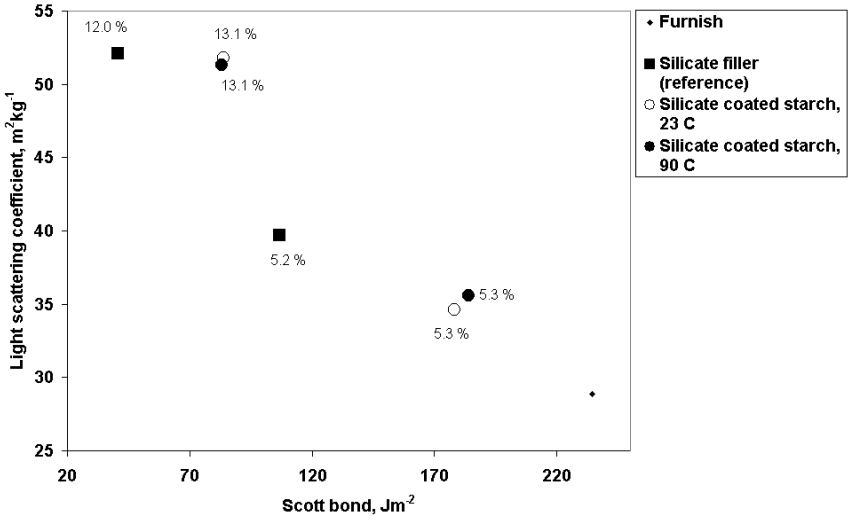

Fig. 25. Light scattering coefficient against Scott bond in different Al-silicate contents. Sample 2. Drying temperature is marked in the legend. Adapted from Publication IV.

The treatment of the handsheets at elevated temperature did not have a significant effect on the results. This suggests the ability of the starch particles to withstand the drying conditions examined.

Complex starch hybrid fillers

The results suggest that the new starch-hybrid fillers can be introduced in paper as fillers using the conventional forming procedure without adverse effects. Forming and visual examination of the sheets suggested feasible behaviour especially with the CMS + ($ZrO(NO_3)_2.xH_2O$) hybrid, which provided superior bulking ability. Fig. 26 presents the bulk values from the calendered sheets. Bulk is largely affected by the filler particle size, the volume occupied by the particles, and the calendering response of the filler. The CMS + $BaCl_2$ hybrid displayed strong bonding and significant densification of the sheets.

CMS + $BaCl_2$ and CMS + ($ZrO(NO_3)_2.xH_2O$) hybrid fillers displayed particle sizes markedly higher than the reference fillers. The volume-based particle size distributions of the hybrid fillers, were centred around 20-60 μm and 10 μm, respectively. Hence, the scattering properties of the hybrids will need further optimisation through PSD modification.

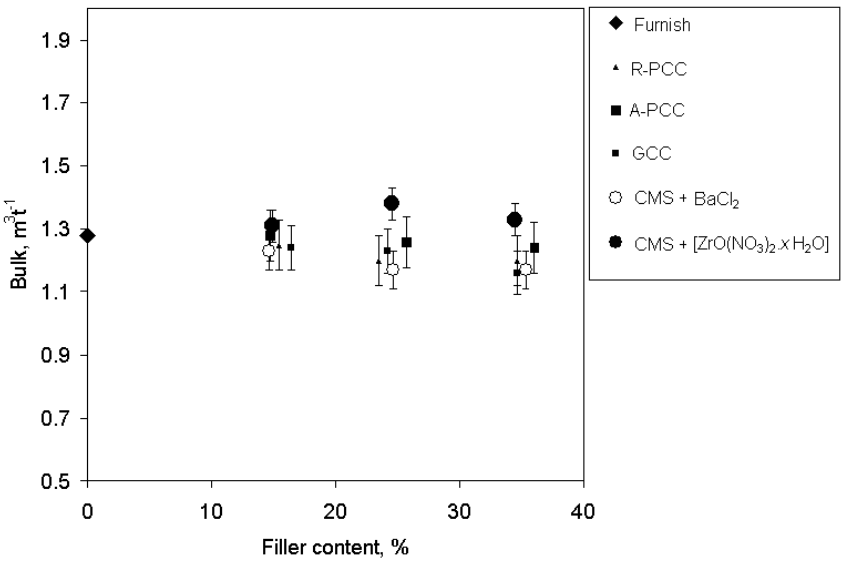

Fig. 26. Bulk of the calendered sheets containing two different starch-hybrid fillers, and inorganic reference fillers. Adapted from Publication V.

Aromatic starch based fillers

Incorporation of aromatic groups contributed to the refractive index of the organic filler. Refractive indices of the reference starch acetate and the aromatic starch benzoate were around 1.47 (Karvinen *et al.* 2007) and 1.50-1.55 (examined with the microscopic method), respectively. As further observed in the microscopic examinations, both fillers had a porous particle structure consisting of aggregated fine particles displaying sizes below 1 µm.

The light scattering coefficient measured from the filled sheets is presented in Fig. 27. These results suggest that with fixed filler content, i.e. fixed filler weight relative to the base paper weight, starch benzoate yields higher light scattering than the other fillers examined. The difference is emphasised when filler content is increased from 9.4 w-% to 18.0 w-%. Further increase to 28.3 w-% filler content displays a slight reduction in the light scattering gain, which might be an indication of optical crowding. Property combination of light scattering coefficient and tensile strength index, presented in Fig. 28, further suggests effective light scattering at fixed debonding.

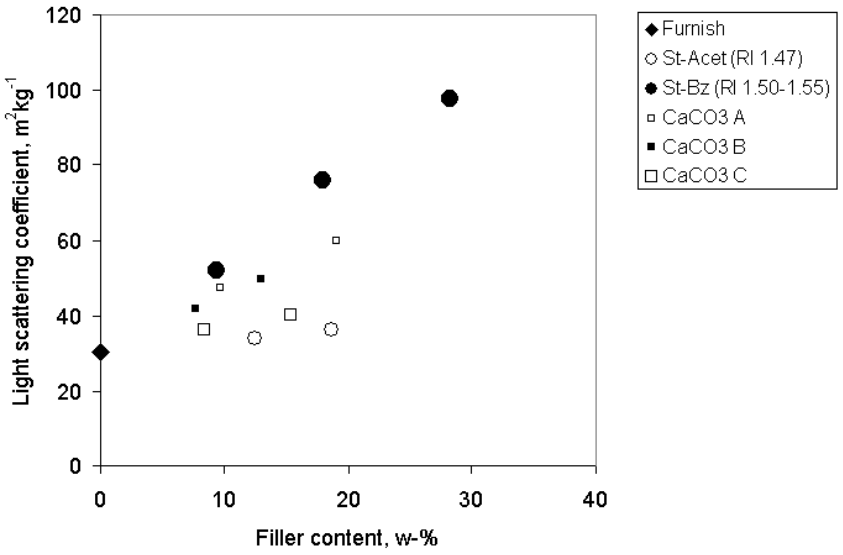

Fig. 27. Light scattering coefficient against filler content. The filler content is expressed as w-%. Sheets filled with organic starch based reference filler (St-Acet), optically enhanced starch based filler (St-Bz), and commercial calcium carbonate fillers (A, B, and C).

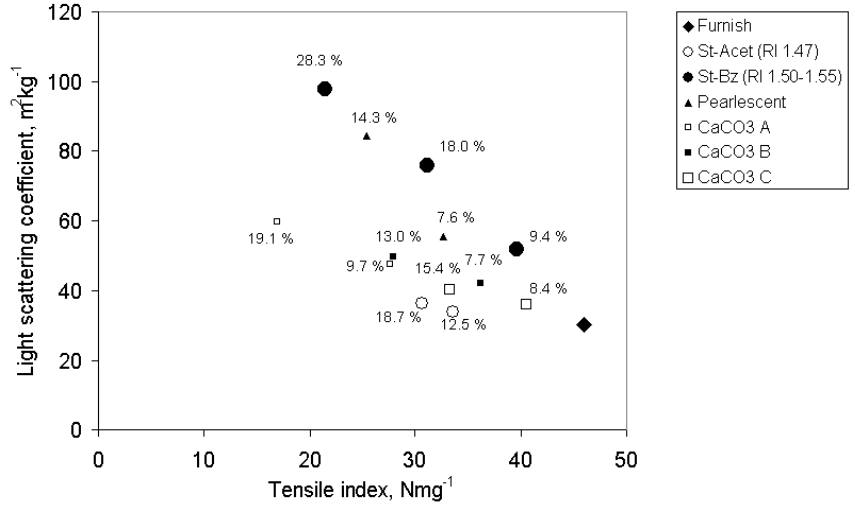

Fig. 28. Combination of light scattering coefficient and tensile strength index of sheets filled with organic starch based reference filler (St-Acet), optically enhanced starch based filler (St-Bz), commercial calcium carbonate fillers (A, B, and C), and a commercial pearlescent pigment. Filler contents of the sheets are expressed in terms of weight-%.

4.4 Discussion

The work described above illustrates three different approaches to tailor starch based materials to be further utilised as paper filler.

A semi-organic filler based on coarse starch granules spot-coated with an optically effective discrete layer of Al-silicate particles was developed in cooperation with research partners. The results suggest significant benefits in the property combinations of light scattering coefficient and strength when Al-silicate is introduced in paper on the starch particle surface instead of through the conventional manner of free addition. Being attached to the host particles, it is at this stage suggested that the silicate particles provide effective light scattering, but may not excessively disrupt the fibre network which would probably be the case if introduced in the conventional way. The reduced deterioration of strength is considered to be due to the coarse particle size provided by the starch host granules. On the other hand, the reduced effect on debonding decreases light scattering. This could explain the lower light scattering coefficient of the sheets when inspected with fixed filler content.

The second thesis hypothesis that organic filler particles can be utilised in novel ways with other materials to increase paper light scattering is partially supported in this case. The Al-silicate spot-coated starch granules yield improved property combinations, but when inspected against filler content, slight reduction in light scattering coefficient can be observed.

The potential of the starch-based hybrid fillers CMS + $BaCl_2$ and CMS + $(ZrO(NO_3)_2.xH_2O)$ will be further evaluated after optimisation of the scattering properties through milling.

An aromatic-modified starch benzoate filler, displaying fine aggregate structure and increased RI, developed in another research cooperation during this study, provided light scattering clearly surpassing the level provided by conventional inorganic fillers on a weight for weight basis. The result indicates that the refractive index of the organic filler particle itself can be increased, and, hence, supports the third thesis hypothesis.

The most frequently used ways to estimate papermaking potential of fillers include plotting the light scattering coefficient against tensile strength, as suggested by Alince (1989), and against filler content in terms of filler weight with relation to the weight of the base paper. In the former approach, with conventional fillers, increase of light scattering coefficient and corresponding decrease of tensile index are displayed, as filler content is increased. In this conventional way of presentation, the light scattering coefficient yielded at fixed tensile is used as the basis of the filler potential evaluation. In the latter standard way of presentation, plotting the property against filler content (w-%) does not provide sufficient basis for comparing fillers with differing specific

gravities in the same plot, as it fully ignores that fillers with lower specific gravity occupy greater volume proportion in respect to the total paper volume, and hence provide more surface for light interaction at fixed weight-%. Therefore, when examined alone, the plot may give distorted view about the light scattering properties of individual filler particles.

The results (Figs. 27-28), presented via the standard evaluation method, indicate that effective light scattering can be achieved by the novel starch benzoate filler, surpassing the level provided by both organic and inorganic reference fillers examined. The light scattering yielded by the starch benzoate filler at fixed tensile (Fig. 28) is higher than that provided by the other fillers, suggesting good potential to be used as filler in paper applications. The benefit can be considered significant, as, for instance, with 20 Nmg^{-1} tensile index, starch benzoate yields over 60 % higher light scattering coefficient than the calcium carbonate references. This might indicate the ability of the filler to promote more efficient use of fibres through, for instance, grammage reduction. That with around 18 w-% filler content the organic fillers yield equal tensile strength, but significantly different light scattering coefficient, indicates that the starch benzoate filler itself contributes scattering more than merely through increased debonding. This refers to the effect of increased RI.

In Fig. 29, the light scattering coefficient is plotted against filler content in terms of filler volume in relation to the base paper volume. The figure is obtained from Fig. 28 by using thickness and specific gravity data of the sheets and the fillers, respectively. The sheets exhibit thickness in the range of 110 µm – 120 µm. The calcium carbonates and the starch acetate filler used in this experiment display densities of 2.71 gcm^{-3} (Lide 1990) and 1.356 gcm^{-3} (Karvinen *et al*. 2007), respectively. For the density of the starch benzoate filler the value of the starch acetate (1.356 gcm^{-3}) is used as an approximation. The effect of filler density is further demonstrated in the case of starch benzoate by using additional density values in the range of 1.2 gcm^{-3} - 1.7 gcm^{-3}.

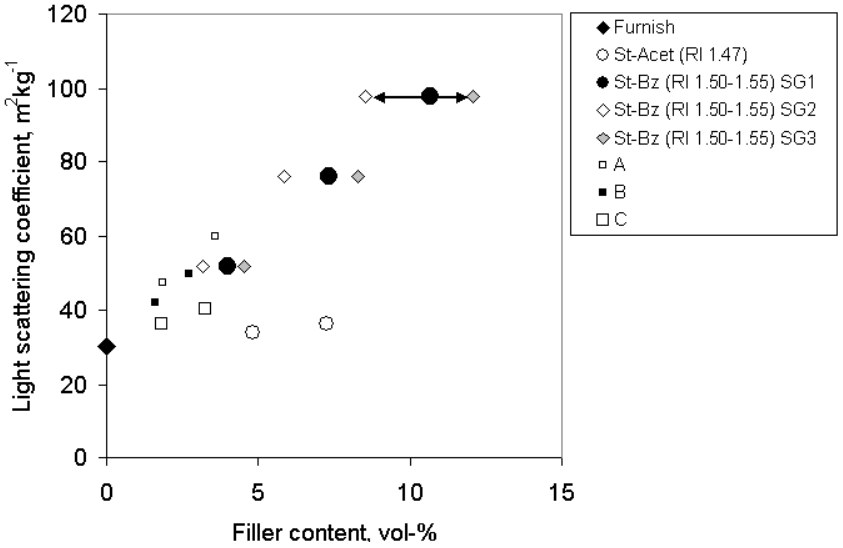

Fig. 29. Light scattering coefficient against filler content. Filler content is expressed in terms of vol-%. Sheets filled with organic starch based reference filler (St-Acet), optically enhanced starch based filler (St-Bz), and commercial calcium carbonate fillers (A, B, and C). SG1, SG2 and SG3 denote the specific gravities, 1.356, 1.7, and 1.2, respectively.

The results in Fig. 29 show that the calcium carbonate fillers A and B impart actually higher light scattering with constant volume-based filler content, suggesting effective scattering from the individual $CaCO_3$ bodies. Starch benzoate would give equally effective scattering with a nominal filler density around 1.7 gcm^{-3}.

All in all, the results suggest effective scattering due to the starch benzoate filler in the light of the three ways of presentation discussed (Figs. 27-29), and illustrate the significant effect of RI increase with optimally-sized particles. The results are also consistent with the current scattering theory based on the framework of the Mie scattering treatment (Mie 1908).

- Part II: Refractive Index in Printing Applications -

5 INTRODUCTION

Paper coatings, formed by application and drying of pigmented coating slurry onto a paper surface at a coating unit, and further, finishing through calendering in the following unit operation, display, in general, lower porosity and higher uniformity than the base paper substrate alone. Coating layers promote beneficial interactions with liquids during printing, limit linting, and improve the optical properties.

The interaction phenomena between the coating matrix and printing inks, such as the competing actions of spreading and absorption, can be influenced in a controlled manner by engineering the coating pore structure. Besides porosity, the pore size distribution, together with surface free energy of the involved phases, linked to external pressure if present, significantly affect the absorption behaviour. A critical factor is the pore connectivity within the coating matrix, enabling liquid absorption into the structure by capillarity in the finest pores, and pore wall wetting in the largest pores. Work done by, for instance, Schoelkopf *et al*. (2000a, b), Gane *et al*. (2004) and Ridgway *et al*. (2006a) highlight the preferred pathway wetting phenomenon of initially rapid wetting front propagation through fine pores at the moment the liquid is contacted with the coating surface. With longer contact times the filling of larger pores is completed, and the point of saturation gradually gains on the wetting front (Schoelkopf *et al.,* 2000a, b, 2003a, b, Gane *et al.* 2004). In other words, the concentration gradient at the wetting front increases as a function of contact time.

The capillary pressure across a wetting liquid meniscus in a cylindrical pore can be described by the Laplace equation

$$P = -\frac{2\gamma_{LV}\cos\theta}{r} \tag{12}$$

where

P is the pressure difference across the liquid meniscus
γ_{LV} is the surface tension of the liquid-vapour interface
θ is the contact angle
r is the radius of the cylindrical pore.

The well-known Lucas-Washburn equation concept of infinite cylindrical capillaries absorbing under viscous resistance-equilibrated flow is not fully comparable in paper coatings displaying to some extent non-uniform interparticle pore geometry, distances, and connectivity.

Actually, liquid propagation through capillary wetting in the finest pores of the coating structure is not at equilibrium within short timescales. In contrast, models by Szekely *et al.* (1971) and Bosanquet (1923) account for energy loss and inertial effects, respectively, as liquid flows in such heterogeneous media. In the Bosanquet model, the acceleration of a liquid in relation to its volume defines the preferential absorption on the nanoscale into the smallest pores before saturation of the larger voids is reached.

As discussed earlier in this study, pigment particle size and shape largely define the resulting interparticle pore structure. Traditional coatings often consist of blends of GCC and clay as beneficial pore structure is not typically achievable using standard GCC alone, except in the case of multicoated sheets. Interparticle pore structure, and the resulting liquid interaction, can be controlled to some extent through latex binder content, and, as suggested by van Gilder and Purfeerst (1994), and Rousu *et al.* (2002), the latex solubility index.

Current demands for higher brightness favour increased usage of GCC (Gane 1998). This has created a need for new structured calcium carbonate grades capable to provide advantageous coating structures as a single pigment. Bimodal pore size distributions of coatings have been shown to be achievable through recently introduced nanofeatured calcium carbonate coating pigments displaying fine intraparticle pores providing additional capillary driving force for liquid propagation (Gane 2006, Ridgway *et al.* 2006b).

Refractive index differences between the paper coating matrix, the liquid phase of the printing ink, or fountain solution, and air can be utilised in developing optical tools providing real-time information about the dynamics of liquid absorption into porous paper coating during printing. Knowledge of absorption behaviour of liquids into coatings is essential for the print quality, and controllability of printing processes. It is also an important factor in terms of the efficiency of print drying processes, such as in heatset web offset or in digital presses, as the distribution of liquid in the coated paper surface determines the relative heat energy required for liquid evaporation.

6 RELATING LIQUID LOCATION AS A FUNCTION OF CONTACT TIME WITHIN A POROUS COATING STRUCTURE TO OPTICAL REFLECTANCE

In the previous Part I of the thesis aggregate particles containing internal voids with distributed RI gradients were used as fillers in papermaking to enhance light scattering potential. In that study, it was highlighted that the effect of RI gradient variation is difficult to confirm alone, as its effect is convoluted with that of particle agglomerate size and internal pore distribution and size. Here, therefore, a further study is undertaken in which the pore size distribution is well-defined, in one case using solid particulate skeletal material (coating GCC pigment) and in a second case an internally porous skeletal material (modified calcium carbonate MCC), exhibiting a discretely bimodal pore size distribution. This latter case models an idealised filler that has internal porosity, but now we can maintain a consistent RI throughout the solid material. Using these model systems allows the RI contrast to be examined in a complementary way to that in the paper filler case, i.e. by reducing contrast rather than increasing it. Effect of changing SSA due to RI modification, observed in the case of PCC in the first part, is eliminated through modifying RI now through liquid absorption. In this way, the RI contrast behaviour can be illustrated without the convolution with the other parameters prevailing in the paper filler study. The link of value to paper coatings in the print process is then also an immediate corollary, and is further highlighted here.

Liquids usually exhibit higher refractive index than air, but lower refractive index than typical coating pigments and binders. Thus, a refractive index contrast modification takes place as liquid replaces air in the interparticle coating pores. This can be observed as intensity decrease of the diffuse reflection, or brightness, as the light scattering from the solid-liquid interfaces is reduced.

Binder can affect the absorption behaviour in a number of ways. Firstly, films formed by soluble binders can reduce the pore connectivity, which has further influence on the distribution of liquid. In the case of latex, liquids can additionally permeate by diffusion into the polymer matrix depending primarily on the similarity in solubility indices of latex and liquid (van Gilder & Purfeest 1994, Rousu *et al.* 2002). Therefore, the binder can swell, leading to a further reduction in pore network connectivity, and hence permeability, and even significant loss of pore volume (Xiang *et al.* 2003).

The objective of this part, as presented in the introduction, is to relate the liquid distribution within the porous coating network to optical reflectance.

6.1 Materials and Methods

Slurries of ground calcium carbonate (GCC[1]) and modified calcium carbonate (MCC[2]) pigments (RI 1.58) were compressed to tablets through wet filtration with a range of pore structures, controlled by the pigment type and binder content. The GCC displays blocky particle shape, and weight median particle size, d_{50}, around 1.5 µm (equivalent spherical diameter, e.s.d.). The MCC pigment exhibits internal nano-featured pore structure, with pore size close to the Bosanquet inertially-defined optimum, < 100 nm, (Schoelkopf *et al.* (2002) and Gane (2006)) at short timescales, and particle size, d_{50}, around 5.1 µm, estimated from micrographs. The binder used is a styrene acrylic latex[3] with narrow particle size distribution around 200 nm. More detailed presentation of the pigments, including the micrographs, can be found from Publication VII.

Specific pore volume and pore size distribution of the tablets were analysed by mercury porosimetry using an Autopore IV porosimeter[4], and corrected with Pore-Comp[5] software to account for mercury and penetrometer effects, as well as sample skeleton compression applying the equation given by Gane *et al.* (1996). The maximum applied pressure in the porosimeter was 415 MPa, able to probe the pore structure on the nanometre scale.

Liquid[6], in the form of a typical offset ink diluent oil (RI ~1.46), was absorbed into the tablets by capillary wicking without external pressure. Liquid uptake was thus driven by the capillarity of the porous tablet in contact with a supersource of the liquid, formed by a reservoir of excess liquid held in a decanting glass dish.

After a series of pre-determined contact times (60, 420, 900, 1 200, 1 500 s with GCC, and 60 s, 240 s, 420 s, 600 s with MCC) the tablet was dried by wiping away any excess surface liquid using a tissue, and the tablet with its contained liquid weighed.

Reflectance, *R*457, or ISO brightness (effective wavelength of $\lambda = 457$ nm), was detected from the exposed surface using an Elrepho[7] SE 070R

[1] Hydrocarb is a product name of Omya AG, Baslerstrasse, CH-4665 Oftringen, Switzerland
[2] The MCC pigment represents a proprietary technology patented by Omya AG, Baslerstrasse, CH-4665, Oftringen, Switzerland
[3] Acronal S 360 D is a product name of BASF, Ludwigshafen, Germany.
[4] Micromeritics, 4356 Communications Dr. Norcross, GA 30093-2901, U.S.A

[5] Pore-Comp is a program software name of the Porous Media Research Group at the University of Plymouth, U.K.

[6] PKWF™ 4/7 is a product name of Haltermann Products, Schopenstehl 15, 20095 Hamburg, Germany
[7] Elrepho is a product name of Lorentzen & Wettre, Kista, Sweden

spectrophotometer. After each measurement, a thin layer was removed from the tablet sample surface by grinding the surface carefully with sandpaper to obtain the reflectance, $R(t, z)$, as a function of height (length of absorption into the sample), z, and absorption time, t (see Fig. 30).

More details on the experimental procedure of the absorption procedure and the reflectance measurement can be found in Publication VI.

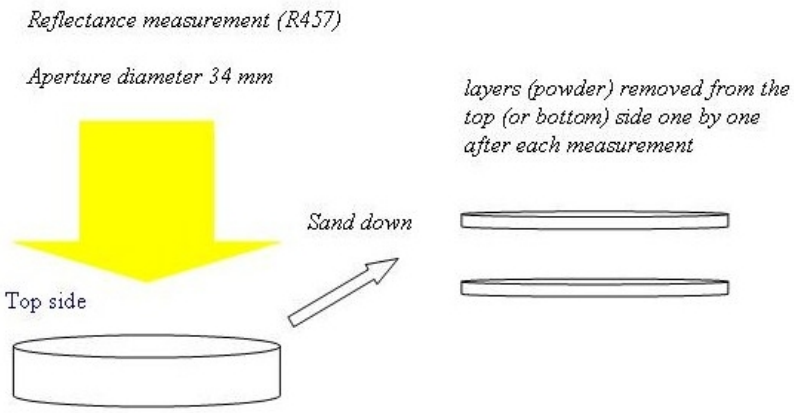

Fig. 30. Measurement of reflectance from exposed tablet. Adapted from Publication VI.

The influence of liquid absorption on latex swelling was examined by introducing and drying some of the latex onto a glass microscope slide, and then measuring the weight increase on immersing it in oil. The excess of oil remaining was removed with a tissue. A more detailed description of the method has been reported by Rousu *et al.* (2002). The swelling can significantly influence the pore structure. In the cases of high interaction, this is especially the case, such as can be observed between aromatic mineral oils and styrene butadiene latices of closely matching solubility index (Van Gilder and Purfeerst (1994), Rousu *et al.* (2002)). According to Xiang *et al.* (2003) with 14 pph latex content, latex with low swellability yields a higher volume of fine pores than latex with high swellability, indicating partial pore closing of the fine pores due to the swelling.

As more specifically explained in Publication VI, the specific pore volume lost by latex swelling, $\Delta\Phi$ cm^3g^{-1}, may be expressed as

$$\Delta\Phi = \Phi + [\varepsilon.n/(100+n)]/\rho_{oil} - w_{measured\ saturation}/\rho_{oil} \quad (13)$$

where

n	is the latex content in the coating, pph
ε	is the weight fraction of oil absorbed in latex
ρ_{oil}	is the density of oil
$w_{measured\ saturation}$	is the measured oil saturated mass of the coating.

If we consider this porosity loss using the parameters of our experimental case, where just 7 w/w% is the measured fractional uptake into the latex, then ε = 0.07. In the case of 12 pph latex content, using Equation (13), the pore volume lost, calculated accordingly, is 0.014 cm^3g^{-1}, adopting a measured density of oil, ρ_{oil}= 0.824 gcm^{-3}. The effect of this pore volume loss is shown in the "corrected" data for 12 pph latex below to illustrate how such a correction could be applied.

6.2 Results

The pore size distributions of the tablets, including the corrections made for compression are presented in Fig. 31. The results illustrate the effect of latex content on the total pore volume of the tablets, and the polydispersity (breadth of distribution) of the pore sizes, which plays an essential role in the development of the liquid front propagation and the liquid uptake capacity.

The GCC coatings exhibit a continuous, mono-modal pore size distribution around 200 nm (Fig. 31, left). With low latex content, a more significant fraction of fine pores are present, contributing to more rapid absorption and enhanced preferred pathway effect of the imbibing liquid, as obtained according to Schoelkopf *et al.* (2000a, b), Gane *et al.* (2004) and Ridgway & Gane (2002). Increasing latex content decreases the specific pore volume, and yields a narrower pore size distribution, centred at 200 nm, the size beneficial for light interaction.

In contrast, MCC yields a discrete, bimodal pore size distribution (Fig. 31, right). The fine, intraparticle nanopores of MCC (size 30 nm – 80 nm), and interparticle microvoids (1 μm) are further connected through throat-like connectivity pores acting as route-providing channels for the absorbing liquid, and bodies for effective interaction with light, in the manner more specifically explained in Publication VII.

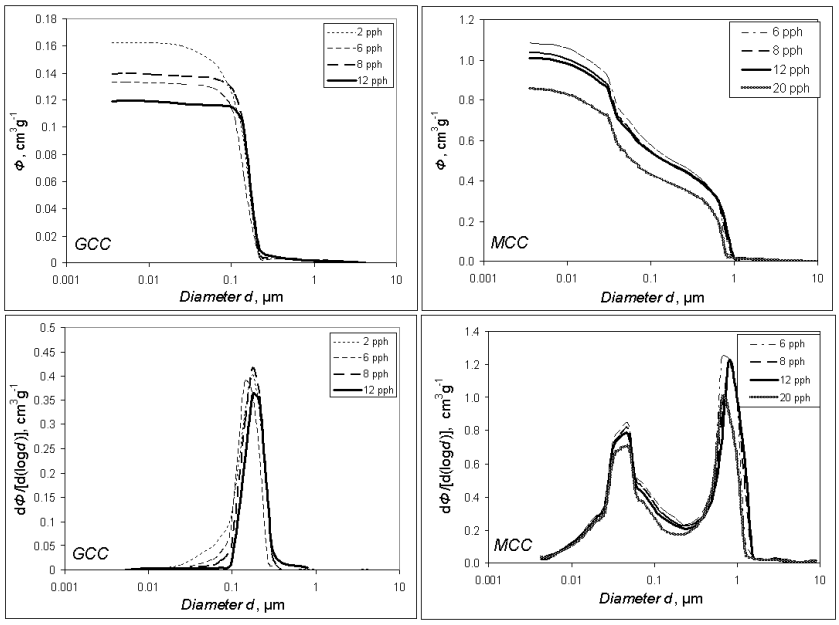

Fig. 31. Cumulative mercury intrusion (top) and differential (bottom) pore size distributions of the tablets formed for absorption study. Adapted from Publication VII.

Before the tablet surface is exposed to the liquid, the fluid present in the coating pores is air, and the refractive index contrast with regard to the coating components is at maximum. At the moment the liquid is contacted with the coating, the liquid starts to replace air, filling the first layer of fine pores first, and so the refractive index difference between the pores and the solid components is reduced. However, the optical effect is not maximised with the involvement of the fine pores. The filling is, in contrast, most clearly observed as decreasing reflectance when the next larger pores, displaying size suitable for light interaction, start to fill. Due to the presence of these optically interactive pores, filled with RI contrast reducing liquid, the reflectance is significantly reduced, as could also be predicted from, for instance, the treatment by Mie theory.

The reflectance data obtained with GCC coatings (Fig. 32) illustrate that the pores fill progressively and not at all fill at the same time, confirming the effects of preferred pathway wicking (Schoelkopf *et al.* 2000a, b, Ridgway *et al.* 2006a, Gane *et al.* 2004). It is known that rapid absorption occurs in the presence of small pores, and this dominates the initial wetting front distribution (Schoelkopf *et al.* 2000a, b, Gane *et al.* 2004, Schoelkopf *et al.* 2001, 2002, 2003a, b). Larger pores are first only partially filled (Schoelkopf *et al.,* 2000a, b, 2003a, b, Gane *et al.* 2004). With longer contact times the filling is completed, and the point of saturation gradually gains on the liquid front as

wetting proceeds through the structure with permeability becoming the progressive controlling parameter.

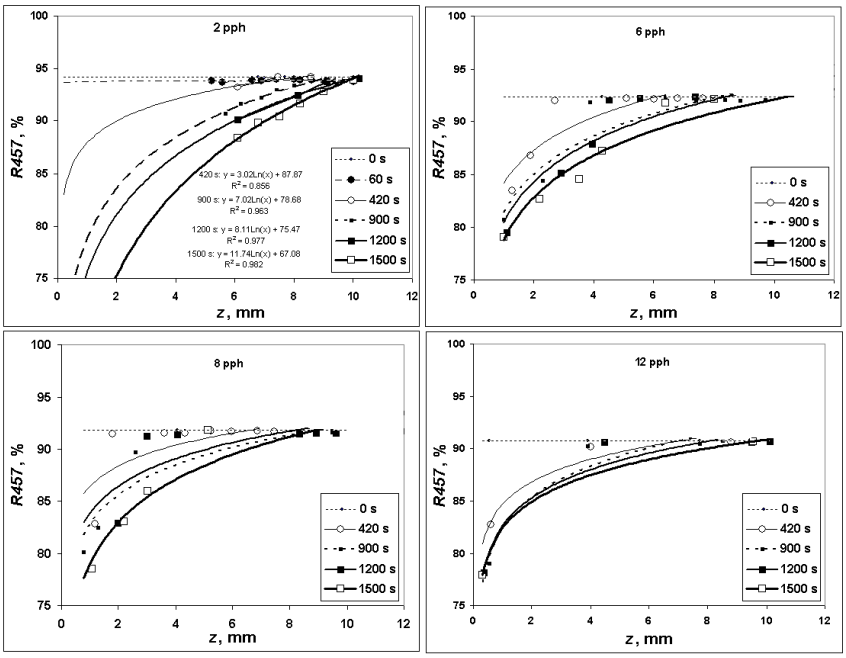

Fig. 32. Reflectance against the distance from the tablet bottom (absorption distance) with different latex contents. GCC coatings. Adapted from Publication VI.

Similar response in reflectance was observed in the case of MCC (see Publication VII). This indicates that with MCC coatings, the liquid distribution follows the same principles of capillarity and permeability with regard to optically active pores. In both coatings, part of the pores which are filled by the liquid, display effective size in terms of interaction with light. This is a prerequisite for observing the liquid distribution through optical reflectance measurements. In MCC coatings, filling of the throat-like connectivity pores can be clearly observed as decreasing reflectance, while the response to filling of the fine intraparticle pores and large interparticle voids is more moderate.

The reflectance data of Fig. 32 are presented as a logarithmic plot in Fig. 33, where a linear relationship can be observed.

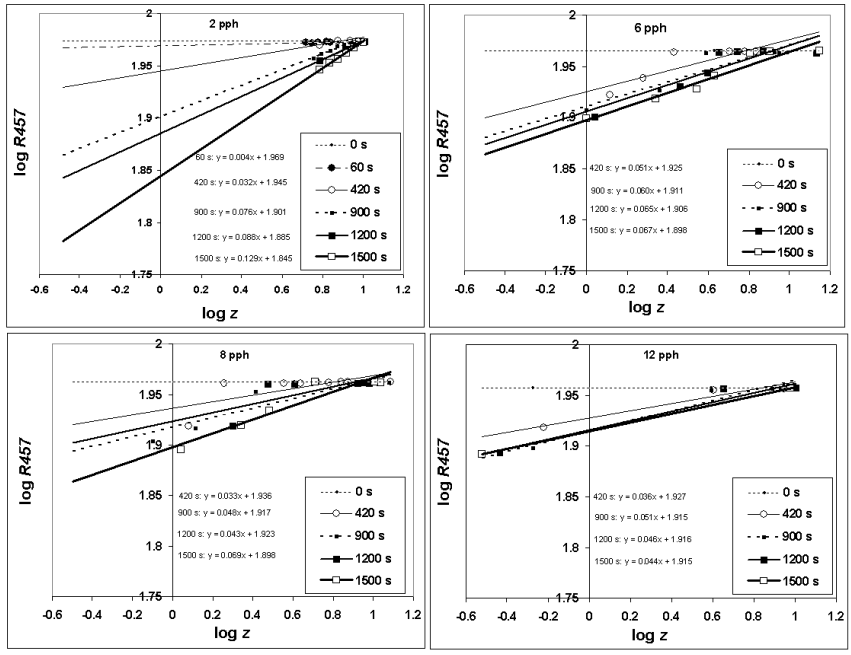

Fig. 33. Reflectance against the distance from the tablet bottom with different latex contents. GCC coatings. Logarithmic plot. Adapted from Publication VI.

The gradients of the lines in the logarithmic plots are re-plotted against contact time in Fig. 34. In the case of GCC, the gradients form a straight line relationship with respect to time over the shorter timescales, and for the 2 pph latex level over the complete timescale range. By contrast, this does not apply for long time scales (t > 1 000 s) in permeability-restricted structures, i.e. at higher latex levels. In fact they level off to a plateau as the absorption becomes defined by permeability alone, shown as dashed curves, i.e. at longer times. In the case of higher latex levels, there are regions in the structure that are unreachable by the liquid and so the gradient of pore filled volume as one approaches the wetting front at infinite time becomes a constant. Furthermore, latex swelling may cause additional blocking of the inter-pore connections. In the case of significant blocking, isolation of entire regions in the coating pore structure could be possible. Furthermore, although not verified, this result could be an indication of structural changes due to shifting of pigment particles from the original positions.

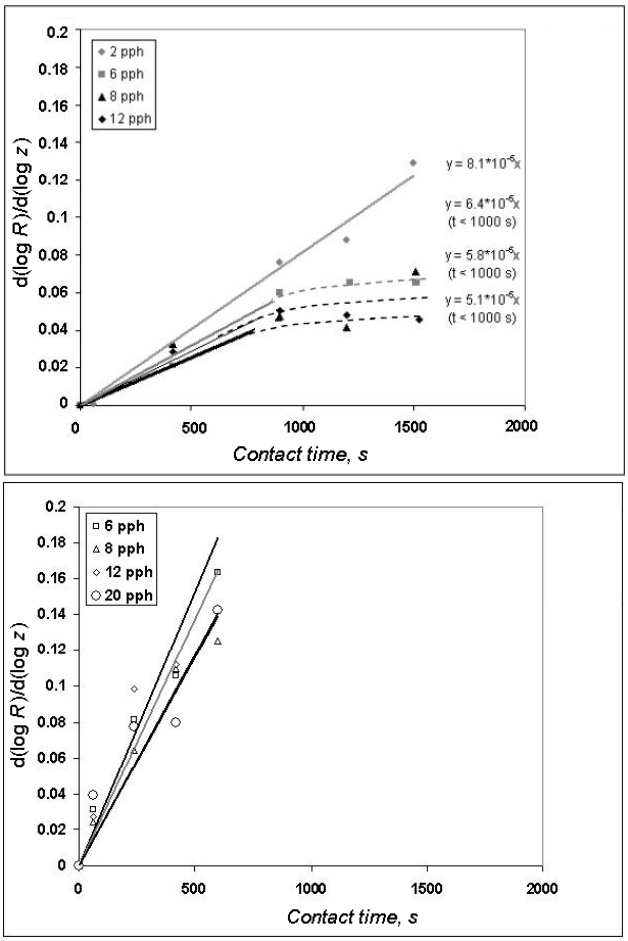

Fig. 34. Logarithmic reflectance gradient against contact time between the tablet and the liquid supersource. GCC (top) and MCC (bottom) coatings. Adapted from Publication VII.

Representing the behaviour seen in Fig. 34 in another way, it is possible to relate the liquid uptake by absorption as a linear function of square root of time, $\sqrt{t}$, by defining the mass absorbed, m_{abs}, per unit area, A, normalised to the sample porosity, ϕ, i.e. $m_{abs}(t)/(A\phi)$ (as presented in Publications VI-VII).

By combining the two linear relationships, the final relation of liquid uptake to optical reflectance can be established (Equation 14). The analysis of results has shown that by plotting the square of the porosity-normalised absorbed liquid mass $(m_{abs}(t)/(A\phi))^2$ against $d\log R(t, z)/d\log z$ we obtain the straight line relationships for absorbed liquid as a function of logarithmic reflectance gradient at a given time, t (Fig. 35).

$$\frac{\mathrm{d}\log R(t,z)}{\mathrm{d}\log z} = k_1 t \quad \text{and} \quad \left(\frac{m_{\mathrm{abs}}(t)}{A\phi}\right)^2 = k_2 t$$
$$\Rightarrow \left(\frac{m_{\mathrm{abs}}(t)}{A\phi}\right)^2 = \frac{k_2}{k_1}\frac{\mathrm{d}\log R(t,z)}{\mathrm{d}\log z} \tag{14}$$

With the GCC coatings, the result indicates increased logarithmic reflectance gradient from the tablets having higher latex contents (Fig. 35). This is due to their more homogeneous pore structure, as reported from the porosimetry, i.e. narrower pore size distribution centred around the size class that is highly interactive with the visible light wavelengths. As expected, the response of reflectance to the filling of the finer pore sizes in the porous structures is more moderate. With the MCC coatings latex content had minor effect.

The effect of pore volume loss due to the latex swelling is illustrated in the case of 12 pph latex content by including the porosity corrected values, $m_{\mathrm{abs}}/(A\phi_{\mathrm{corrected}})$, and comparing them together with the original values. The effect of swelling of the styrene acrylic latex on the relationship in Fig. 35, due to the aliphatic mineral oil, is only slight to moderate, which could also be expected from the observations reported by Rousu *et al*. (2002).

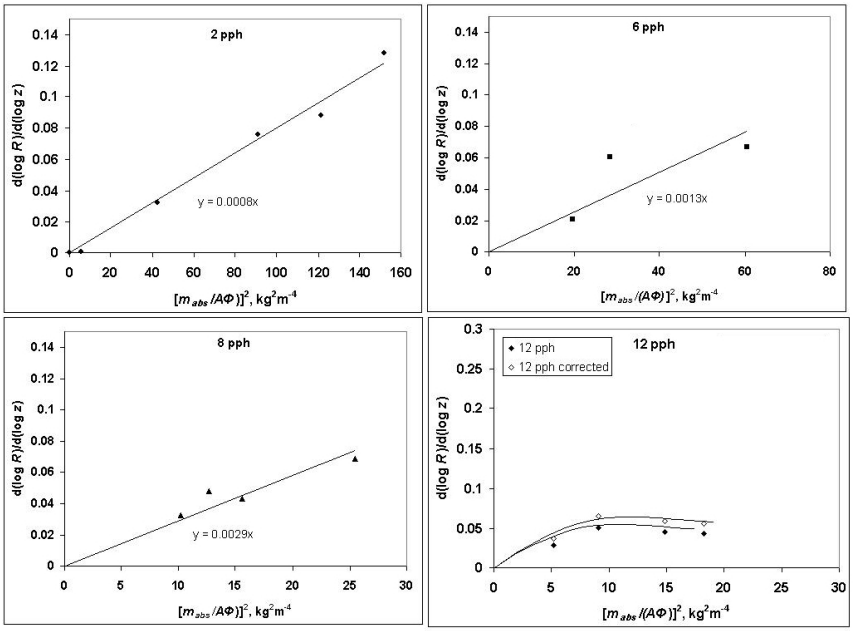

Fig. 35. The logarithmic reflectance gradient as a function of the square of the absorbed liquid mass. GCC coatings. The pore volume loss corrected data of tablets with 12 pph latex content, calculated according to Equation 13, is referred to as "12 pph corrected" in the legend. Adapted from Publication VII.

6.3 Discussion

This outcome is the first step in the development of a remote sensing tool enabling the detection of liquid distribution in porous systems under dynamic conditions, such as in printing applications, where only non-contact measurements can be considered. This is achievable through optical methods, for instance reflectance measurements based on diffuse illumination, and detection perpendicular to the coating surface, as illustrated in this study. That the liquid distribution can be monitored by reflectance measurements supports the fourth hypothesis of the thesis.

The preferred pathway propagation of liquid is gradually decelerated as a function of contact time, due to the effect of the viscous drag, and the point of saturation, $\sigma_{sat}(z)$, progressively gains on the wetting front position. The magnitude of the concentration gradient, i.e. the change in concentration per unit length, increases with time, and theoretically approaches infinity. This is illustrated by Equation 15, and further in the schematic diagram displayed in Fig. 36.

$$\left| -\left(\frac{\mathrm{d}\sigma}{\mathrm{d}z} \right)_{t_2} \right| > \left| -\left(\frac{\mathrm{d}\sigma}{\mathrm{d}z} \right)_{t_1} \right|, t_2 > t_1 \tag{15}$$

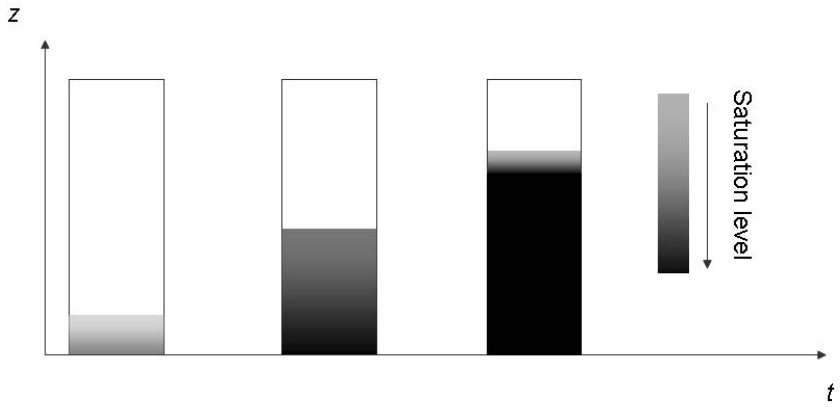

Fig. 36. The effect of liquid concentration gradient as a function of time. Adapted from Publication VI.

As the pore size varies within the range that is effective in terms of light interaction, it is possible to illustrate the concentration gradient increase with contact time through reflectance measurements. This is consistent with the fifth thesis hypothesis. Furthermore, the relationship between reflectance change in the *z*-direction of the coating structure, as a function of contact time, and the liquid uptake, was established. That the relationship is valid for both GCC and MCC coatings examined, suggests that in both cases the liquid distribution follows the same principles of capillarity and permeability with regard to optically active pores.

Knowing the relationship, the liquid uptake could be monitored in the future by scanning beneath the coating surface with non-destructive non-contact tools such as near-infra-red (NIR).

Reflectance was measured from surfaces of macroscopic blocks of tablets representing typical paper coatings. This was followed by removal of layers displaying thickness up to thousand-fold with regard to the size of the pigments used, after which the reflectance measurement was repeated. When incident diffuse light interacts with a coating layer, it is scattered back partly from the surface, while the rest of the backscattering comes from the underlying structure. Therefore, the reflectance values obtained are not purely surface-reflected values. The usage of macroscopic blocks of tablets enables the measurements with millimetre-wide intervals in the *z*-direction, suggesting that this approximation is justified.

As described in the introductory section of this thesis, the base paper is an extremely heterogeneous network consisting of fibres, various fibrous fragments, filler particles, and interconnected voids between the particles. The base sheet structure further affects the coating uniformity through the small-scale grammage and density variation (i.e. formation), and in particular, surface roughness (see for instance Dahlström & Uesaka 2009).

Naturally, the coating uniformity largely depends on the pigment, the binder, the degree of pigment flocculation, and the coating process. Variations in the coating structure have influence on the nature of the interaction between the coating and the liquids contacted with the coating in printing, and tend to contribute to mottling, or unevenness of printed image (Gliese & Gane 2005). Uniform coating displaying even distribution of well-dispersed pigments promotes beneficial interaction with liquids, such as ink and fountain solution, by absorbing them in a controlled way before reaching the base paper, protecting the base paper from being subjected to uneven moisture profile (which may further cause increased number of web breaks, blistering, and waving), reducing print-through, and, finally, improving the quality of the resulting image.

In the heat-set offset printing process, external heat energy is applied on the printed paper immediately after the printing units, to immobilise and set the oil-based offset inks and the fountain solution on the image- and non-image areas, respectively, through evaporation of the liquid phase involved. Information on the liquid distribution in the thickness of the coating is essential in terms of the print quality, runnability, and economics, as it determines the relative heat energy required, promoting more efficient control of the process variables.

7 CONCLUSIONS

The first objective of this study was to improve the paper optical properties, arising from diffuse reflectance, through introducing RI contrast in paper structure by new means. The RI approach was used due to the reasons crystallised in the following:

A) Current paper grades exhibit lack of interparticle and inter material RI contrast, as fibres, fines, fillers, coating pigments, and binders usually display similar refractive indices. Hence, significant light scattering is not generated at the solid-solid contact interfaces. Instead, interparticle pores, imparted by filler specific surface area and fibre debonding in the base paper, and coating particle dimensions and shapes in the coating, play a significant role in this respect by defining the pore space between particles. In uncoated grades, such as WFU, the role of fillers is critical.

B) It is advantageous, therefore, to introduce as much filler as possible. This however results in increased fibre debonding, reducing paper strength. The particle crowding effect may also negate any potential scattering benefit when high filler contents are used. Also process performance can be deteriorated. Hence, with conventional practices only, filler contents cannot be significantly increased.

C) As a consequence from B), filler particles must be optimised with limited dose. However, lot of work has already been done to affect particle size distribution, specific surface area, interparticle pore size, and flocculation, while RI contrast modification has received less attention.

D) According to current scattering theory, already a minor increase in RI of fine particles, displaying size around half the wavelength of light, can boost light scattering of the matrix. Fine pigments and fillers as RI modifying particles are, therefore, most beneficial.

Therefore, different fillers with increased RI, verified by spectrometric and microscopic methods, were developed in the laboratories during this study, and their effects in paper studied.

The results suggest beneficial light scattering potential of many of the novel fillers proposed. Also improved combinations of light scattering coefficient – strength properties were observed. The results indicate that the light scattering effects in paper can be contributed to by small-scale deposition of optically effective, fine particles on the filler surface, and by affecting the intrinsic filler RI through modification at the molecular level. Advantages with both inorganic and organic materials were observed.

Effective RI of clustered scalenohedral PCC filler was increased through introduction of high RI-particles as spots on the PCC surface. This was achieved through simple extension of the conventional carbonation process by utilising soluble RI modifying additives during the PCC precipitation. From the additives examined, especially Zn resulted in beneficial optical properties. Zn was deposited as ZnO spots (RI 2.0) displaying at least partially optimum size and inter-spot distances with regard to light interaction. In laboratory handsheet filler experiments, the novel PCC, displaying effective RI adjusted to 1.63-1.67 with the ZnO particles, improvement in reflectance, measured from standard filled handsheets, was achieved.

Besides adjusting the effective RI of PCC, the ZnO particles increased the filler SSA, and, further, had a beneficial contribution to interparticle spacing through increasing the number of optically effective pores in the sheet. With low ZnO content, yielding only slightly increased effective RI (about 1.60), the spacing effect was moderate, and no benefit in light scattering coefficient was observed. However, as the results suggested, calendering significantly increased the volume in the region of optically effective pores, and the light scattering coefficient was consequently boosted by increasing filler content, without adverse effects on bonding. This might be an indication of the synergistic effect due to the ZnO modified PCC filler, occurring in compressed highly-filled structures. In addition, no indications about the crowding effect were observed, and light scattering efficiency increased monotonically with increasing filler content. These findings enabled the mechanisms of filler structure and RI change to be differentiated.

In the light scattering modelling study from simulated model PCC coatings, incrementing effective RI from the original level, 1.58, to 1.60 – 1.62 through introduction of ZnO particles, displaying size around 150 nm, resulted in 4 - 7 % improvement in reflectance. The modelling study further suggested that increasing the effective RI of PCC through the used method, i.e. ZnO introduction, is more beneficial for light scattering than increasing the RI of bulk PCC particles. This was supported in practice when comparing the effects of densification of RI modified pigments by calendering sheets with high filler content. However, the approximations, especially in the radiative transfer (RT) approach in the case of multiple scattering calculations made for a piece of coating comprising several aggregates, and in the estimation of complex refractive index, must be considered as limitations to this modelling approach, and the results are therefore only indicative of possible mechanisms.

Using linear combination averaging, the Rayleigh criterion expression for a composite particle, consisting of smaller ZnO particles, exhibiting size around 50 nm, on the surface of an optimally sized PCC (for scattering in air), showed that the composite provided similar scattering power to that of separate PCC particles having the same total volume as the sum of the host PCC particles and the volume of the host plus attached ZnO particles, i.e. a scattering power similar to twice the loading by PCC alone.

The light scattering mechanisms due to the ZnO spot-coated PCC are suggested to be due to local RI contrast enhancement, increased SSA, both of which were verified, and the additional spacing effects, as suggested by the micrographs, and the pore size analyses. More work is needed to study the relative effects of the mechanisms.

The results obtained with the ZnO spot-coated PCC support the first hypothesis of the thesis. PCC filler can be used as a platform for optically effective fine RI enhancing structures, which further contribute to light scattering coefficient of paper.

From the soluble RI-modifying additives examined, also Sr had a beneficial effect on the optical performance of PCC. In contrast to Zn modification, the Sr additive yielded at least partly aragonitic PCC crystals. Even with low degree of modification, benefits in the pore structure and light scattering coefficient of the filled sheets were observed. Calendering reduced the volume related to optically effective pores, but did not significantly reduce the light scattering. This might be an indication that the light scattering advantage yielded by this filler is more dominated by the RI gradient with regard to the surrounding particles. A crowding effect was, however, observed with the Sr modified sample. However, as the results observed with Nano-S-PCC 3 arise from the conventional aragonitic structure, Sr modification as an approach was not found to support the first hypothesis.

The second thesis hypothesis was that light scattering effects in paper can be enhanced by utilising organic filler particles with other materials in novel ways. The results indicate that introduction of Al-silicate on the starch granule carrier with coarse particle size yields better combination of light scattering coefficient and strength property than conventional introduction of free addition. SEM images indicate that Al-silicate is distributed on starch granules in discrete manner, which supports the discussion on increased RI gradients when contrasted to densely packed configuration displayed by conventional Al-silicate filler. To verify that the interfaces occur in the paper structure in a similar way, closer examination of the filled sheet structures is required. The second thesis hypothesis is partially supported in this case. The Al-silicate spot-coated starch granules yield improved property combinations, but when inspected against filler content, slight reduction in light scattering coefficient can be observed. The novelty aspect was supported by a patent that was granted for this innovation.

In general, increase in RI contrast was most beneficially realised in increased light scattering with fillers displaying a particle size close to the optimal for light interaction. This observation is consistent with the scattering theory based on the Mie solution. An aromatic-modified starch benzoate filler, displaying fine aggregate structure and increased RI, developed in research cooperation during this study, provided light scattering clearly surpassing the level provided by conventional inorganic fillers on a weight for weight basis. An increase in the bulk filler particle refractive index was verified, which supports the third

thesis hypothesis. The handsheet results suggest that the starch benzoate filler itself contributes to light scattering more than merely through increased debonding effect. This refers to the increased RI.

The fillers examined behave mostly without disturbances or adverse effects in papermaking, as simulated by the Moving Belt former (MBF) experiments in this study. A lot of work remains to be done to examine the potential of these fillers further, for instance their impact on printability, as in some cases linting/dusting might be an issue. In the future work, biological aspects must also be considered, and optimal manufacturing and calendering conditions should be found. More work is needed to study the ability of the composite structures to stand the shear forces of a paper machine. Economic feasibility of the fillers is also to be evaluated, and their environmental impact considered.

In the second part of the study, due to the convolution problem recognised in the first part, i.e. identification of the response of light scattering coefficient to the increase of local refractive index contrasts in complex structures with simultaneous changes of particle configurations and overall pore structure, the response to decreased contrast was studied through liquid absorption in more uniform structures of coatings. This allowed the effect of RI contrast to be studied without the effects of the other parameters present in the first part.

The objective was to relate the liquid uptake and its distribution in the pore structure to optical reflectance measured from the coating surface exposed to contact with a chosen liquid supersource for a defined range of contact times.

The results suggest that the liquid distribution in a coating as a function of contact time can be detected by reflectance measurements. This is consistent with the fourth thesis hypothesis. As higher RI liquid replaces air in the pores, a significant decrease in reflectance is observed. A porosity normalised formula for reflectance change as a function of absorbed liquid mass was derived.

Using the reflectance measurement method utilised in this study, it was possible to observe the consistency of the results with the earlier findings made in the study field of liquid absorption into coatings, displaying rapid and uneven initial absorption of the liquid front, driven by the fine pore capillarity, and followed by subsequent filling of larger pores. This, finally, supports the fifth thesis hypothesis. As time progresses the saturation point of the liquid filling the structure gradually approaches that of the advancing wetting front, eventually making the wetting front more evenly distributed.

In coatings comprising standard GCC pigment the structural effect of latex content significantly influenced the reflectance change. The reflectance change with regard to the mass taken up by the coating structure was most significant with coating structures displaying narrow pore size distribution centred around the particle size suitable for effective light interaction, i.e. half the wavelength of light. This observation is in line with the considerations of the Mie solution,

suggesting highest effect in RI change in light scattering with particles or pores displaying half-wavelength size.

The results obtained with GCC were contrasted with coatings containing modified calcium carbonate (MCC) displaying unique internal nano-featured pore structure. The results suggest similar response in reflectance with the MCC coatings, which indicate that the liquid distribution in the coating structure follows the same principles of capillarity and permeability with regard to pores displaying optically effective size. The results emphasise the role of the refractive index gradients at optimal pores as an important factor defining the magnitude of the optical response.

The outcome of the second part is further considered useful as a first step in the development of on-line measurements for observing dynamic liquid uptake into porous coating structures. Applications of such methods are foreseen as being of value in controlling printing press properties and efficiency, for example in the case of heatset web offset, where ink and fountain solution drying efficiency depends on the distribution of these liquids within the pore structure of the paper.

In conclusion, the combination of the publications and complementary results bound together in this work suggest that the methods studied provide potentially important new means to utilise RI contrast modification in paper making, finishing and printing applications.

REFERENCES

Adams, J. M. (1993): Particle Size and Shape Effects in Materials Science: Examples from Polymer and Paper Systems. Clay Miner. 28: 509-530.

Agnihotri, R., Mahuli, S. K., Chauk, S. S., Fan, L. S. (1999): Influence of Surface Modifiers on the Structure of Precipitated Calcium Carbonate. Ind. Eng. Chem. Res. 38: 2283-2291.

Alince, B. (1986): Light scattering of pigments in papermaking. Pap. Puu 68: 545-547.

Alince, B. (1989): Optimisation of pigment performance in paper. Transactions of the Fundamental Research Symposium, Vol 1. Ed. C. F. Baker. Mechanical Engineering Publications, Cambridge, pp. 495-510.

Alince, B. & Lepoutre, P. (1983): Interaction of cationic clay particles with pulp fibers. Tappi J. 66(2): 92-95.

Alince, B. & Lepoutre, P. (1985): Light scattering in filled sheets - separating the contribution of the pigment and of debonding, Tappi J. 68(4): 122-123.

Alince, B., Porubska, J., van de Ven, T.G.M. (2002): Light scattering and microporsity in paper. J. Pulp Pap. Sci. 28(3): 93-98.

Aspnes, D. E. (1982): Local-Field Effects and Effective-Medium Theory: A Microscopic Perspective Am. J. Phys. 50: 704-709.

Pat. DE3014620. Modifiziertes Calciumcarbonat und Verfahren zu dessen Herstellung. Nicolaus MD Papier, DE (M. Baumeister & H.-P. Hofmann). App. DE19803014620, 1980—04-16. Publ. 1981-10-29.

Borch, J. & P. Lepoutre, P. (1978): Light reflectance of spherical pigments in paper coatings. A comparison with theory. Tappi 61(2): 45-48.

Bosanquet, C. H. (1923): On the flow of liquids into capillary tubes. Philos. Mag. Ser. 6 45(267): 525-53.

Bourlinos, A. B., Karakassides, M. A., Petridis, D. (2001): Synthesis and characterization of hollow clay microspheres through a resin template approach. Chem. Commun. 16: 1518-1519.

Bown, R. (1997a): A Review of the Influence of Pigments on Papermaking and Coating. Proceedings of the 1997 Cambridge FRC Symposium. pp. 83-137.

Bown, R. (1997b): Particle size, shape and structure: Effects of fillers on paper. Pira International conference on use of minerals in papermaking. Manchester, UK. Pira publications. pp. 62-78.

Boyd, R. W. & Sipe, J. E. (1994): Nonlinear optical susceptibilities of layered composite materials. J. Opt. Soc. Am. B 11: 297 -303.

Braybrook, A.L., Heywood, B.R., Jackson, R.A., Pitt, J.K. (2002): Parallel computational and experimental studies of the morphological modification of calcium carbonate by cobalt. J. Crystal Growth 243(2): 336-344.

Breunig, A., Fischer, C., & Farber, K (1990): Use of calcium carbonate-kaolin mixtures in supercalendered papers – advantages in quality and determination of calcium carbonate-kaolin portions. Wochenbl. für Papierf. (118)20: 903-905.

Brunauer, S., Emmet P. H., & Teller, E. (1938): Absorption of gases and multimolecular layers. J. Am. Chem. Soc. 60: 309-319.

Buijnsters, P., Donners, J. J. J. M., Hill, S. J., Heywood, B. R., Nolte, R .J. M., Zwanenburg, B., Sommerdijk, N.A.J.M. (2001): Oriented Crystallization of Calcium Carbonate under Self-Organized Monolayers of Amide-Containing Phospholipids. Langmuir 17: 3623-3628.

Chylek, P. & Videen, G. (1998): Scattering by a composite sphere and effective medium approximations. Opt. Commun. 146: 15-20.

Climpson, N. A. & Taylor, J. H. (1976): Pore size distributions and optical scattering coefficients of clay structures. Tappi 59: 89-92.

Dahlström, C. & Uesaka, T. (2009): New Insights into Coating Uniformity and Base Sheet Structures. Ind. Eng. Chem. Res. 48(23): 10472-10478.

Demirors, A. F., van Blaaderen, A., & Imhof, A. (2010): A General Method to Coat Colloidal Particles with Titania. Langmuir 26(12): 9297-9303.

Djurišic, A. B. & Leung, Y. H. (2006): Optical properties of ZnO nanostructures.
Small (8-9): 944-961.

Draine, B. T. & Flatau, P. J. (1994): The discrete dipole approximation for scattering calculations. J. Opt. Soc. Am. A 11: 1491-1499.

Eiden-Assmann, S., Widoniak, J., & Maret, G. (2004): Synthesis and Characterization of Porous and Nonporous Monodisperse Colloidal TiO_2 Particles. Chem. Mater. 16(1): 6-11.

Enomae, T., Tsujino., K. (2004): Application of spherical hollow calcium carbonate particles as filler and coating pigment. Tappi J. 3(6): 31.

Evans, R.C. (1954): Einführung in die Kristallchemie. Barth Verlag, Leipzig.

Fairchild, G. H. (1992): Increasing the Filler Content of PCC-Filled Alkaline Papers. Tappi J. 75(8): 85-90.

Feynman, R.P., Leighton, R.B., Sands, M. (1964): The Feynman Lectures on Physics. Volume 1, Mainly mechanics, radiation and heat. Addison-Wesley Publishing Company. Reading, MA. P. 31-1.

Flaim, T., Wang, Y., Mercado, R. (2004): High Refractive Index Polymer Coatings for Optoelectronics Applications. Proceedings of the SPIE – The International Society for Optical Engineering, Advanced in Optical Thin Films, pp. 423-434.

Pat. JP 62207714. Production of calcium carbonate. Maruo Calcium (T. Fujiwara, T. Maida., & H. Shibata). App. 19860051209 1986-03-08. Publ. 1987-09-12.

Gane, P. A. C. (1998): New Flexibility for Print-surface Design from 100% Natural Ground Calcium Carbonate. TAPPI 1998 Coating/Papermakers Conference. New Orleans. p. 807-817.

Gane, P. A. C. (2001): Mineral pigments for paper: Structure, function and development potential. Wochenbl. Papierfabr.129(3): 110-116.

Gane, P. A .C. (2006) Decoupling capillarity and permeability for rapid liquid absorption: Nanotechnology solution to super absorbers, 6th International Paper and Coating Chemistry Symposium. Stockholm. June 7-9, 2006.

Gane, P. A. C., Buri, M., Blum, R. (1999): Pigment co-structuring: New opportunies for higher brightness coverage and print-surface design. International Symposium on Paper Coating Coverage, Helsinki. February 1999. AEL Metsko. pp. 2-17.

Gane, P. A. C., Kettle, J.P, Matthews, G.P., Ridgway, C.J. (1996): Void space structure of compressible polymer spheres and consolidated calcium carbonate paper-coating formulations. Ind. Eng. Chem. Res. 35: 1753-1764.

Gane, P. A. C., Ridgway, C.J., Schoelkopf, J. (2004): Absorption rate and volume dependency on the complexity of porous network structures. Transp. Porous Med. 54(1): 79-106.

Pat. EP0270103 (1998): A method and apparatus for manufacturing filler-containing paper. Mo och Domsjoe AB, SE (Gavelin, G.). App. EP19870117847, 1987-12-02. Publ.
1988-06-08. 16 p.

Giertz, H.W. (1951): Opaciteten hos pappersmassor. Svensk Papperstidn. 54(8): 267-274.

Gill, R. A. (1990): The Performance of Precipitated Calcium Carbonate Fillers in Fine Quality Printing and Writing Papers. Proc. Materials Res. Soc. Symp. 197: 325-341.

Gill, R. A. (1991): The effect of precipitated calcium carbonate filler characteristics on the optical and permeability aspects of paper. 1991 International paper physics conference proceedings. Kona, Hawaii. September 22-26, 1991. Tappi Press. Atlanta. pp. 211-218.

Gliese, T. & Gane, P. A. C. (2005): Mottling-Phänomene bei holzfreien, gestrichenen Papieren. Wochenbl. Papierfabr. 133(6): 274-279.

Gruber, E., Bothor, R, Dintelmann, T. (1998): Modified granular starches for wet end application. EUCEPA symposium 1998 - chemistry in papermaking. Florence, Italy. Oct. 12-14 1998. pp. 379-391.

Hadiko, G., Han, Y. S., Fuji, M., Takahashi, M. (2005): Synthesis of hollow calcium carbonate particles by the bubble templating method. Materials Letters 59: 2519-2522.

Hagemeyer, R. W. (1960): The effect of pigment combination and solids concentration on particle packing and coated paper characteristics. Tappi 43(3): 277-288.

Hamm, U. (1998): Final fate of waste from recovered paper processing and non-recycled paper products. Recycled Fiber and Deinking. Ed. L. Göttsching, and H. Pakarinen. Fapet Oy. Jyväskylä. pp. 507–591.

Han, Y. R. & Seo, Y. B. (1997): Effect of Particle Shape and Size of Calcium Carbonate on Physical Properties of Paper. J. Korea Tappi 29(1): 7-12.

Hanecker, E. (1994): Alternative Verwertung von Reststoffen – ausser thermische Nutzung – getrennt nach Fasern und Füllstoffen, INDEGE Report 2892 PTS, Papiertechnische Stiftung, Munich.

Hatakeyama, H., Matsumura, H., & Hatakeyama, T. (2005): Lignin-based polyurethane composites with inorganic fillers. Appita Conference Proceedings, pp. 573-576.

Heiser, E. J. & Shand, A. (1973): Lightweight Polymeric Pigment, Tappi 56(2): 101-104.

Hemstock, G.A. (1962): The effect of clays upon the optical properties of paper. Tappi 45(2): 158A-159A.

Holm, M. (2007): Building paper performance through filler design. Fillers and Pigments for Papermakers. Berlin, Germany. June 13-14 2007. Pira International. pp. 20-56.

Holm, M. & Manner, H. (2001): Increasing filler content of fine paper by using preflocculation. 28th DITP International Annual Symposium, Bled, Slovenia. November 14-16, 2001. pp. 167-170.

Howard, G. J. (1983): The influence of polymers on the light scattering of TiO_2 pigment in paper. Tappi 66(6): 87-91.

Hsu, W.P., Yu, R., & Matijevich, E. (1993): Paper Whiteners I : Titania Coated Silica. J. Colloid Interface Sci. 156(1): 56-65.

Husband, J. & Nutbeem, C. (2001): A practical approach to engineered pigments. Paper Technology 42(8): 57-66.

Ingmanson, W. L. & Thode, E. F. (1959): Factors contributing to the strength of a sheet of paper. II. Relative bonded area. Tappi 42: 83-93.

Ishikawa, M. & Ichikuni, M. (1984): Uptake of sodium and potassium by calcite. Chem. Geol 42: 137-146.

Jaakkola, P. & Manner, H. (2001): Comparison of Methods for Stabilization of PCC against Dissolution at Acid Papermaking Conditions. Nord. Pulp Pap. Res. J. 16(2):113-117.

Jaffe, H.W. (1996): Crystal Chemistry and Refractivity. 2nd Edition. Dover Publications, Mineola, New York. 335 p.

Johnson, J. A., Heidenreich, J. J., Mantz, R. A., Baker, P. M., Donley, M. S. (2003): A multiple-scattering model analysis of zinc oxide pigment for spacecraft thermal control coatings. Prog. Org. Coat. 47(3-4): 432-442.

Karvinen, P., Oksman A., Silvennoinen R., Mikkonen, H. (2007) Complex refractive index of starch acetate used as a biodegradable pigment and filler of paper. Opt. Mater. 29(9): 1171-1176.

Ketola, H., Andersson., T. (1998): Dry-strength additives. Papermaking Chemistry. Ed. L. Neimo. Fapet Oy. Jyväskylä. pp. 269-287.

Kim, I.W., Robertson, R.E., Zand, R. (2005): Effects of Some Nonionic Polymeric Additives on the Crystallization of Calcium Carbonate. Cryst. Growth Des. 5(2): 513-522.

Kitano, Y. (1962): The behavior of various inorganic ions in the separation of calcium carbonate from a bicarbonate solution. Bull. Chem. Soc. Japan 35: 1973-1980.

Klein, C. & Hurlbut, C. S. (1999): Manual of Mineralogy (After James D. Dana). 21st edition. John Wiley & Sons. New York. 681 p.

Krevelen, D.W. (1976) Properties of Polymers: Part III, Properties of Polymers in Fields of Force. Elsevier. New York.

Krogerus, B. (1998): Fillers and Pigments. Papermaking Chemistry. Ed. L. Neimo. Fapet Oy. Jyväskylä. pp. 117-149.

Kubelka, P. & Munk, F. (1931): Ein Beitrag zur Optik der Farbanstriche. Ann. Techn. Phys. 11: 593-601.

Lakhtakia, A. (2001): Application of strong permittivity fluctuation theory for isotropic, cubically nonlinear, composite mediums. Opt. Commun. 192: 145-151.

Lattaud, K., Vilminot, S., Hirlimann, C., Parant, H., Schoelkopf, H., Gane, P. (2006): Index of refraction enhancement of calcite particles coated with zinc carbonate. Solid State Sci. 8: 1222-1228.

Laufmann, M. (2006): Pigments as fillers. Handbook of paper and board. Ed. H. Holik. Wiley-VCH Verlag GmbH&Co. Wenheim.

Leskelä, M. (1997): Simulation of Particle Packing for Modelling the Light Scattering Characteristics of Paper. Doctoral Thesis. Helsinki University of Technology. Department of Forest Products Technology. Otaniemi 1997. 255 p.

Leskelä, M. (1998): Optical properties. Paper Physics. Ed. K. Niskanen. Fapet Oy. Jyväskylä. pp. 117-137.

Lide, D. R. (1990): CRC handbook of chemistry and physics: a ready-reference book of chemical and physical data. 71st ed. Boca Raton, CRC.

Lord Rayleigh (1871): On the scattering of light by small particles. Philos. Mag. 4-41(275): 447-454.

Luukko, K. (1999): Characterization and Properties of Mechanical Pulp Fines. Acta Polytechnica Scandinavica. Chemical Technology Series No. 267. The Finnish Academy of Technology. Espoo. 60 p.

Maxwell, J. C. (1865): A Dynamical Theory of the Electromagnetic Field, Philosophical Transactions of the Royal Society of London 155, 459-512

McLain, L. & Wygant, R. (2006): Balancing Filler Characteristics Maximizes Sheet Performance. Pulp Pap. 80(3): 46-49.

Merrill, L., & Bassett, W.A. (1975): The Crystal Structure of $CaCO_3$ (II), a High-Pressure Metastable Phase of Calcium Carbonate. Acta Cryst. B31: 353-349.

Mie, G. (1908): Beiträge zur Optik trüber Medien, speziell kolloidaler Metallösungen. Ann. Phys. 25(3): 377-445.

Middleton, S. R., Desmeules, J., and Scallan, A.M. (1994): The Kubelka-Munk Coefficients of Fillers. J. Pulp Pap. Sci. 20(8): 231-235.

Pat. FI-20086261. Uudet polysakkaridi-pohjaiset pigmentit ja täyteaineet. Valtion teknillinen tutkimuskeskus, FI (H. Mikkonen, K. Putkisto, S. Peltonen, S. Hyvärinen, K. Koivunen). App. FI-20086261, 2008-12-31. Publ. 2010-07-01.

Nassrallah-Aboukaïs N., Boughriet A., Fischer J. C., Wartel M., Langelin H. R., Aboukaïs A. (1996): Electron paramagnetic resonance (EPR) study of Cu2+ and Mn2+ ions interacting as probes with calcium carbonate during the transformation of vaterite into cubic calcite. J. Chem. Soc., Faraday Trans. 92(17): 3211- 3216.

Nelson, K. (2007): Enhanced Performance and Functionality of TiO_2 Papermaking Pigments with Controlled Morphology and Surface Coating. Doctoral thesis, Georgia Institute of Technology.

Niskanen, K., Kajanto, I., and Pakarinen, P. (1998) Paper structure. Paper physics. Ed. K. Niskanen. Fapet Oy. Jyväskylä. pp. 13-53.

Niskanen, I., Räty, J., Peiponen K.-E. (2006): A multifunction spectrophotometer for measurement of optical properties of transparent and turbid liquids. Meas. Sci. Technol. 17: N87 –N91.

Okumura, M. & Kitano, Y. (1986): Coprecipitation of alkali metal ions with calcium carbonate. Geochim. Cosmochim. Acta 50(1): 49-58.

Olshavsky, M. & Allcock, H.R. (1997): Polyphosphazenes with High Refractive Indices: Optical Dispersion and Molar Refractivity. Macromolecules 30: 4179-4183.

Page, D. H. (1989): The beating of chemical pulps – the action and the effect. Fundamentals of Papermaking, Vol. 1. Transactions of the Ninth Fundamental research Symposium. Ed. C. F. Baker, V. W. Punton. Cambridge. September 1989. Mechanical Engineering Publications Limited. London. pp. 1-38.

Papp, J. (1989): The Use of Calcined Clay in Lightweight Papers. Nord. Pulp Pap. Res. J. 1: 4-7.

Paquet, C., Cyr, P.W., Kumacheva, E., Manners, I. (2004): Polyferrocenes: metallopolymers with tunable and high refractive indices. Chem. Commun. 234-235.

Partington, J.R. (1960): An Advanced Treatise of Physical Chemistry:Physico-Chemical Optics, Vol. IV, Longmans, Green and Co, London.

Passe-Coutrin, N., Ph. N'Guyen, Ph., R. Pelmard, R., A. Ouensanga, A. C., Bouchon, C. (1995): Water desorption and aragonite—calcite phase transition in scleractinian corals skeletons. Thermochimica Acta 265: 135-140.

Pauler, N. (1998): Paper Optics. AB Lorentzen & Wettre. Kista, Sweden. 93 p.

Peiponen, K.-E., Vartiainen, E. M., and Asakura, T. (1999): Dispersion, Complex Analysis and Optical Spectroscopy. Springer. Heidelberg.

Penttilä, A. & Lumme, K. (2004): The effect of particle shape on scattering – A study with a collection with axisymmetric particles and sphere clusters. Journal of Quantitative Spectroscopy & Radiative Transfer 89: 303-310.

Penttilä, A. I., and Lumme, K. (2008): Unpublished report.

Plummer, L.N. & Busenberg, E. (1982): The solubilities of calcite, aragonite and vaterite in CO_2-H_2O solutions between 0 and 90 °C, and an evaluation of the aqueous model for the system $CaCO_3$-CO_2-H_2O. Geochim. Cosmochim. Acta 46: 1011-1040.

Porubska, J., Alince, B., van de Ven, T.G.M. (2002): Homo- and heteroflocculation of papermaking fines and fillers", Colloids Surf. 210(2-3): 223-230.

Pummer, H. (1973): Selektive Füllstoffretention und optische Eigenschaften des Papiers. Papier 27: 417-422

Rasmussen, W.L.C. (2001): Novel Carbazole Based Methacrylates, Acrylates, and Dimethacrylates to Produce High Refractive Index Polymers. Doctoral Thesis. Virginia Polytechnic Institute and State University. Virginia. 166 p.

Rennel, J. (1969): Opacity in relation to strength properties of pulps III: Light scattering coefficient of sheets of model fibers. Tappi 52: 1943-1947.

Retulainen, E., Niskanen, K., and Nilsen, N. (1998) Fibres and bonds. Paper physics. Ed. K. Niskanen. Fapet Oy, Jyväskylä. pp. 55-87.

Ridgway, C. J. & Gane, P. A. C. (2002): Dynamic absorption into simulated porous structures. Colloids Surf. A. 206(1-3): 217-239.

Ridgway, C. J. & Gane, P. A. C. (2003): On Bulk Density Measurement and Coating Porosity Calculation for Coated Paper Samples. Nord. Pulp Pap. Res. J. 18(1): 24-31.

Ridgway, C. J. & Gane, P. A. C. (2004): Ink-coating adhesion: The importance of pore size and pigment surface chemistry. J. Dispersion Sci. and Technol. 25(4): 469-480.

Ridgway, C. J., Gane, P. A. C., El Abd, A. E.-G., Czachor, A. (2006a): Water absorption into construction materials: comparison of neutron radiography data with network absorption models. Transp. Porous Med. 63(3): 503-525.

Ridgway, C. J., Gane, P. A. C., Schoelkopf, J. (2006b): Achieving rapid absorption and extensive liquid uptake capacity in porous structures by decoupling capillarity and permeability: Nanoporous modified calcium carbonate. Transp. Porous Med. 63(2): 239-259.

Ross, W. D. (1971): Theoretical computation of light scattering power: Comparison between and air bubbles. J. Paint Technol. 43(563): 50-66.

Rousu, S., Lindstöm, M., Gane, P.A.C., Pfau, A., Shädler, V., Wirth, T., Eklund, D., (2002): Influence of latex-oil interaction on offset ink setting and ink oil distribution in coated paper. Journal of Graphic Technology, 1(2): 45-56.

Rozanov, V. V. & Kokhanovsky, A.A. (2006): The solution of the vector radiative transfer equation using the discrete ordinates technique: Selected applications. Atm. Res. 79: 241-265.

Räisänen, K. (1998): Water removal by flat boxes and a couch roll on a paper machine wire section. Doctoral Thesis. Helsinki University of Technology, Espoo.

Scaffardi, L. B. & Tocho, J. O. (2006): Size dependence of refractive index of gold nanoparticles Nanotechnology 17: 1309-1315.

Scallan, A. & Borch, J. (1972): An Interpretation of paper reflectance based upon morphology. Tappi 55(4): 583-588.

Scallan, A. & Borch, J. (1974): An Interpretation of paper reflectance based upon morphology: general applicability. Tappi 57(5): 143-147.

Scallan, A.M. & Borch, J. (1976) in ”The Fundamental Properties of Paper Related to Its Use”, (F. Bolam, ed), tech. Section Brit. Paper and Board Maers Assoc. London, p. 152.

Schoelkopf, J., Gane, P.A.C., Ridgway, C.J., Matthews, G.P. (2000a): Influence of inertia on liquid absorption into paper coating structures. Nord. Pulp Pap. Res. J. 15(5): 422-430.

Schoelkopf, J., Ridgway, C.J., Gane, P.A.C., Matthews, G.P., Spielmann, D.C. (2000b): Measurement and network modeling of liquid permeation into compacted mineral blocks. J. Colloid Interface Sci. 227(1): 119-131.

Schoelkopf, J., Gane, P.A.C., Ridgway, C.J., Spielmann, D.C., Matthews, G.P. (2001): Rate of vehicle removal from offset inks: a gravimetric determination of the imbibition behaviour of pigmented coating structures. Tappi 2001 Advanced Coating Fundamentals Symposium Proceedings. San Diego, Atlanta. pp.1-18.

Schoelkopf, J., Gane, P.A.C., Ridgway, C.J., Matthews, G.P. (2002): Practical observation of deviation from Lucas-Washburn scaling in porous media. Colloids Surf. A: Physicochem. and Eng. Asp. 206(1-3): 445-454.

Schoelkopf, J., Gane, P.A.C., Ridgway, C.J., Spielmann, D.C., Matthews, G.P. (2003a): Imbibition behaviour of offset inks: I Gravimetric determination of oil imbibition rate into pigmented coating structures. Tappi J. 2(6): 9-13.

Schoelkopf, J., Gane, P.A.C., Ridgway, C.J., Spielmann, D.C., Matthews, G.P. (2003b): Imbibition behaviour of offset inks: II: Gravimetric determination of vehicle imbibition rate from an offset ink into pigmented coating structures. Tappi J. 2(7): 19-23.

Seferis, C. J. (1999): Refractive Indices of Polymers. Polymer Handbook, 4th edition. Ed. Brandrup, J.. Publ. Wiley, New York. pp. 571-582.

Shalaev, V. M. (2002): Optical Properties of Nanostructured Random Media. Springer, Heidelberg.

Silenius, P. (2002): Improving the combinations of critical properties and process parameters of printing and writing paper and paperboards by new paper-filling methods. Doctoral thesis. Helsinki University of Technology, Espoo.

Starr, R.E. & Young, R.H. (1976): A study of the light scattering coefficients of various filler pigments using the Kubelka-Munk analysis. Tappi 59(12): 103-106.

Stokes, G. G. (1860): On the intensity of the light reflected from or transmitted through a pile of plates. Proc. R. Soc. London 11: 545-557.

Suhara, T., Esumi, K., Meguro, K. (1983): Effect of Surfactant on Formation of Calcium Carbonate. Bull. Chem. Soc. Jpn. 56(10): 2932-2936.

Szekely, J., Neumann, A.W., Chuang, Y.K (1971): The Rate of Capillary Penetration and the Applicability of the Washburn Equation. J. Colloid Interface Sci. 35(2): 273-278.

Van Gilder, R. & Purfeerst, R. (1994): Latex binder modification to reduce coating pick on six-color offset presses. Tappi J. 77(5): 230-239.

Varjos, P., Mikkonen, H., Kataja, K., Kuutti, L., Luukkanen, S., Peltonen, S., Qvintus-Leino, P. (2004): Non-mineral starch based pigments. PulPaper 2004: coating. Helsinki, Finland. June 1-3, 2004. pp. 131-134.

Videen, G., and Chýlek, P. (1998): Scattering by a composite sphere with an absorbing inclusion and effective medium approximations. Optics Communications 158(1-6): 1-6.

Walsh, D., Mann, S. (1995): Fabrication of hollow-porous shells of calcium carbonate from self-organizing media. Nature 377(6547): 320-323.

Weigl, J., Zeuner, M., and Baumgarten, H.L. (1981): Function, technological and economical aspects of pretreatment of fillers for groundwood-containing printing papers, Papier 35(10A): V46-V55.

White, A.F. (1975): Sodium and potassium coprecipitation in calcium carbonate. Doctoral Thesis. Northwestern University.

White, A.F. (1977): Sodium and potassium coprecipitation in aragonite. Geochim. Cosmochim. Acta 41: 613-625.

Xyla, A.G., Giannimaras, E. K., Koutsoukos, P. G. (1991): The Precipitation of Calcium Carbonate in Aqueous Solutions. Colloids Surf. 53(3-4): 241-255.

Xiang Y, Bousfield D.W., Hayes P.C., Kettle J. (2003): Effect of latex swelling on ink setting on coated paper. J. of Graphic Tech.1: 13-25.

Pat. JP 5116936. Production of highly dispersible platy calcium carbonate. K.K. Fine Ceramics JP (Y.Yakushiji, H. Sugihara, & K. Sugawara). App. JP19910307077 1991-10-25. Publ. 1993-05-14.

Yurkin, M. A., Maltsev, V. P., Hoekstra, A.G. (2007): The discrete dipole approximation for simulation of light scattering by particles much larger than the wavelength. J of Quant. Spec. and Rad. Transf. 106: 546-557.

Zeng, X. C., Bergman, D. J, Hui, P. M. (1988): Effective medium theory for weakly nonlinear composites. Phys. Rev. B 38: 10970-10973.

ERRATA

Paper I

Page 479, second column: "…in steps of 0.05"
Should be: "…in steps of 0.01-0.05"

Page 481, first column: "…refractive indices were 1.62 and 1.67"
Should be: "…refractive indices were 1.63 and 1.67".

Paper II

Page 6, Table I. Dosage 200 mg/g
Should be 0.2 mg/g.

Page 6, second column: "...pH and temperature of the stock were around 7 °C and 20 °C, respectively."
Should be: "…pH and temperature of the stock were around 7 and 20 °C, respectively."

Paper IV

Page 3186, Table 1, $Mg(OH)_2$ dosage 1:1 g
Should be 1.1 g

Aalto-DD 11/2011

ISBN: 978-952-60-4034-9 (pdf)
ISBN: 978-952-60-4033-2
ISSN-L: 1799-4934
ISSN: 1799-4942 (pdf)
ISSN: 1799-4934

Aalto University
School of Chemical Technology
Department of Forest Products Technology
aalto.fi

BUSINESS +
ECONOMY

ART +
DESIGN +
ARCHITECTURE

SCIENCE +
TECHNOLOGY

CROSSOVER

DOCTORAL
DISSERTATIONS